Wave Propagation in Stratified Plasmas

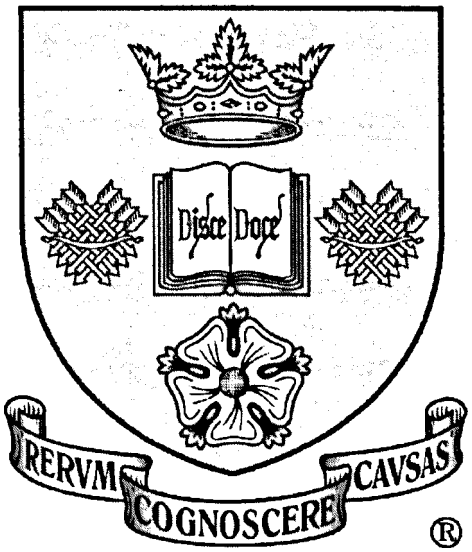

The University of Sheffield

James Hargreaves
Department of Applied Maths
Submission for the degree of PhD.

March, 2008

Abstract

In this Thesis the theoretical aspects of MHD wave propagation in stratified magnetic flux tubes are studied. In particular the focus is directed firstly to the study of wave propagation in flux tubes with the presence of a background flow and secondly to wave propagation in non-ideal, i.e. viscous, media. Recent observational evidence from the Hinode satellite shows clearly that plasma flows are ubiquitous in the solar atmosphere. Longitudinal and transverse tube waves in flux tubes with a background flow are studied, with the governing equations being derived and solved for a number of footpoint drivers. Applications to the Sun are made and some interesting and important effects on wave propagation are found. The solar atmosphere is widely recognised as a dissipative medium, although most previous studies of wave propagation in stratified atmospheres have assumed an ideal medium. In the second half of the Thesis the effect of viscosity on wave propagation is investigated for both longitudinal and transverse tube waves in a stratified flux tube. The governing equations are derived and solved for both temporal and spatial boundary conditions.

Acknowledgements

I am deeply indebted to Prof. Robertus von Fáy-Siebenbürgen for his excellent supervision and guidance. I am very grateful for all at the Applied Maths Department at the University of Sheffield and in particular Dr. Istvan Ballai for many helpful discussions and ideas. Thanks must also go to Ben, Ian, Craney, Carlos, Eamon and the rest of my friends for helping me do the math. Last, but not least, I would like to thank my family and especially my parents for their invaluable support and encouragement.

Contents

1 Introduction **1**

1.1 Introduction 2
1.1.1 The solar interior 3
1.1.2 The solar atmosphere 3
1.2 The equations of magnetohydrodynamics 5
1.2.1 Summary of MHD equations 8
1.3 MHD waves in a uniform atmosphere 9
1.4 MHD waves in structured atmospheres 13
1.4.1 Overview of atmospheric wave observations 16
1.5 The Klein-Gordon Equation 17
1.5.1 Properties and solutions of the Klein-Gordon equation 19
1.5.2 Summary of wave propagation characteristics for temporal boundary conditions 21
1.6 Outline of thesis 23

2 Longitudinal wave propagation in steady stratified waveguides **24**

2.1 Introduction 25
2.1.1 Observational evidence of flows 26
2.2 Longitudinal wave propagation with steady background flow 26
2.2.1 Equilibrium considerations 27
2.2.2 Small perturbations about the steady equilibrium 29
2.2.3 Formulation of solution by means of Laplace transforms 32
2.2.4 Solution by Maple 32
2.2.5 Solution by perturbation methods 33
2.2.6 The inverse Laplace transform 35
2.2.7 Atmospheric response to various photospheric drivers 36
2.3 Application to the Sun 45
2.4 Conclusions 48

3 Transverse wave propagation in steady stratified waveguides **52**

3.1 Introduction 53
3.2 Transverse tube waves 53
3.2.1 Solution by Laplace transforms and perturbation methods 57
3.2.2 Atmospheric response to various photospheric drivers 58
3.3 Application to the Sun 60
3.4 Conclusions 63

4 Longitudinal MHD waves in stratified and viscous plasmas **66**

4.1 Introduction 67
4.2 Governing equations 67
4.3 Variation in Q occurs over length scales much larger than the scale height . . . 70

4.3.1 Solving for various footpoint drivers 72
4.4 Variation in Q occurs over length scales much smaller than the scale height . . 74
4.4.1 Spatial boundary conditions 75
4.4.2 Temporal boundary conditions 79
4.5 Application to the Sun 81
4.6 Conclusions 83

5 Transverse MHD waves in stratified and viscous plasmas **85**
5.1 Introduction 86
5.2 Governing equations 86
5.3 Case 1: Variation in Q occurs over length scales much larger than H 88
5.3.1 Solving for various footpoint drivers 90
5.4 Case 2: Variation in Q occurs over length scales much smaller than H 91
5.4.1 Spatial boundary conditions 92
5.4.2 Temporal boundary conditions 92
5.5 Conclusions 93

6 Conclusions **96**
6.1 Overview of Thesis 96
6.2 Summary of results 96
6.3 Outlook 98
6.4 Concluding Remarks 99

A Thin flux tube equations **100**
A.1 The MHD equations 101
A.1.1 Continuity 101
A.1.2 Momentum 103
A.1.3 Induction 104
A.1.4 Energy 105
A.1.5 Ideal Gas 105
A.1.6 Solenoidal 105
A.2 Summary 105

B Multiple Scales **106**

C Alternative derivation for Section 4.2 **109**
C.1 Governing equations 109

List of Figures

1.1 Diagram of the solar structure highlighting the core, radiative and convection zones as well the atmospheric regions of the photosphere, chromosphere and corona (NASA). 2

1.2 Image of the photosphere and a sunspot group near disk centre. The granulation of the photosphere is clearly seen. Tick marks are 1000 km apart. (Royal Swedish Academy of Sciences) 4

1.3 Positions of sunspot groups observed at the Mt. Wilson Observatory (MWO). . 5

1.4 Polar plot showing the phase speed, c_{ph} of the two magnetoacoustic modes and the Alfvén wave at the angle to the magnetic field. a) $c_T < c_0 < v_A < c_F$, b) $c_T < v_A < c_0 < c_F$ 13

1.5 Dispersion diagram for magnetic cylinder plotted for typical coronal conditions. 15

2.1 Equilibrium configuration of the thin magnetic flux tube. The equilibrium pressure, density and bulk flow are denoted by p_0, ρ_0 and U_0 respectively. 27

2.2 The maximum value of footpoint flow, $U_0(0)$, against the maximum height considered. 46

2.3 The variation of the flow timescale, λ, with height plotted for two magnitudes of footpoint flow, $U_0(0)$. The dotted line corresponds to $z_{max} = 500$, giving $U_0(0) = e^{-500/2H}$. The solid line corresponds to $z_{max} = 2000$. 46

2.4 The forced atmospheric oscillations for the monochromatic driver against time. Curve plotted for z=500 km, $U_0(0) = e^{-500/2H}$ and a driver period of 50 s. . . . 47

2.5 The percentage increase in amplitude of the forced atmospheric oscillations between the steady and static flux tubes. The solid, dotted and dashed curves correspond to ω =0.13, 0.06 and 0.04 s^{-1} respectively. All curves are plotted to $z_{max} = 2000$, giving $U_0(0) = e^{-2000/2H}$ 48

2.6 The free atmospheric oscillations for the monochromatic driver against time. Curve plotted for z=500 km and $U_0(0) = e^{-500/2H}$. 49

2.7 The percentage increase in amplitude of the free oscillations between the steady and static cases against height. Two sets of curves are plotted; the leftmost corresponds to a footpoint flow valid up to $z = 500$ km, the rightmost to a footpoint flow valid up to $z = 2000$ km. The solid, dotted and dashed lines correspond to times of $t = 1000, 2000$ and 3000 s respectively. 49

2.8 The percentage increase in amplitude of the free oscillations between the steady and static cases against footpoint flow. The curve is plotted for $z = 500$ km and the solid, dashed, dotted and dot-dashed lines correspond to $t = 1000, 2000, 3000$ and 4000 s respectively. 50

2.9 The phase angle between against footpoint flow. The curve is plotted for $z =$ 500 km and the solid, dashed, dotted and dot-dashed lines correspond to $t =$ 1000, 2000, 3000 and 4000 s respectively. 50

3.1 The variation of the flow timescale, λ_k, with height plotted for two magnitudes of footpoint flow, $U_0(0)$. The dotted line corresponds to $z_{max} = 500$, giving $U_0(0) = \exp(-500/2H)$. The solid line corresponds to $z_{max} = 2000$. 62
3.2 The percentage increase in amplitude of the forced atmospheric oscillations between the steady and static flux tubes. The solid, dotted and dashed curves correspond to ω =0.13, 0.06 and 0.04 s^{-1} respectively. All curves are plotted to $z_{max} = 2000$, giving $U_0(0) = e^{-2000/2H}$ 63
3.3 The percentage increase in amplitude of the free oscillations between the steady and static cases against height. Two sets of curves are plotted; the leftmost corresponds to a footpoint flow valid up to $z = 500$ km, the rightmost to a footpoint flow valid up to $z = 2000$ km. The solid, dotted and dashed lines correspond to times of $t = 1000, 2000$ and 3000 s respectively. 64
3.4 The percentage increase in amplitude of the free oscillations between the steady and static cases against footpoint flow. The curve is plotted for $z = 500$ km and the solid, dashed, dotted and dot-dashed lines correspond to $t = 1000, 2000, 3000$ and 4000 s respectively. 64
3.5 The phase angle between against footpoint flow. The curve is plotted for $z =$ 500 km and the solid, dashed, dotted and dot-dashed lines correspond to $t =$ 1000, 2000, 3000 and 4000 s respectively. 65

4.1 The integration contour and the branch cuts for the inverse Laplace transforms of the quantities Eq. (4.47) and Eq. (4.48). The branch cuts are shown by crosses. 76
4.2 Temperature and density as a function of height based on the VALIIIc model; a)temperature against height b) density against height. 81
4.3 Viscosity coefficient against height, based on the VALIIIc model. 82
4.4 Change in cutoff period, $P_{T\nu}$, versus viscosity coefficient. 82
4.5 The exponential multiplier versus viscosity for times $t = 1000$ s (solid line) to $t = 5000$ s (dash-dot-dot-dot line). 83

5.1 Change in cutoff period, $P_{k\nu}$, plotted against the viscosity coefficient. 94
5.2 The exponential multiplier versus viscosity coefficient for times $t = 1000$ s (solid line) to $t = 5000$ s (dash-dot-dot-dot line). 94

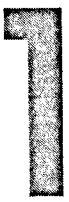

Introduction

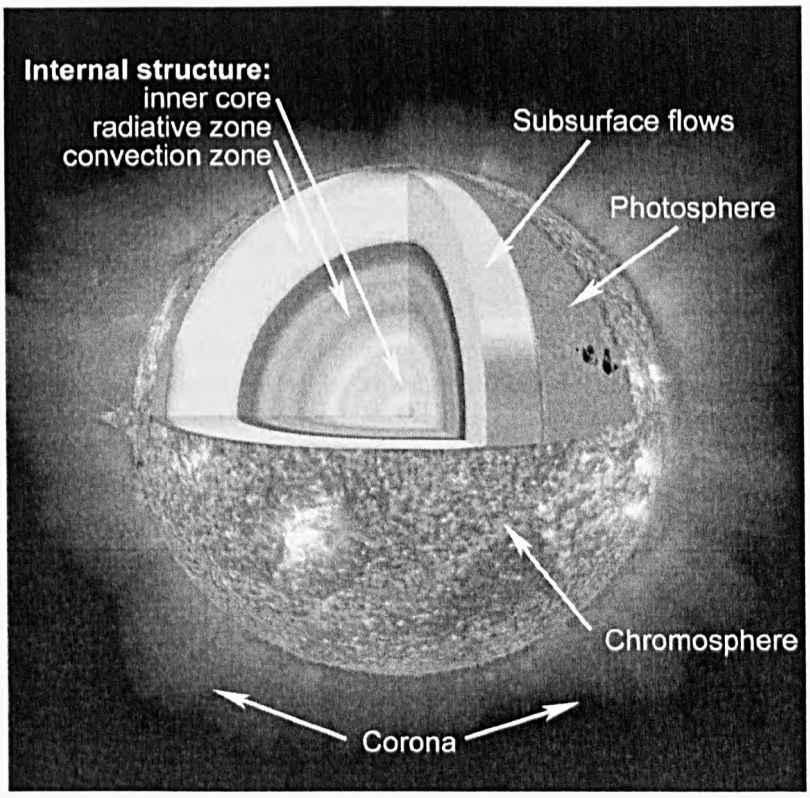

Figure 1.1: Diagram of the solar structure highlighting the core, radiative and convection zones as well the atmospheric regions of the photosphere, chromosphere and corona (NASA; http://www.solarviews.com/cap/vss/VSS00031.html).

1.1 Introduction

The Sun, the source of life on Earth, is in every sense a middling kind of star. There are millions like it in our galaxy, others however may be a hundred times bigger, others not even a tenth of the size. To solar physicists however it is the Sun's proximity to the Earth that offers the unique opportunity to study it in extraordinary detail. The Sun formed some 4.5 billion years ago in a huge cloud of interstellar gas which slowly collapsed under its own gravity. The cloud rotated faster as it shrank, forming a flat disc at its outer edge from which the planets eventually formed. In the centre, the nascent Sun heated to a point where, after several million years, thermonuclear processes were ignited and the Sun began to shine. Like all stars the Sun is a giant ball of plasma held together by its own gravity. It is, in human terms, almost incomprehensibly large, being around 330,000 times more massive than the Earth and with a radius of 696,000 km, is more than a million times larger in volume. It loses a million tonnes a second in the form of sunlight and has been doing so, without noticeable shrinkage, for over four billion years. It consists of hydrogen and helium, in a ratio of around nine to one, with minute quantities of heavier elements. In crudest terms the Sun can be thought of as being structured in concentric regions, namely the core, radiative zone and convection zone, each with specific properties, see Fig. 1.1.

1.1.1 The solar interior

The solar core extends to around a quarter of the solar radius ($0.25R_\odot$) and generates, through the process of nuclear fusion, 99% of the Sun's energy. The temperature of the core is around 15 million K and, with a density ten times greater than the Earth's centre, fusion is made possible. The main reaction is the proton-proton cycle; hydrogen is converted into helium and energy in the form of γ rays. The four particles making up the helium nucleus have a larger mass prior to their fusion than after it. This loss of mass has an energy production equivalent given by Einstein's equation, $E = mc^2$.

Moving outwards from the core the temperature drops to a point where fusion is no longer sustainable and energy leaks outwards by radiative diffusion. This is the radiative zone and extends from $0.25R_\odot$ to around $0.7R_\odot$ and, although as opaque as a brick wall, a steady flow of light makes it through (Zirker, 2004). The mean free path is so small that a photon takes around 10^7 years to reach the surface. Photons are continuously absorbed and re-emitted at lower and lower temperatures, such that the wavelength is increased from that of the high energy γ rays to the visible range by the solar surface. Throughout this region the temperature drops from 7 million K to 2 million K, with a corresponding drop in density from 20,000 kg/m^3, slightly greater than the density of gold, to a mere 200 kg/m^3, a fifth of the density of water.

Moving further outward, beyond $0.7R_\odot$, the temperature decreases and heavy ions retain more of their electrons, rendering the plasma more opaque. The temperature gradient becomes steep enough for convective instability. Static equilibrium can no longer be maintained and energy is transported most efficiently by convection, which manifests itself in distinct scales, namely the supergranules, mesogranules and granules. The supergranules are around 30,000 km across and have a lifetime of 1-2 days. The centre of the cell is made up of hot, rising plasma and cooler, descending plasma at the edges. Typical speeds for this large scale plasma flow is of the order of 0.1 km/s. The mesogranules and granules are smaller in size and found nearer the surface, with the granules at the top of the convection zone. The temperature at this point has fallen to around 6,600 K with a density of around 2×10^{-4} kg/m^3, which is about one ten thousandth the density of air at sea level.

The interface between the radiative zone and the convection zone is another important region in the Sun as it is believed that it is the source of the magnetic field that dominates so much of the Sun's dynamics. The tachocline, as it is called, generates the magnetic field in accordance with dynamo theory. Above the convection zone lies the solar atmosphere, which, in the classical view can also be considered to consist of three layers; the photosphere, the chromosphere and the corona.

1.1.2 The solar atmosphere

At the top of the convection zone lies the photosphere, a thin layer of plasma some 500 km thick, from which most of the Sun's visible light is emitted. Only in the sense that there is a very rapid drop in density does the Sun have a 'surface'. The photosphere extends up to the temperature minimum, where the temperature falls to around 4,100 K and displays a cobblestone pattern, being the top of the granular cells, having diameters of the order of 1,500 km and a lifetime of around 5 minutes. Sunspots, a common photospheric feature, have been observed with telescopes since the time of Galileo, since they appear as dark blemishes on an otherwise smooth background. Fig. 1.2 shows a sunspot group observed near disk centre. The sunspot is dark against the background due to the extremely high magnetic field (of the order 3,000

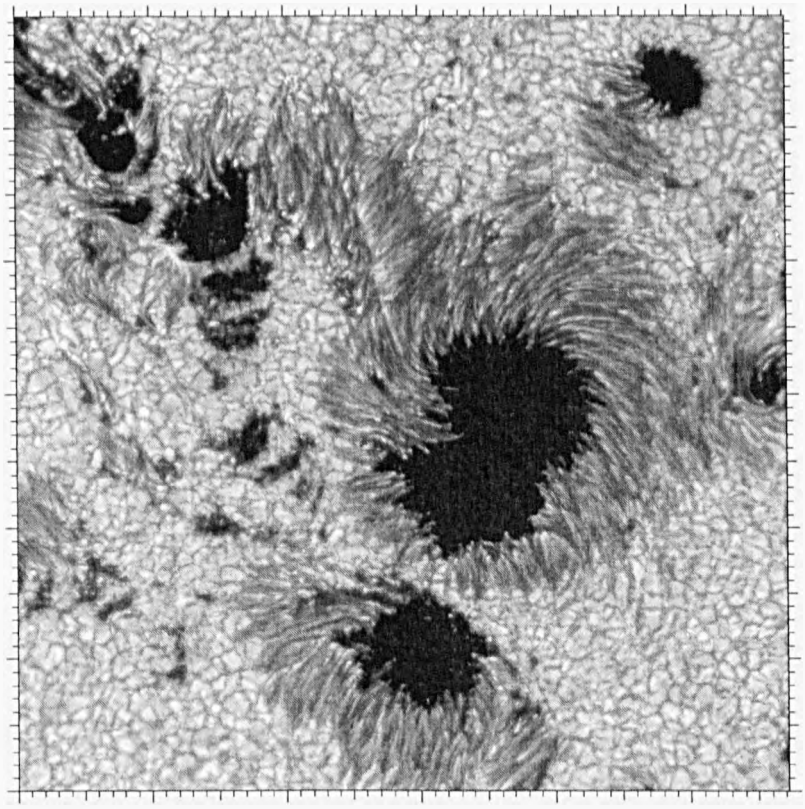

Figure 1.2: Image of the photosphere and a sunspot group near disk centre. The granulation of the photosphere is clearly seen. Tick marks are 1000 km apart. (Royal Swedish Academy of Sciences)

Gauss) that locally suppresses energy transport by convection meaning the temperature is decreased. The study of sunspots has given a clear indication of the Sun's solar cycle; a variation in activity over an approximately 11 year period. During each cycle sunspots emerge at high latitudes and over the course of the cycle their emergence migrates to lower and lower latitudes. Plotting their appearance against time produces the well-known 'butterfly diagram' shown in Fig. 1.3. Sunspots typically appear in pairs, one with emerging flux, the other submerging and are aligned east-west in the northern hemisphere, west-east in the southern hemisphere and switching every solar cycle.

Above the photosphere lies the chromosphere, so named from early eclipse observations where it was seen ruby-red in colour, and now known to be H_α emission. Above the photosphere and the temperature minimum the temperature actually rises, to around 50,000 K, but the structure of the chromosphere is far from uniform. Features include the chromospheric network and internetwork of magnetic field, observed 3 min oscillations and the dynamic spicules, which eject chromospheric material to higher layers. The chromospheric network is formed by the convective motions of supergranular cells which tend to push magnetic flux toward cell boundaries. The internetwork field refers to regions where the field is weak and corresponds to cell interiors. Above this region lies the transition region, a thin and irregular layer of plasma in which the temperature rises dramatically to over 1 million K and the density falls to around 10^{-10} kg/m^3. The light emitted at these temperatures is in the ultraviolet, x-ray and even shorter wavelength

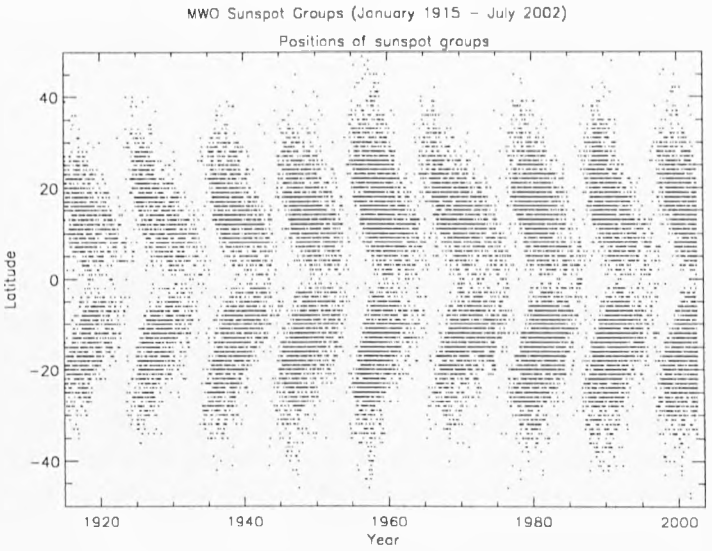

Figure 1.3: Positions of sunspot groups observed at the Mt. Wilson Observatory (MWO).

regions, and consequently visible only from space.

The outer atmosphere of the Sun is called the corona, an extremely tenuous plasma that extends millions of kilometers into space and has temperatures well over 1 million K. The corona may be observed in visible light only during total eclipses when the solar disk is obscured. The fact that the temperature rises from the temperature minimum to the high coronal values is counter-intuitive and remains a largely unanswered question and a hot topic for research. The corona exhibits a wealth of features such as loops, streamers, plumes, coronal holes, coronal mass ejections and many others, which are often observed in x-ray wavelengths due to the corona's high temperature. The Sun emits a low density stream of particles in all directions and at extremely high speeds, known as the solar wind. The source is the solar corona but the exact method of acceleration of the solar wind is another current area of research.

1.2 The equations of magnetohydrodynamics

Magnetohydrodynamics (MHD) is the study of the interaction between an electrically conducting fluid and a magnetic field, in which the plasma can be considered to be a continuous medium. MHD is essentially the combination of Maxwell's equations of electromagnetism and the Navier-Stokes equation which governs the motions of a neutral fluid. An alternative starting point would be the Boltzmann equations for electrons and protons, and thus taking the two-fluid approach, e.g. Boyd & Sanderson (1969). We adopt the single-fluid approach, e.g. Cowling (1976), and start with Maxwell's equations which describe the change in electric field, $\mathbf{E}$, and the magnetic field, $\mathbf{B}$, with currents of density, $\mathbf{j}$, and electric charges of density, ρ_c. We have

$$\nabla \times \mathbf{B} = \mu \mathbf{j} + \frac{1}{c^2} \frac{\partial \mathbf{E}}{\partial t}, \tag{1.1}$$

$$\nabla \cdot \mathbf{B} = 0, \tag{1.2}$$

$$\nabla \times \mathbf{E} = -\frac{\partial \mathbf{B}}{\partial t}, \tag{1.3}$$

$$\nabla \cdot \mathbf{E} = -\frac{\rho_c}{\varepsilon}. \tag{1.4}$$

Eq. (1.1) is Ampere's law, where μ is the magnetic permeability, Eq. (1.2) is the solenoidal condition, stating that there are no magnetic sources, Eq. (1.3) is Faraday's law of induction, and Eq. (1.4) is Poisson's equation stating conservation of charge, where ε is the permittivity of free space. The term c is the speed of light in a vacuum. When formulating a fluid description of the plasma, we assume that the times scales of interest are long in comparison to with the time scales associated with particle motions and that the spatial scales of interest are large when compared to the Debye length and the thermal gyroradius. In particular we may consider Eq. (1.3) such that

$$\nabla \times \mathbf{E} \sim \frac{E}{L}, \quad \frac{\partial \mathbf{B}}{\partial t} \sim \frac{B}{\tau}, \tag{1.5}$$

where L and τ are typical spatial and timescales respectively, such that a typical plasma velocity is of the order $v = L/\tau$, yielding the estimate $E \sim vB$. Examining the time derivative of the electric field in Eq. (1.1) in terms of these estimates gives

$$\frac{1}{c^2}\frac{\partial \mathbf{E}}{\partial t} \sim \frac{1}{c^2}\frac{E}{\tau} = \frac{v^2}{c^2}\frac{B}{L}. \tag{1.6}$$

For non-relativistic perturbations, such that $v \ll c$, we see that the second term on the RHS of Eq. (1.1) can be dropped, allowing us to restate Ampere's law in the MHD limit as

$$\nabla \times \mathbf{B} = \mu \mathbf{j}. \tag{1.7}$$

The above equations are taken in conjunction with Ohm's law which states that the current is proportional to the total electric field. Neglecting Hall terms, which results in the assumption that the all wave motion frequencies are much lower than the ion cyclotron frequency, allows us to use a simple form of Ohm's law given by

$$\mathbf{j} = \sigma(\mathbf{E} + \mathbf{v} \times \mathbf{B}), \tag{1.8}$$

where σ is the electric conductivity and $\mathbf{v}$ is the plasma velocity. In general $\mathbf{v}$ and $\mathbf{B}$ are taken as the primary variables and the electric field and current are secondary. Using Eq. (1.8) we may eliminate the electric field and the current density from Eq (1.1) and Eq. (1.3) to obtain

$$\frac{\partial \mathbf{B}}{\partial t} = \nabla \times (\mathbf{v} \times \mathbf{B}) - \nabla \times (\eta \nabla \times \mathbf{B}), \tag{1.9}$$

where $\eta = 1/(\mu\sigma)$ is the magnetic diffusivity. Assuming a constant η and employing the identity $\nabla \times (\nabla \times \mathbf{B}) = \nabla(\nabla \cdot \mathbf{B}) - (\nabla \cdot \nabla)\mathbf{B}$ along with the solenoidal condition, Eq. (1.2), we find

$$\frac{\partial \mathbf{B}}{\partial t} = \nabla \times (\mathbf{v} \times \mathbf{B}) + \eta \nabla^2 \mathbf{B}, \tag{1.10}$$

known as the induction equation. Consideration of the ratio between the first and second terms in the induction equation yields the magnetic Reynolds number

$$R_m = \frac{vL}{\eta}. \tag{1.11}$$

R_m is the magnitude of the ratio of the convective term to the diffusive term and measures the strength of coupling between flow and magnetic field. In typical solar atmosphere applications $R_m \gg 1$, thus the diffusive term in Eq. (1.10) may be neglected. Under these conditions the plasma is considered to be perfectly conducting and the induction equation is reduced to

$$\frac{\partial \mathbf{B}}{\partial t} = \nabla \times (\mathbf{v} \times \mathbf{B}). \tag{1.12}$$

In this limit Alfvén's frozen flux theorem holds, which states that magnetic field lines are frozen to the plasma. Plasma motion along the field line does not effect the magnetic field but transverse motions tend to drag the field lines with it. Equally movement of field lines may push the plasma. The frozen flux idea breaks down when small length scales are considered, such that $R_m \ll 1$ and the diffusive term in the original induction equation dominates.

Turning our attention to the hydrodynamic equations we see that continuous fluid may be described by equations of continuity, momentum and energy. The mass continuity equation is given by

$$\frac{\partial \rho}{\partial t} + \nabla \cdot (\rho \mathbf{v}) = 0, \tag{1.13}$$

where ρ is the mass density. The continuity equation states that a convergence of mass flux yields a density increase and vice versa. Eq. (1.13) may be rewritten as

$$\frac{D\rho}{Dt} + \rho \nabla \cdot \mathbf{v} = 0, \tag{1.14}$$

where

$$\frac{D}{Dt} \equiv \frac{\partial}{\partial t} + \mathbf{v} \cdot \nabla. \tag{1.15}$$

The momentum equation is given by

$$\rho \frac{D\mathbf{v}}{Dt} = -\nabla p + \mathbf{j} \times \mathbf{B} + \mathbf{F}_g + \mathbf{F}_v, \tag{1.16}$$

where p is the plasma pressure, $\mathbf{j} \times \mathbf{B}$ is the Lorentz force and $\mathbf{F}_g$ and $\mathbf{F}_v$ are gravitational and viscous forces respectively. Employing Ampere's law, given by Eq. (1.7), the Lorentz force can be shown to comprise of a magnetic tension component and a magnetic pressure component. Thus

$$\mathbf{j} \times \mathbf{B} = \frac{1}{\mu}(\nabla \times \mathbf{B}) \times \mathbf{B} = \frac{(\mathbf{B} \cdot \nabla)\mathbf{B}}{\mu} - \nabla\left(\frac{B^2}{2\mu}\right), \tag{1.17}$$

where $B = |\mathbf{B}|$ is the magnitude of the magnetic field. The ratio of the plasma pressure to the magnetic pressure can thus be readily defined, yielding the dimensionless parameter

$$\beta = \frac{p}{B^2/2\mu}, \tag{1.18}$$

and is termed the plasma-β. In a low-β plasma the magnetic pressure is dominant and in general characterises the solar atmosphere. The plasma may be termed 'cold' if the plasma-β is zero.

This has the consequence of effectively setting the sound speed to zero, resulting in the absence of any pressure perturbations. The energy equation has the form (Priest, 1982)

$$\frac{\rho^\gamma}{\gamma-1}\frac{D}{Dt}\left(\frac{p}{\rho^\gamma}\right) = -\mathcal{L}, \tag{1.19}$$

where γ is the ratio of the specific heats at constant pressure and volume respectively, also known as the adiabatic index and $\mathcal{L}$ is the energy loss function, representing the energy lost to thermal conduction, radiation etc. Taking the loss function to be zero, i.e. energy is conserved, we may rewrite Eq. (1.19) as

$$\frac{Dp}{Dt} = \frac{\gamma p}{\rho}\frac{D\rho}{Dt} = -\gamma p \nabla \cdot \mathbf{v}. \tag{1.20}$$

We close the hydrodynamic equations with the ideal gas law

$$p = \frac{R}{\tilde{\mu}}\rho T, \tag{1.21}$$

where R is the gas constant and $\tilde{\mu}$ is the mean atomic weight. It should be noted that $\tilde{\mu}$ may often be included in the gas constant term and Eq. (1.21) may be written in terms of the Boltzmann constant and the mean particle mass.

1.2.1 Summary of MHD equations

The basic equations of MHD that shall form the basis for further study are

$$\mathbf{j} = \frac{\nabla \times \mathbf{B}}{\mu}, \tag{1.22}$$

$$\frac{\partial \mathbf{B}}{\partial t} = \nabla \times (\mathbf{v} \times \mathbf{B}) + \eta \nabla^2 \mathbf{B}, \tag{1.23}$$

$$\nabla \cdot \mathbf{B} = 0, \tag{1.24}$$

$$\frac{\partial \rho}{\partial t} + \nabla \cdot (\rho \mathbf{v}) = 0, \tag{1.25}$$

$$\rho \frac{D\mathbf{v}}{Dt} = -\nabla p + \mathbf{j} \times \mathbf{B} + \mathbf{F}_g + \mathbf{F}_v, \tag{1.26}$$

$$\frac{Dp}{Dt} - \frac{\gamma p}{\rho}\frac{D\rho}{Dt} = 0, \tag{1.27}$$

$$p = \frac{R}{\tilde{\mu}}\rho T, \tag{1.28}$$

being Ampere's law in the MHD limit, the induction equation, the solenoidal condition, equations of continuity, momentum, energy and the ideal gas law respectively. It is worth reviewing the assumptions under which the preceding equations may be employed. The plasma has been treated as a continuum, such that the equations of hydrodynamics may be employed. This requires that typical length scales are much greater than the internal plasma scales such as the ion gyroradius and the electron inertia length. Further it is assumed that length scales are much grater than the mean free path of the particles. Plasma motions and the magnitudes of characteristic speeds are considered small when compared with c, the speed of light. Relativistic effects

are therefore ignored. Hall effects have been ignored by using a simple form of Ohm's law, thus assuming that wave frequencies are much lower than the ion cyclotron frequency. Charge neutrality is assumed such that the number density of the ions is of the order of the electron number density. Finally we have assumed that the magnetic diffusivity, η, and the magnetic permeability, μ, are constants. Strictly speaking MHD requires plasma to be collisional, but for many structures in the solar corona, where the plasma is so tenuous it is in fact collisionless, MHD may be still applied to give qualitative description of solar processes.

1.3 MHD waves in a uniform atmosphere

A physical system under the influence of a perturbation will commonly respond with the emission of waves. Sound waves reach one's ears by means of a pressure perturbation produced at the wave source. A local compression or rarefaction creates a pressure gradient which acts to restore the original equilibrium. The properties of acoustic waves may be examined by considering a reduced set of the governing equations of MHD presented in the previous section. Taking the continuity equation, Eq. (1.25), the adiabatic energy equation, Eq. (1.27) and a reduced form of the momentum equation given by

$$\rho \frac{D\mathbf{v}}{Dt} = -\nabla p, \tag{1.29}$$

where the only restoring force is given by the plasma pressure, we examine wave-like properties by examining linear perturbation theory. Properties are taken to be a sum of equilibrium and perturbation quantities, where, if the amplitudes of the waves are small, products of perturbed quantities may be considered small and thus neglected. Thus we consider

$$p = p_0 + p_1(\mathbf{r},t), \quad \rho = \rho_0 + \rho_1(\mathbf{r},t), \quad \mathbf{v} = 0 + \mathbf{v}_1(\mathbf{r},t) \tag{1.30}$$

where the subscript '0' denotes an equilibrium quantity and the subscript '1' denotes a perturbed quantity. We shall consider the atmosphere to be uniform such that the equilibrium pressure and density are constant. Linearising the governing equations yields

$$\frac{\partial \rho_1}{\partial t} + \nabla \cdot (\rho \mathbf{v}_1) = 0, \tag{1.31}$$

$$\rho_0 \frac{\partial \mathbf{v}_1}{\partial t} = -\nabla p_1, \tag{1.32}$$

$$\frac{\partial p_1}{\partial t} = c_0^2 \frac{\partial \rho_1}{\partial t}, \tag{1.33}$$

where

$$c_0^2 = \frac{\gamma p_0}{\rho_0}, \tag{1.34}$$

is the (constant) sound speed. Combining Eq. (1.31), Eq. (1.32) and Eq. (1.33) for the perturbation velocity $\mathbf{v}_1$ yields

$$\frac{\partial^2 \mathbf{v}_1}{\partial t^2} = c_0^2 \nabla (\nabla \cdot \mathbf{v}_1). \tag{1.35}$$

Arbitrary perturbations may be decomposed into Fourier components such that we seek plane-wave solutions of the form

$$\mathbf{v}_1(\mathbf{r},t) = \mathbf{v}_1(0)e^{i(\mathbf{k}\cdot\mathbf{r}-\omega t)}, \tag{1.36}$$

where $\mathbf{k}$ is the wavenumber vector and ω is the frequency. Thus the period of the wave is given by $2\pi/\omega$ and the wavelength by $2\pi/k$ in the direction of $\mathbf{k}$, being the wavenumber unit vector. Substituting Eq. (1.36) into Eq. (1.35), with the assumption that $\mathbf{k}\cdot\mathbf{v}_1$ (and thus $\nabla\cdot\mathbf{v}_1$) is non-zero, yields

$$\omega^2 = c_0^2 k^2, \tag{1.37}$$

where k is the magnitude of the wavenumber vector. Eq. (1.37) is known as a dispersion relation, linking the frequency with the wavenumber. The dispersion relation shows that acoustic waves propagate equally in all directions with a phase speed, given by ω/k, of

$$c_{ph} = c_0, \tag{1.38}$$

and a group speed in the direction $\mathbf{k}$, given by $d\omega/dk$ and describing the velocity of energy transfer, of

$$c_g = c_0. \tag{1.39}$$

The speed of propagation, since not a function of frequency, is therefore non-dispersive and the requirement that $\mathbf{k}\cdot\mathbf{v}_1$ is non-zero highlights the fact that acoustic waves owe their existence to the compressibility of the plasma. Waves are longitudinal since the velocity perturbation is in the direction of propagation, $\mathbf{k}$.

We now turn our attention to magnetic waves in a uniform medium. We use the MHD equations presented in Section 1.2.1 and in order to demonstrate the fundamental MHD wave modes we neglect gravity and viscous effects, such that $\mathbf{F}_g = \mathbf{F}_v = 0$ in Eq. (1.26). The medium is taken to be ideal such that $\eta = 0$ in the induction equation. The equilibrium magnetic field, $\mathbf{B}_0$, pressure, p_0, and density, ρ_0, are taken as uniform and we align the magnetic field along the z-axis, such that $\mathbf{B}_0 = B_0\hat{\mathbf{z}}$, where $\hat{\mathbf{z}}$ denotes the unit vector in the z-direction. Consideration of the momentum equation, Eq. (1.26), along with the expression for the Lorentz force, given by Eq. (1.17), yields the condition of pressure balance such that the total pressure is conserved. In the same way as for the acoustic case, we may consider perturbed quantities about the equilibrium given by

$$\mathbf{B} = \mathbf{B}_0 + \mathbf{B}_1(\mathbf{r},t), \quad \mathbf{v} = 0 + \mathbf{v}_1(\mathbf{r},t), \quad p = p_0 + p_1(\mathbf{r},t), \quad \rho = \rho_0 + \rho_1(\mathbf{r},t). \tag{1.40}$$

Substituting the total perturbed quantities into the equations for continuity, momentum, induction and energy, along with the solenoidal condition yields the linearised equations

$$\frac{\partial \rho_1}{\partial t} + \rho_0 \Delta = 0, \tag{1.41}$$

$$\rho_0 \frac{\partial \mathbf{v}_1}{\partial t} = -\nabla p_1 + \frac{1}{\mu}(\nabla \times \mathbf{B}_1) \times \mathbf{B}_0, \tag{1.42}$$

$$\frac{\partial \mathbf{B}_1}{\partial t} = \nabla \times (\mathbf{v}_1 \times \mathbf{B}_0), \tag{1.43}$$

$$\frac{\partial p_1}{\partial t} = c_0^2 \frac{\partial \rho_1}{\partial t}, \tag{1.44}$$

$$\nabla \cdot \mathbf{B}_1 = 0, \tag{1.45}$$

where $\Delta = \nabla \cdot \mathbf{v}_1$, after Cowling (1976). Taking the derivative with respect to time of Eq. (1.42) and eliminating perturbed quantities of pressure and magnetic field using Eq. (1.31), Eq. (1.43) and Eq. (1.44) yields a single equation for the velocity perturbation $\mathbf{v}_1 = (v_x, v_y, v_z)$, given by

$$\frac{\partial^2 \mathbf{v}_1}{\partial t^2} = c_0^2 \nabla \Delta + v_A^2 \left[\left(\frac{\partial^2 v_x}{\partial x^2} + \frac{\partial^2 v_x}{\partial z^2} + \frac{\partial^2 v_y}{\partial x \partial y} \right), \left(\frac{\partial^2 v_y}{\partial y^2} + \frac{\partial^2 v_y}{\partial z^2} + \frac{\partial^2 v_x}{\partial y \partial x} \right), 0 \right], \tag{1.46}$$

where $v_A = B_0/(\mu \rho_0)^{1/2}$ is known as the Alfvén speed (Alfvén, 1942). We may rewrite the second term on the right hand side of this equation in terms of the divergence of the velocity perturbation such that

$$\frac{\partial^2 \mathbf{v}_1}{\partial t^2} = c_0^2 \nabla \Delta + v_A^2 \left[\frac{\partial}{\partial z} \left(\frac{\partial \mathbf{v}_1}{\partial z} - \Delta \hat{\mathbf{z}} \right) - \nabla \left(\frac{\partial v_z}{\partial z} - \Delta \right) \right]. \tag{1.47}$$

The z-component and the divergence of this equation respectively yield

$$\frac{\partial^2 v_z}{\partial t^2} = c_0^2 \frac{\partial \Delta}{\partial z}, \tag{1.48}$$

$$\frac{\partial^2 \Delta}{\partial t^2} = c_0^2 \nabla^2 \Delta + v_A^2 \nabla^2 \left(\Delta - \frac{\partial v_z}{\partial z} \right), \tag{1.49}$$

giving the governing linear equations for MHD waves in unbound, uniform plasma (Lighthill, 1960; Roberts, 1981). These two equations may be combined to give the single partial differential equation

$$\frac{\partial^4 \Delta}{\partial t^4} - (c_0^2 + v_A^2) \frac{\partial^2}{\partial t^2} \nabla^2 \Delta + c_0^2 v_A^2 \frac{\partial^2}{\partial z^2} \nabla^2 \Delta = 0. \tag{1.50}$$

It should be noted that if the magnetic field is removed, by setting $v_A^2 = 0$, the preceding equation may yield

$$\frac{\partial^2 v_z}{\partial t^2} = c_0^2 \frac{\partial^2 v_z}{\partial z^2}, \tag{1.51}$$

being a one-dimension wave equation describing purely acoustic waves. Consideration of Eq. (1.47) and Eq. (1.50) in turn yields the three fundamental MHD waves modes.

If the perturbation is considered to be incompressible, such that $\Delta = 0$ and $v_z = B_z = p_1 = \rho_1 = 0$, Eq. (1.47) readily reduces to

$$\frac{\partial^2 \mathbf{v}_1}{\partial t^2} = v_A^2 \frac{\partial^2 \mathbf{v}_1}{\partial z^2}, \tag{1.52}$$

which describes Alfvén waves traveling along magnetic field lines. Alfvén waves are driven by the magnetic field line tension, shown by the decomposition of the Lorentz force in Eq. (1.17), and can be thought of as similar to transverse waves traveling along a taught string. Fourier analysing Eq. (1.52) by means of Eq. (1.36) results in the dispersion relation

$$\omega^2 = v_A^2 k_z^2 = v_A^2 k^2 \cos^2 \theta_B, \tag{1.53}$$

where k_z is the z-component of the wavenumber vector, k is given by $k = (k_x + k_y + k_z)^{1/2}$, and

θ_B is the angle between the wavenumber vector and the magnetic field. Thus $\theta_B = 0$ denotes propagation along the magnetic field lines and for $\theta_B = \pi/2$ we find $\omega = 0$ showing Alfvén waves are unable to propagate across the field lines. The group velocity of Alfvén waves is given by $\mathbf{c}_g = \pm v_A \hat{\mathbf{z}}$ showing that energy is transferred only along the field lines at the Alfvén speed regardless of the direction of propagation.

Fourier analysing Eq. (1.50) using $\Delta(\mathbf{r},t) = \Delta(0)e^{i(\mathbf{k}\cdot\mathbf{r}-\omega t)}$ yields the dispersion relation

$$\omega^4 - (c_0^2 + v_A^2)k^2\omega^2 + c_0^2 v_A^2 k^4 \cos^2\theta_B = 0. \tag{1.54}$$

Solving this quadratic equation in ω^2 yields two distinct solutions given by

$$\omega^2 = \frac{k^2}{2}\left[(c_0^2 + v_A^2) \pm \sqrt{(c_0^2 + v_A^2)^2 - 4c_0^2 v_A^2 \cos^2\theta_B}\right], \tag{1.55}$$

where the positive sign corresponds to the so-called fast magnetoacoustic mode and the negative sign corresponds to the slow magnetoacoustic mode. The modes are dependent on the Alfvén speed and the sound speed. The two modes are driven by both magnetic tension and pressure (magnetic and kinetic) forces. When the magnetic field vanishes, i.e. $v_A^2 = 0$, it can bee seen that the slow wave is non-existent and the fast wave is a pure acoustic wave. For the case of $c_0^2 = 0$ (called the cold plasma approximation) the slow mode again disappears and the fast wave becomes a compressional Alfvén wave. We may rewrite Eq. (1.55) as

$$\omega^2 = \frac{k^2}{2}(c_0^2 + v_A^2)\left[1 \pm \sqrt{1 - \frac{4c_T^2\cos^2\theta_B}{c_0^2 + v_A^2}}\right], \tag{1.56}$$

where

$$c_T = \frac{c_0 v_A}{\sqrt{c_0^2 + v_A^2}}, \tag{1.57}$$

where c_T is the known as the cusp or tube speed, being less than both the sound and the Alfvén speeds. The behaviour of the three modes can be seen in Fig. 1.4 in which we plot a polar diagram of the phase speed ($c_{ph} = \omega/k$) and the angle of propagation. Fig. 1.4a is plotted with the ordering of the speeds given by $c_T < c_0 < v_A < c_F$, where $c_F = (c_0^2 + v_A^2)^{1/2}$ is known as the fast speed and is the highest of the MHD speeds. It can be seen that the fast mode is practically isotropic in that it may propagate at all angles to the magnetic field, being fastest perpendicular to the field, with $c_{ph} = c_F$ in this case, and slowest parallel to the field, with $c_{ph} = v_A$. The Alfvén wave and the slow wave are field guided, in that they cannot propagate perpendicular to the field and have their maximum phase speed along the field. Fig. (1.4b) shows the alternative case where the ordering of the speeds is given by $c_T < v_A < c_0 < c_F$. The behaviour of the magnetoacoustic modes may be understood by considering the relationship between the kinetic and magnetic pressures. For the fast wave the kinetic and magnetic pressures are in phase with one another and thus the total pressure is greatest when the angle of propagation reaches $\pi/2$. For the slow mode, the two pressures are out of phase, such that the total pressure perturbation falls zero as the propagation angle is $\pi/2$. Thus the slow waves carry energy mainly along the field lines whereas fast waves may propagate in all directions.

This section has dealt with MHD wave propagation in a uniform environment and is extensively covered in many textbooks and reviews; see, for example, the textbooks Priest (1982), Roberts (1991), Aschwanden (2006) and Nakariakov & Verwichte (2005), Erdélyi (2007), Erdélyi & Ballai (2007), Banerjee *et al.* (2007) for the latest reviews. While this is a useful starting point,

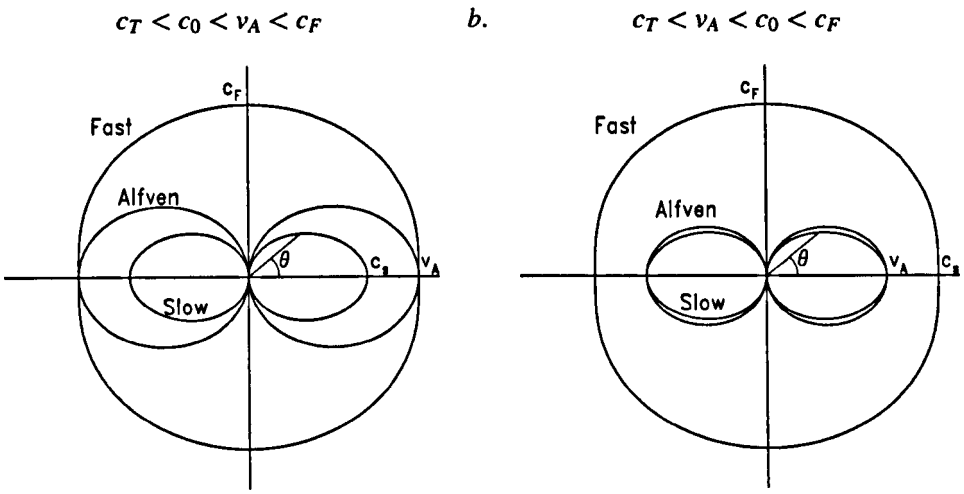

Figure 1.4: Polar plot showing the phase speed, c_{ph} of the two magnetoacoustic modes and the Alfvén wave at the angle to the magnetic field. a) $c_T < c_0 < v_A < c_F$, b) $c_T < v_A < c_0 < c_F$

readily highlighting the fundamental modes, such a uniform environment is rarely met in solar applications. The following chapters study wave propagation in structured, non-uniform and non-ideal environments which better model solar phenomena.

1.4 MHD waves in structured atmospheres

Since the three MHD modes met in the previous chapter are highly dependent on the angle of propagation to the magnetic field, it is clear that magnetic structuring will strongly affect these MHD modes. The fundamental theoretical building block to model the complex oscillatory nature of the solar atmosphere is the magnetic cylinder. Propagation of MHD waves in a magnetic cylinder embedded in a magnetic atmosphere was studied comprehensively by Edwin & Roberts (1983). They considered a straight flux tube with magnetic field $B_0\hat{\mathbf{z}}$ and radius a, filled with a uniform plasma of pressure p_0 and density ρ_0 embedded in a magnetic environment, $B_e\hat{\mathbf{z}}$, in the absence of gravity. The equilibrium condition of pressure balance is given by

$$p_0 + \frac{B_0^2}{2\mu_0} = p_0 + \frac{B_e^2}{2\mu_e}, \tag{1.58}$$

where the subscript e refers to the environment. The internal and external sound speeds, c_0 and c_e, Alfvén speeds, v_{A0} and c_{Ae} and tube speeds, c_{T0} and c_{Te}, may be defined. Considering perturbations of the form $R(r)\exp[i(\omega t + \theta n - k_z z)]$ for frequency, ω, azimuthal number, $n = 0, 1, 2...$, and wavenumber (longitudinal), k_z, the magnetoacoustic wave modes may be shown to be governed by the Bessel equation

$$\frac{d^2R}{dr^2} + \frac{1}{r}\frac{dR}{dr} - \left(m_0^2 + \frac{n^2}{r^2}\right)R = 0, \tag{1.59}$$

where

$$m_0^2 = \frac{(k_z^2 c_0^2 - \omega^2)(k_z^2 v_{A0}^2 - \omega^2)}{(c_0^2 + v_{A0}^2)(k_z^2 c_{T0}^2 - \omega^2)}. \tag{1.60}$$

In the external environment a corresponding term, m_e^2, may similarly be defined. Inside the tube ($r < a$) the solution to Eq. (1.59) is given by

$$R(r) = \begin{cases} A_0 I_n(m_0 r), & m_0^2 > 0, \\ A_0 J_n(n_0 r), & n_0^2 = -m_0^2 > 0, \end{cases}$$

where I_n and J_n are Bessel functions of order n. For the region external to the tube it is necessary to take $m_e^2 > 0$, corresponding to confined solutions i.e. evanescent radial perturbations. The solution for $r > a$ is thus

$$R(r) = A_1 K_n(m_e r). \tag{1.61}$$

Considering continuity of perturbation across the tube boundary, Edwin & Roberts (1983) found the following dispersion relations

$$\rho_0(k_z^2 v_{A0}^2 - \omega^2) m_e \frac{K_n'(m_e a)}{K_n(m_e a)} = \rho_e(k_z^2 v_{Ae}^2 - \omega^2) m_0 \frac{I_n'(m_0 a)}{I_n(m_0 a)}, \tag{1.62}$$

for surface waves ($m_0^2 > 0$) and

$$\rho_0(k_z^2 v_{A0}^2 - \omega^2) m_e \frac{K_n'(m_e a)}{K_n(m_e a)} = \rho_e(k_z^2 v_{Ae}^2 - \omega^2) n_0 \frac{J_n'(m_0 a)}{J_n(m_0 a)}, \tag{1.63}$$

for body modes ($n_0^2 > 0$). Body modes have an oscillatory nature inside the tube and are evanescent outside the tube. Surface modes are evanescent both inside and out and exist as a consequence of the surface. The azimuthal number, n, describes the shape of the tube; $n = 0$ yields symmetrical pulsations where the central axis of the tube is undisturbed, these are known as sausage modes, $n = 1$ corresponds to antisymmetric pulsations such that the tube supports lateral displacements and the axis of the tube is snake-like, these are known as kink modes, and finally $n \geq 2$ gives the so-called fluting modes which effectively ripple the tube's boundary. A dispersion diagram for a typical coronal loop is shown in Fig. (1.5). The ordering of of speeds is $v_{Ae} > c_k > v_A > c_0 > c_{T0} > c_{e0} > c_{T0}$ and under these conditions Fig. (1.5) shows all the possible modes are body modes, there are no surface modes. The phase speeds of the modes fall into two distinct bands called the fast waves and the slows waves, in an analogous manner to waves propagating in a uniform atmosphere. The fast modes are strongly dispersive and exist only if $v_{Ae} > v_A$, otherwise they disappear. At longer wavelengths there is a cut-off for the sausage modes such that trapped sausage modes do not exist. In the long wavelength limit the kink and fluting modes tend to c_k, the so-called kink speed, defined by

$$c_k = \sqrt{\frac{\rho_0 v_{A0}^2 + \rho_e v_{Ae}^2}{\rho_0 + \rho_e}}, \tag{1.64}$$

being a average, density weighted, Alfvén speed. The slow modes exist in a band between c_{T0} and c_0 and are only weakly dispersive. If there is a strong internal magnetic field the tube speed and the sound speed are approximately equal and the tube provides a one dimensional waveguide for the propagation of sound waves. A more detailed discussion of MHD modes found in a magnetic cylinder may be found in e.g Edwin & Roberts (1983), Roberts (2000), Nakariakov & Verwichte (2005) and more recently in Erdélyi (2007).

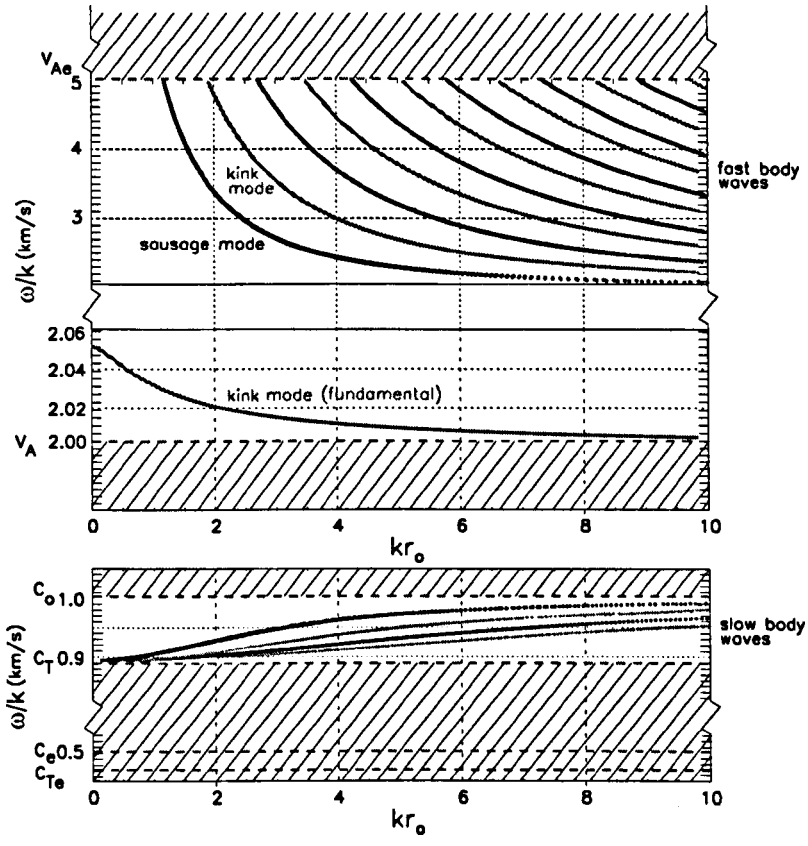

Figure 1.5: Dispersion diagram for magnetic cylinder plotted for typical coronal conditions. (Image credit: Viktor Fedun).

1.4.1 Overview of atmospheric wave observations

Perhaps the most well known evidence for fast kink modes in the solar corona results from studies into a flare generated event on the 14th July 1998 (Aschwanden *et al.*, 1999; Nakariakov *et al.*, 1999). The oscillations were found to be harmonic with a period in the order of 250 s with rapid damping and have been interpreted as a global standing kink mode of the loop. Using an estimate of the total loop length along with the observed period, the phase speed may be estimated and was found to be around 1000 km s^{-1}. This led Nakariakov & Ofman (2001) to estimate the magnetic field strength inside a typical coronal loop to be 13 $\pm$9 G. The magnetic field is a parameter that is not readily detectable by direct or indirect methods. Thus the estimate by Nakariakov & Ofman (2001) marks the first application, based on direct observation of the kink mode, of the technique of coronal seismology. The technique, in which the use of observed wave characteristic allows the determination of otherwise unknown coronal parameters, was given a sound theoretical footing and first applied to the corona by Roberts *et al.* (1984). In contrast, propagating fast waves are much harder to observe. The time resolution of the TRACE (Transition Region and Coronal Explorer, a high cadence telescope) is around 20-30 s, corresponding to a minimum observable period of 2-3 min. Thus for coronal conditions this means observable wavelengths are of the order of the loop length, and such loop guided fast waves will not be observed. However using the ground based and extremely high cadence SECIS instrument, Williams et al. (2001, 2002) observe coronal loops on the solar limb supporting rapidly propagating compressible wave trains. The speed was observed to be in the order of 2100 km s^{-1} and thus interpreted as a fast MHD mode. The exact nature of the mode, whether it be kink or sausage, could not be determined due to uncertainties in the measurement of the amplitude.

Observations of slow modes, since the launch of SOHO (the Solar and Heliospheric Observatory) and TRACE, are abundant. Such modes are longitudinal, with perturbations in density observable by variations in EUV (extreme ultra-violet) emission and disturbances in velocity by periodic Doppler shifts. Using SUMER (a spectral instrument aboard SOHO) Kliem *et al.* (2002), Wang *et al.* (2002, 2003a,b) reported intensity oscillations and Doppler shifts in coronal emission lines. These oscillations were interpreted in terms of the global standing acoustic mode by Ofman & Wang (2002) and have been modelled by Taroyan *et al.* (2007). Evidence for propagating slow modes is extensive. The standard approach is the so-called stroboscopic method in which the emission intensities form a time-distance map. Thus periods, relative amplitudes and propagation speeds are readily determined. The observed speeds are much lower than inferred coronal Alfvén speeds and coupled with the fact that they are seen to propagate along coronal structures, and hence the magnetic field, has led to their interpretation as slow magnetoacoustic waves. The first detection of longitudinal waves came from analysing brightness fluctuations (Ofman *et al.*, 1997). DeForest & Gurman (1998) found propagating intensity perturbations at distances of 1.01-1.2 $R_{\odot}$, with periods of around 10-15 min and projected speeds of 75-150 kms^{-1}. Similar observations were made near the footpoints of coronal loops using the EIT (Extreme ultra-violet Imaging Telescope aboard SOHO) (Berghmans & Clette, 1999) and TRACE (Nightingale *et al.*, 1999; De Moortel *et al.*, 2000, 2002a,b) instruments. Waves were seen to propagate along the loops towards the loop apex at speeds lower than the sound speed. An extensive review of propagating longitudinal oscillation observations is given by De Moortel *et al.* (2002a), Nakariakov (2003) and Banerjee *et al.* (2007). Projected propagation speeds are in the range 35-165 kms^{-1} with amplitudes $<$10% in intensity (corresponding to 5 % in density). Disturbances are observed mainly to be outwardly propagating, such that propagation is from loop footpoint to loop apex. Disturbances with 3 min periods have been associated with loops with footpoints in sunspot groups, whereas longer 5

min periods are linked with loops with footpoints not in sunspot groups (De Moortel *et al.*, 2002c). However this remains somewhat unclear since King *et al.* (2003) reported both 3 and 5 min oscillations in the same coronal structure. The properties presented above, the propagation directions and speeds along with the fact that the waves are compressive has led to their interpretation as slow magnetoacoustic waves. Further, 3 min oscillations have been observed in sunspot umbra (Bogdan, 2000) and have been interpreted in terms of slow waves.

The dominant oscillations of the solar photosphere are at 5 min, being the superposition of myriad global resonant oscillation modes. These are predominantly acoustic modes (although their propagation is modified by gravity, the internal stratification, the magnetic field and by bulk flows) trapped inside the Sun, and are hence sometimes termed cavity-modes. At the chromospheric level, however, the observed oscillations are of somewhat different nature and origin. Lites *et al.* (1993) observed oscillations of different periods in the chromospheric network and internetwork. Periods of $\sim$ 5-20 min were observed in network regions whereas they found oscillations of shorter periods of $\sim$3 min in internetwork regions. McAteer *et al.* (2004) reported similar oscillations using TRACE. De Pontieu (2003a,b) reported oscillations of the so-called moss, the bright upper TR emission above active region plage. They found periods of 200 to 600 s and showed some correlation with *p*-modes in the photosphere. They also found moss oscillations are strongly associated with periodic flows in spicules. Oscillations in regions of the chromosphere and TR associated with sunspot umbra are well established and are connected to *p*-modes. It is proposed that *p*-modes undergo mode conversion into slow magnetoacoustic waves in regions where the magnetic field is strong. Marsh & Walsh (2006) presented observations of the propagation of such slow magnetoacoustic *p*-modes, along the magnetic field, through the TR and into the corona. Curdt & Heinzel (1998) found intensity oscillations in hydrogen Lyman lines. In cell interiors they detected significant periodic intensity variations with peak power at 3.3-3.5 min, being consistent with the 3 min internetwork oscillations. In the network they detected oscillations of around 7 min. These observed oscillations and in particular the 3 min internetwork oscillations have been the subject of extensive analytical work. Since the oscillations are observed at chromospheric heights, with the photosphere acting as a likely wave source, the effect of gravity becomes important. Wave propagation in atmospheres stratified by gravity typically gives rise to the Klein-Gordon (KG) equation, see e.g. Roberts (2004).

1.5 The Klein-Gordon Equation

The Klein-Gordon equation is perhaps most widely encountered in the field of quantum physics, where it holds for spinless particles and is the relativistic version of the Schrödinger equation. In the context of wave propagation, however, the KG equation describes waves propagating in a gravitationally stratified environment. The 1-D homogeneous KG equation is given by (e.g. Rae & Roberts, 1982; Sutmann *et al.*, 1998)

$$\frac{\partial^2 Q}{\partial t^2} - c^2 \frac{\partial^2 Q}{\partial z^2} + \Omega^2 Q = 0, \tag{1.65}$$

where Q is the physical quantity in question (e.g. density, velocity etc.), often reduced by an exponential term, z is the spatial direction, in this Thesis the coordinate parallel to the gravitational vector, c is the propagation speed and Ω represents the cutoff frequency of the medium, which is related to the magnitude of the gravitational acceleration vector.

The effect of gravitational stratification is perhaps most simply shown for the case of sound

waves propagating vertically in an isothermal field free environment. Lamb (1908, 1932) pioneered the study of such waves and found their propagation is affected by pressure and temperature gradients. Lamb introduced the acoustic cut-off frequency, defined as

$$\Omega_A = \frac{c_0}{2H}, \tag{1.66}$$

where H is the pressure scale height. Ω_A is the natural frequency of the atmosphere, such that any wave source will trigger an atmospheric response at this frequency. Lamb was also the first to note that waves with frequency less than Ω_A will always be evanescent, i.e. the waves are unable to transmit appreciable energy to higher atmospheric layers. The theory governing these waves shows that the propagation of, say, a pulse will leave an oscillating wake. Fleck & Schmitz (1991) were the first to suggest that the observed 3 min modes in the chromosphere may be the atmospheric response at its natural frequency, Ω_A, to propagating acoustic waves. Sutmann *et al.* (1998) extended this idea and formulated a general method for determining acoustic wave propagation in a semi-bounded isothermal atmosphere. More specifically they solved the governing homogenous KG equation with inhomogeneous boundary conditions chosen to represent the introduction of a wave source at the lower boundary of the semi-infinite atmosphere.

The magnetic field in solar and stellar atmospheres tends not to be diffuse but, instead, to concentrate in magnetic flux tubes or magnetic loops. In these tubes the magnetic field can be, as a first approximation, considered to be axial. Such structures are a perfect medium for MHD wave propagation, playing the role of waveguides. There is clear observational evidence that strong, isolated and vertical magnetic fields, in other words magnetic flux tubes, can exist other than in sunspot structures and in particular at the boundaries of supergranulation cells (e.g. Solanki, 1993) and give rise to the chromospheric emission network of the quiet Sun. Such magnetic flux tubes act as windows providing a direct link between the photosphere and chromosphere. Thus large amplitude chromospheric disturbances may be expected if there exists a dynamic coupling to the photosphere, since energy densities are much larger than in the rarified atmosphere above. In general magnetic flux tubes allow the propagation of longitudinal, transverse and torsional MHD waves. The KG equation for longitudinal MHD waves (often termed tubes waves and denoted by subscript T) was first derived by Rae & Roberts (1982) and independently by Musielak *et al.* (1989) who studied the efficiency of generation of longitudinal tube waves. Rae & Roberts (1982) use the linearised slender magnetic flux tube equations (Roberts & Webb (1978), discussed further in Chapter 2), which allows a complete analytical description, and studied the pulse propagation in the tube. For an unstratified magnetic tube (e.g. Defouw, 1976; Roberts & Webb, 1978) the propagation of symmetric pulses is at the slow tube speed, c_T, and yields the dispersion relation $\omega^2 = k^2 c_T^2$. Propagation is non-dispersive ($c_{ph} = c_g = \pm c_T$), thus an initial compression will have a wavefront that travels at c_T and will leave an undisturbed atmosphere behind it. Propagation in a stratified tube (e.g. Roberts, 2004, 2006), such that disturbances are governed by Eq. (1.65), yields the dispersion relation $\omega^2 = k^2 c_T^2 + \Omega_T^2$, after employing a normal mode analysis ($Q \sim e^{i(\omega t - kz)}$). Propagation is now dispersive. Longer wavelengths (smaller k) will have a faster c_{ph} given by

$$c_{ph} = \pm\sqrt{c_T^2 + \frac{\Omega_T^2}{k^2}}, \tag{1.67}$$

but a slower c_g given by

$$c_g = \frac{\pm k c_T^2}{\sqrt{k^2 c_T^2 + \Omega_T^2}}. \tag{1.68}$$

The maximum c_g is c_T, when $k \to \infty$. Thus the effect of stratification is to increase the propagation speed of an individual mode above c_T but the wavefront for the initial disturbance moves at max $c_g = c_T$. By analogy with the acoustic case, the slender magnetic flux tube with an initial compression results in a disturbance that propagates along the tube at c_T (max c_g) with an oscillating wake behind at Ω_T. The atmosphere behind the wavefront is disturbed and remains in motion long after the pulse has passed. Musielak & Ulmschneider (2003a) also studied longitudinal wave propagation in a thin magnetic flux tube and developed solutions for various footpoint drivers. Transverse oscillations were considered in Musielak & Ulmschneider (2003b). The main results of these studies shall be examined later in the section but first the general properties and solutions of the KG equation are examined.

1.5.1 Properties and solutions of the Klein-Gordon equation

Probably the simplest non-trivial solution of the KG equation is the uniform wave train solution of the form $Q = A\cos k\theta$ where $\theta = z \pm c_{ph}t$, where c_{ph} is given by Eq. (1.67). The KG equation is a particular case of the so-called telegrapher's equation (see, e.g. Coulson, 1955). For any function $u(t,z)$ satisfying the telegrapher's equation

$$a\frac{\partial^2 u}{\partial t^2} + 2b\frac{\partial u}{\partial t} + cu = \frac{\partial^2 u}{\partial z^2}, \quad u = u(t,z), \tag{1.69}$$

with $a > 0$, b and c constants, we can introduce the a new function $Q(t,z) = u(t,z)e^{(b/a)t}$, which transforms the telegrapher's equation into the KG equation

$$\frac{\partial^2 Q}{\partial t^2} - m^2\frac{\partial^2 Q}{\partial z^2} + n^2 Q = 0, \tag{1.70}$$

where

$$m^2 = \frac{1}{a}, \quad n^2 = \frac{ac - b^2}{a^2}. \tag{1.71}$$

It can be shown that the KG equation can be reduced to a Bessel equation of order zero. Let us introduce the new independent variables

$$\xi = \frac{n}{m}(mt + z), \quad \zeta = \frac{n}{m}(mt - z), \tag{1.72}$$

Eq. (1.70) can be reduced to the canonical form

$$\frac{\partial^2 Q}{\partial \xi \partial \zeta} + \frac{Q}{4} = 0, \tag{1.73}$$

which is a linear hyperbolic differential equation. Introducing the new variable

$$w = (\xi - \xi_0)(\zeta - \zeta_0), \tag{1.74}$$

then the differential equation transforms into an ordinary differential equation

$$w\frac{d^2 Q}{dw^2} + \frac{dQ}{dw} + \frac{1}{4}Q = 0. \tag{1.75}$$

Changing the variable $w = \alpha^2$, we obtain

$$\frac{d^2Q}{d\alpha^2} + \frac{1}{\alpha}\frac{dQ}{d\alpha} + Q = 0, \tag{1.76}$$

which is a Bessel equation of order zero with solutions in form of $AJ_0(\alpha) + BY_0(\alpha)$, where J_0 and Y_0 are the zero-th order Bessel functions of first and second kind respectively, and A and B are constants. The solution can be further simplified by neglecting the solution containing $Y_0(\alpha)$ since it is divergent at zero. Therefore, the solution of the differential equation, Eq. (1.70), is

$$Q = AJ_0\left(\sqrt{(\xi - \xi_0)(\zeta - \zeta_0)}\right), \tag{1.77}$$

The solution of the KG equation in form of Bessel functions will be used throughout further derivations. Returning to the original variables used in Eq. (1.65) yields

$$Q = AJ_0\left(\frac{\Omega}{c}\sqrt{c^2(t - t_0)^2 - (z - z_0)^2}\right). \tag{1.78}$$

This result has been obtained without considering any initial and/or boundary conditions, other than the condition that the solution is convergent at zero. Nevertheless this solution serves as an initial guess of the form of the final solution. In order to find the value of A, initial and/or boundary conditions have to be taken into account.
Depending on the type of the initial condition (spatial or temporal) the form of the solution will differ. Let us first suppose that the KG equation is subject to the conditions

$$Q\,|_{t=0} = f(z), \quad \left.\frac{\partial Q}{\partial t}\right|_{t=0} = g(z), \quad -\infty < z < \infty, \tag{1.79}$$

supplemented by the requirement that at $\pm\infty$ the function $Q(t,z)$ vanishes (boundary condition). Initially the tube is set to motion with the shape $f(z)$ and is also accelerating with the given shape $g(z)$. Using a Laplace transform, the KG equation can be reduced to an ordinary differential equation of the form

$$\frac{d^2\Psi(s,z)}{dz^2} - q^2\Psi(s,z) = -s\frac{f(z)}{c^2} - \frac{g(z)}{c^2}, \tag{1.80}$$

where

$$\Psi(s,z) = \int_0^\infty Q(t,z)e^{-st}dt, \quad q^2 = \frac{s^2 + \Omega^2}{c^2} \tag{1.81}$$

with the solution

$$\Psi(s,z) = \frac{1}{2c^2q}\left[\int_{-\infty}^{z} e^{-q(z-\eta)}\left[sf(\eta) + g(\eta)\right]d\eta + \int_z^\infty e^{-q(\eta-z)}\left[sf(\eta) + g(\eta)\right]d\eta\right]. \tag{1.82}$$

In order to obtain a solution for the KG equation, Eq. (1.65), we have to invert Eq. (1.82) using an inverse Laplace transform (Bromwich integral) in the form

$$Q(t,z) = \frac{1}{2\pi i}\int_{\gamma-i\infty}^{\gamma+i\infty} e^{st}\Psi(s,z)ds, \tag{1.83}$$

where γ is chosen such that all singular points of $\Psi(s,z)$ lie on the left of the line $\Re(s) = \gamma$

in the complex s-plane. Calculating the inverse Laplace transform of Eq. (1.82) we obtain the solution of the Klein-Gordon equation

$$Q(t,z) = \frac{1}{2}[f(z-ct)+f(z+ct)] + \tag{1.84}$$
$$+\frac{1}{2c}\int_{z-ct}^{z+ct}\left[g(\eta)J_0\left(\frac{\Omega}{c}\sqrt{c^2t^2-(z-\eta)^2}\right) - f(\eta)\frac{\Omega ctJ_1\left(\frac{\Omega}{c}\sqrt{c^2t^2-(z-\eta)^2}\right)}{\sqrt{c^2t^2-(z-\eta)^2}}\right].$$

This solution can be interpreted as follows; there are two propagating waves each half of the original displacement moving in opposite directions, followed by an oscillating tail with decaying amplitude. In obtaining Eq. (1.84) we have used the properties of the Laplace transform (Erdélyi *et al.*, 1954)

$$\mathcal{L}\left[cJ_0\left(\frac{\Omega}{c}\sqrt{c^2t^2-z^2}\right)\mathcal{H}\left(t-\frac{z}{c}\right)\right] = \frac{e^{-qz}}{q}, \quad z>0, \tag{1.85}$$

$$\mathcal{L}\left[c\delta\left(t-\frac{z}{c}\right) - \frac{c\Omega tJ_1\left(\Omega\sqrt{t^2-\frac{z^2}{c^2}}\right)}{\sqrt{t^2-\frac{z^2}{c^2}}}\mathcal{H}\left(t-\frac{z}{c}\right)\right] = \frac{se^{-qz}}{q}, \quad z>0, \tag{1.86}$$

where $\delta(z)$ and $\mathcal{H}(z)$ are the Dirac-delta and Heaviside functions, respectively.
The nature of the solution is changed when we suppose an initial condition such as

$$Q|_{t=0}=0, \quad \left.\frac{\partial Q}{\partial t}\right|_{t=0}=0, \quad Q|_{z=0}=A_0(t), \quad 0<z<\infty. \tag{1.87}$$

These initial conditions suggest that the entire tube is at rest at $t=0$ and no part is accelerating, however, the footpoint of the tube ($z=0$) is driven by a velocity perturbation $A_0(t)$. In this case, the solution of the KG equation is (Sutmann *et al.*, 1998)

$$Q(t,z) = A_0\left(t-\frac{z}{c}\right)\mathcal{H}\left(t-\frac{z}{c}\right) + \int_0^t A_0(t-\tau)W(\tau,z)d\tau, \tag{1.88}$$

where

$$W(\tau,z) = -\frac{\Omega zJ_1\left(\Omega\sqrt{\tau^2-\left(\frac{z}{c}\right)^2}\right)}{\sqrt{c^2\tau^2-z^2}}\mathcal{H}\left(\tau-\frac{z}{c}\right). \tag{1.89}$$

1.5.2 Summary of wave propagation characteristics for temporal boundary conditions

In this section we summarise the main results of the analytical studies given in e.g. Sutmann *et al.* (1998) and Musielak & Ulmschneider (2003a,b), since they form the starting point for much of the following work. Sutmann *et al.* (1998) studied acoustic wave propagation in a semi-bounded isothermal atmosphere with various drivers at the lower boundary. The system is governed by the KG equation where the terms c and Ω given in Eq. (1.65) are replaced with c_0 and Ω_A respectively, being the sound speed and the acoustic cutoff. They considered a piston like driver, a delta function pulse, a sinusoidal pulse and a wavetrain of random pulses. In general two classifications of oscillations are found. The so-called forced atmospheric oscilla-

tions exist when the driver is continuous and thus are driven at the driving frequency, ω. Their behaviour is well known and represent propagating acoustic waves for $\omega > \Omega_A$ and evanescent acoustic waves for $\omega < \Omega_A$. The free atmospheric oscillations are always present regardless of the form of the driver. They decay in time with $t^{-3/2}$, have a linear increase in amplitude with height and crucially are at the acoustic cutoff frequency, Ω_A. Sutmann *et al.* (1998) found that a wavetrain of random pulses may sustain the free atmospheric oscillations despite their temporal decay since they are driven in a continuous manner by the source. For photospheric conditions the corresponding period of the free atmospheric oscillations , $P_A (= 2\pi/\Omega_A)$, is approximately 3 min, hence providing a plausible explanation for the 3 min oscillations seen in the internetwork of the chromosphere.

Musielak & Ulmschneider (2003a) study wave propagation in a thin vertical magnetic flux tube embedded in a field free environment. Given conditions of pressure balance and flux conservation it is seen that the tube has an expanding geometry. The spreading tube model is perhaps not ideal for the crowded network region, since neighbouring tubes will run into one another yielding questionable results at appreciable heights. The model holds however for regions in which there is enough room to cope with the expansion as well as internetwork regions. It is interesting to note that the equation governing the propagation of longitudinal tube waves is of the same form as that for acoustic waves, i.e. the KG equation, except that one has c_T and Ω_T rather than their acoustic counterparts, being the tube speed and cutoff frequency for longitudinal tube waves. Thus it is clear that the solutions developed in Sutmann *et al.* (1998) hold, albeit with the concomitant changes. Applying the model to the Sun, Musielak & Ulmschneider (2003a) find that $P_T \approx 3$ min and is relatively insensitive to changes in the magnetic field strength. Thus the tube oscillations and those in an external field free environment would be practically indistinguishable. The free atmospheric oscillations at Ω_T may be sustained by a wavetrain of random pulses and thus the observed 3 min oscillations may be equally explained by processes either inside or outside a magnetic flux tube. They point out that is unwise to conclude that there may be no flux tube present in the internetwork merely from the lack of a network bright point, since the expanding tube is poorly heated (Fawzy *et al.*, 1998). They also conclude that the observed 7 min oscillations (e.g. Curdt & Heinzel, 1998) must be of a different origin.

Musielak & Ulmschneider (2003b) studied transverse tube waves in a slender vertical magnetic flux tube. It is found that the system is once again governed by the KG equation, in this case with the appropriate speed, c_k, and kink cutoff frequency, Ω_k. Thus the discussion above concerning the acoustic and longitudinal cases holds, such that free atmospheric oscillations will always be excited at Ω_k regardless of the driver. For conditions relevant to the photosphere the period of the free atmospheric oscillations , P_k, is between 7-10 min, depending on the strength of the magnetic field. Thus at first sight appear to be a candidate for the observed oscillations in the chromospheric network. However, as Musielak & Ulmschneider (2003b) point out, they contribute no Doppler signal and hence are not visible at disk center. Hasan & Kalkofen (1999) suggest that they may be detected after transformation into longitudinal waves that have corresponding periods and thus have the required Doppler signal. Musielak & Ulmschneider (2003b) refute this assumption and show that any generated longitudinal waves would have periods of P_T rather than P_k. Thus the cause of the 7 min network oscillations remains unclear.

This Thesis is concerned with the addition of realistic solar features such as bulk flows and non-ideal effects into the slender solar flux tube model.

1.6 Outline of thesis

Chapter 1 has introduced the basic properties of the Sun, highlighted the important aspects of the MHD approach and given a brief summary of the current state of our observational knowledge of waves in the solar atmosphere. The primary focus of this Thesis is the study of wave propagation in atmospheres that are stratified by gravity. With that in mind, Chapter 1 finished with an introduction to the previous studies of waves in such atmospheres and demonstrated the ubiquity of the Klein-Gordon equation which governs their behaviour, along with the important concept of the cutoff frequency.

The aim of Chapter 2 is to study the effect of the inclusion of a steady background flow in the thin magnetic flux tube model and to examine the effect on longitudinal (slow) wave propagation. Linear waves are considered and the governing equations are solved by means of Laplace transforms and perturbation methods, for boundary conditions modeling various forms of footpoint driver. The solutions are applied to the solar atmosphere using conditions appropriate for the photosphere.

Chapter 3 investigates the effect of background flow on transverse wave propagation in one-dimensional stratified waveguides. Governing equations are solved for various footpoint drivers and then applied to the Sun. The similarities and differences between longitudinal and transverse are highlighted.

Chapter 4 describes the effect of viscosity on longitudinal wave propagation in stratified waveguides. Equations governing the propagation of linear waves are derived and the effect of viscosity is shown. Solutions to the governing equations are derived for two limiting cases; the variation in Q, the scaled velocity parameter occurs over lengths scales much larger (smaller) than the scale height. In the first case the governing equation is solved for various footpoint drivers in terms of a modified cutoff frequency. In the second case a solution is derived by means of the Bromwich integral. Various applications to the Sun are finally discussed.

Chapter 5 presents a similar study but for the case of transverse tube waves propagating in a viscous medium. The analysis is carried out and the similarities and differences are highlighted.

Finally Chapter 6 summarises the most important conclusions and presents suggestions for future work.

2

Longitudinal wave propagation in steady stratified waveguides

In this Chapter the propagation of longitudinal magnetic tube waves in a stratified isothermal flux tube with the presence of an internal equilibrium background flow is studied. The governing differential equation is solved by means of Laplace transforms and temporal and spatial solutions are developed, with boundary conditions given by various footpoint drivers, namely a monochromatic source, a delta function pulse and a sinusoidal pulse. The effect of the background flow is to introduce an increase in amplitude of the wave perturbation and changes in phase shift when compared with the corresponding static case. Results are presented and are applied to conditions relevant to the solar atmosphere. When the source is driven continuously the forced atmospheric oscillations are shown to have large percentage differences over the corresponding static case. For the free atmospheric oscillations, percentage increases in amplitude merely of the order of a few percent are found and vary greatly in height but are practically unaltered in time. Phase shifts of up to a radian are introduced and weakly depend on both height and time. The results presented in this paper may have interesting observational consequences especially using the tools of magnetic seismology of solar atmospheric wave guides (i.e. flux tubes from photosphere to corona) in light of the present and near-future high spatial and temporal resolution space missions, e.g. Hinode, Solar Dynamics Observatory or Solar Orbiter.

2.1 Introduction

The solar atmosphere is extremely complex, being both highly structured and highly dynamic, supporting a vast array of wave and oscillatory phenomena. Theoretical descriptions of these waves and oscillations have been given fresh vigor in recent years through the detailed observational studies made with the high resolution SOHO and TRACE satellites, e.g Aschwanden (2006), Banerjee *et al.* (2007), Nakariakov & Verwichte (2005) and references therein. A major question still to be addressed is the exact nature of the coupling between disturbances in the lower layers of the solar atmosphere and their manifestation as wave-like phenomena in higher layers (see e.g. the reviews Erdélyi, 2006; De Pontieu & Erdélyi, 2006). What is the connection between waves observed at coronal temperatures and waves in the chromosphere and transition region (TR), or even lower to the photosphere? How is this connection affected by the dynamic state of the flux tubes, e.g. flows from photosphere to TR? The concept of an intense flux tube provides an obvious tool to model the link between photospheric and chromospheric (or even higher) regions, in which the high energy densities associated with the dense photosphere can communicate directly to the considerably more tenuous chromosphere (plasma density in the order of 10^4 smaller) above. A recent study on intensity oscillations in the upper TR above active region plage suggests the potential role of photospheric drivers in so-called moss oscillations. De Pontieu (2003a,b) reported on strong ($\sim$ 5 - 15 %) intensity oscillations in the upper TR, with periods from 200s to 600s persisting typically for 4-7 cycles. They find a general correspondence between solar global acoustic p-modes and the upper TR oscillations. A model noting the link between photospheric drivers and TR oscillations is put forward by De Pontieu, Erdélyi & James (2004). The concept has been extended into the solar corona first by De Pontieu *et al.* (2005). Similar coupling was reported in sunspot regions, e.g. Marsh & Walsh (2006). The propagation of acoustic waves driven at the photosphere in a non-magnetic atmosphere has been recently numerically studied by Malins & Erdélyi (2007) and Erdélyi *et al.* (2007). Despite the proposed links, the exact relationship between the TR oscillations and the photospheric p-modes remains unclear. Moreover, many of the upper TR oscillations are associated with upper chromospheric oscillations seen in H_α, i.e. periodic flows in spicular structures. Aspects such as these provide the motivation to study the wave propagation in the lower solar atmosphere (where the effect of gravity is important, since the gravitational scale height is comparable to the characteristic scales of the medium) with the presence of flows.

The effect of steady state flows on MHD waves in a uniform magnetic slab-geometry was investigated by e.g. Nakariakov & Roberts (1995), Tirry *et al.* (1998), Joarder *et al.* (1997). They found the dispersion relation for such steady states and also have shown the presence of negative energy waves. Joarder *et al.* (2000), Somasundaram *et al.* (1999) and Narayanan (1991) generalised the slab studies to flux tubes but their derivation is valid only for limited applications and parameters. A detailed and comprehensive derivation of steady flow effects on uniform MHD waveguides in cylindrical geometry (with stratification due to gravity ignored) can be found in, e.g. Terra-Homem *et al.* (2003). They derived the dispersion relation for photospheric and coronal flux tubes, and determined the propagation windows that are Doppler shifted when compared to their static counterparts.
In this Chapter the focus is on the linear propagation of MHD waves in *stratified*, isothermal flux tubes with a *steady* background flow, and the derivation of the governing equations for linear waves. The governing equation for propagating waves is then solved subject to various photospheric drivers namely a monochromatic source, mimicking solar global oscillations, a delta-function type impulse and a wider range impulse. The theoretical description is provided within the framework of the slender flux tube approximation (e.g. Roberts & Webb, 1978).

The classic case of longitudinal wave propagation in a static tube stratified by gravity has been discussed in Section 1.5. It is the purpose of this chapter to investigate the effect of introducing a background flow to the magnetic flux tube.

2.1.1 Observational evidence of flows

Further to the points discussed above, many recent high-resolution imaging observational studies have indicated the existence of flows in the solar atmosphere, in particular in magnetic flux concentrations. The presence of a fast wind originating from the polar coronal holes has been long established (e.g., Watanabe, 1975; Gloeckner & Geiss, 1998). Recent SOHO and TRACE observations have shown the presence of steady flows in the south polar coronal hole and the equatorial quiet Sun-region (Buchlin & Hassler, 2000). The chromosphere also exhibits flows (often termed chromospheric down-flow) associated with thousands of small scale explosions (e.g., Innes *et al.*, 1997; Perez *et al.*, 1999; Teriaca *et al.*, 1999, etc.). Background flows have been noted in arched isolated magnetic flux tubes, steady flows have been observed in slender magnetic flux tubes and in return flows from spicules. Flows cause not just considerable observable Doppler shifts, but can also be responsible for complex dynamical interactions (e.g. flow instabilities, development of boundary layers etc.). These examples and the most recent high cadence and resolution movies released on the Hinode website show the clear need to investigate the effect of such flows on the wave characteristics in the solar atmosphere. In fact one of Hinode's major discoveries is the presence of a ubiquitous background flow in the solar atmosphere. Since resistivity is relatively diminishing, it may follow from induction equation that the flows follow the magnetic field lines, i.e. the field-aligned equilibrium flow concept is a reasonable initial approximation in modelling efforts.

2.2 Longitudinal wave propagation with steady background flow

This Chapter predominantly follows Erdélyi & Hargreaves (2008). To investigate wave propagation in a flux tube with a background flow, the so-called thin flux tube equations, e.g. Roberts & Webb (1978), shall be employed. A detailed derivation of the thin flux tube equations is given in Appendix A. An isolated elastic tube with a background flow, embedded in a field free, isothermal and hydrostatic environment is considered. The tube is considered to be thin, free from twists and with circular cross-section. The tube is aligned vertically, thus the z-axis is the tube axis and gravity acts such that $\mathbf{g} = -g\hat{\mathbf{z}}$. The system is assumed to be governed by the non-linear equations, Eq. (A-44) to Eq. (A-47), such that

$$\rho\left(\frac{\partial v_z}{\partial t} + v_z v_z'\right) + p' + \rho g = 0, \tag{2.1}$$

$$\frac{\partial}{\partial t}\left(\frac{\rho}{B_z}\right) + \left(\frac{\rho v_z}{B_z}\right)' = 0, \tag{2.2}$$

$$\frac{\partial p}{\partial t} + v_z p' - c^2\left(\frac{\partial \rho}{\partial t} + v_z \rho'\right) = 0, \tag{2.3}$$

$$p + \frac{B_z^2}{2\mu} = P_e, \tag{2.4}$$

where v_z, p, ρ, B_z and P_e are the vertical velocity (i.e along the tube axis), pressure, density, vertical component of magnetic field and the total external pressure, respectively, and the dashes denote derivatives with respect to z.

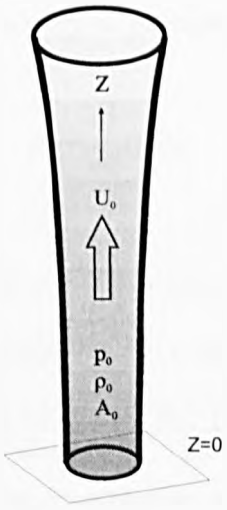

Figure 2.1: Equilibrium configuration of the thin magnetic flux tube. The equilibrium pressure, density and bulk flow are denoted by p_0, ρ_0 and U_0 respectively.

2.2.1 Equilibrium considerations

Consider the equilibrium configuration by letting $U_0(z)$, $B_0(z)$, $\rho_0(z)$ and $p_0(z)$ be the undisturbed quantities of bulk flow, magnetic field, density and pressure respectively, inside the flux tube and with $\partial/\partial t = 0$. The equilibrium configuration of the tube may be seen in Figure 2.1 and has previously been considered for isolated arched magnetic flux tubes by Thomas (1988). For a vertical flux tube the flux conservation equation, Eq. (2.2), may be written

$$\frac{\rho_0'}{\rho_0} + \frac{U_0'}{U_0} = \frac{B_0'}{B_0}, \tag{2.5}$$

and the momentum equation, Eq. (2.1), gives

$$U_0 U_0' = \frac{-p_0'}{\rho_0} - g, \tag{2.6}$$

which may be integrated directly to give Bernoulli's equation. Assuming the external atmosphere (denoted by subscript e) is hydrostatically stratified such that one has

$$p_e = \rho_e R T_e, \tag{2.7}$$

$$p_e' = -\rho_e g, \tag{2.8}$$

and one assumes T_e is constant, thus $p_e = p_e(0)e^{-z/H}$ and $\rho_e = \rho_e(0)e^{-z/H}$ with $H_e = RT_e/g = p_e/\rho_e g$ being the external pressure scale height. Suppose a very rapid radiative exchange between the internal and external atmosphere, such that the tube has the same temp as the external gas, i.e. $T_e = T_0$. Thus it is assumed that the bulk flow (but not it's perturbation) in the tube is isothermal such that $c_0^2 = RT_e \equiv \bar{c}^2$ where $\bar{c}$ is an isothermal sound speed. Using Eq. (2.5) and Eq. (2.6) to eliminate density one obtains

$$\frac{B_0'}{B_0} + \frac{U_0'}{U_0}\left(\frac{U_0^2}{\bar{c}^2} - 1\right) + \frac{g}{\bar{c}^2} = 0, \tag{2.9}$$

this (after Thomas, 1988) is a field-velocity-height relation. From the required condition of pressure balance one obtains

$$p_0 + \frac{B_0^2}{2\mu} = p_e, \tag{2.10}$$

and substituting into Eq. (2.6) gives

$$\rho_0 U_0 U_0' = \left(\frac{B_0^2}{2\mu}\right)' + g(\rho_e - \rho_0). \tag{2.11}$$

The magnetic field may be eliminated from Eq. (2.11) (by making use of Eq. (2.9)) to give

$$\left(1 - \frac{U_0^2}{\bar{c}_T^2}\right)\frac{U_0'}{U_0} = \left(1 - \frac{\rho_e - \rho_0}{\rho_0}\frac{\bar{c}^2}{v_A^2}\right)\frac{g}{\bar{c}^2}, \tag{2.12}$$

where $\bar{c}_T^2 = \bar{c}^2 v_A^2/(\bar{c}^2 + v_A^2)$. A relation describing the magnetic field expansion as a function of height may be formed by using Eq. (2.9) and Eq. (2.12) to eliminate the derivatives of the bulk flow, to give

$$\left(1 - \frac{U_0^2}{\bar{c}_T^2}\right)\frac{B_0'}{B_0} = \frac{-g}{v_A^2}\left(\frac{\rho_e - \rho_0}{\rho_0}\right)\left(1 - \frac{U_0^2}{c_1^2}\right), \tag{2.13}$$

where $c_1^2 = \bar{c}^2(\rho_e - \rho_0)/\rho_e$. Using the horizontal pressure balance one can see that

$$\frac{\rho_e - \rho_0}{\rho_0} = \frac{v_A^2}{2\bar{c}^2}, \quad c_1^2 = \frac{\bar{c}^2 v_A^2}{v_A^2 + 2\bar{c}^2}, \tag{2.14}$$

where $c_1^2 < \bar{c}_T^2 < \min(\bar{c}^2, v_A^2)$. Using Eq. (2.14) and Eq.(2.12) one obtains

$$\left(1 - \frac{U_0^2}{c_T^2}\right)\frac{U_0'}{U_0} = \frac{1}{2}\frac{g}{\bar{c}^2}, \tag{2.15}$$

and with Eq. (2.13) it is seen that

$$\left(1 - \frac{U_0^2}{c_T^2}\right)\frac{B_0'}{B_0} = -\left(1 - \frac{U_0^2}{c_1^2}\right)\frac{g}{2\bar{c}^2}. \tag{2.16}$$

In order to simplify the analysis and facilitate an analytical solution it is assumed that the flow to be small, i.e. $U_0^2 \ll c_1^2 < \bar{c}_T^2$ at all heights, meaning the flow is much smaller than the other characteristic speeds. Noting that $g/\bar{c}^2 = 1/H$, we find

$$\frac{U_0'}{U_0} = \frac{1}{2H}, \quad \frac{B_0'}{B_0} = \frac{-1}{2H}, \quad \frac{\rho_0'}{\rho_0} = \frac{-1}{H}. \tag{2.17}$$

Thus there is a flow profile that is exponentially increasing. This clearly indicates that caution needs to be exercised when applications are considered. The model considered here, with the tube expanding with height and bulk flow increasing in magnitude with height, represents well, for example, the footpoint region of a steeply rising arched flux tube or loop, or secondly a tube situated at the boundary of supergranulation cells where the tube has enough room to expand with height, or finally an tube located inside a cell. Clearly any results evaluated at considerable heights will have to be treated with care since in the extreme case of taking $z \to \infty$ one would have an infinite flow, a situation which is clearly unphysical. However considering the flow to be small in comparison to the other relevant speeds allows an analytical insight into the complicated flow problem.

2.2.2 Small perturbations about the steady equilibrium

Considering small amplitude perturbations about the equilibrium described above, one may find the linearised forms of Eq. (2.1) to Eq. (2.4) to be

$$\rho_0\frac{Du}{Dt}+\rho_0U_0'u+p'+(U_0U_0'+g)\rho=0, \tag{2.18}$$

$$B_0\frac{D\rho}{Dt}-\rho_0\frac{DB}{Dt}-U_0B_0\frac{\rho_0'}{\rho_0}\rho+U_0\rho_0\frac{B_0'}{B_0}B+\rho_0B_0\left(\frac{\rho_0'}{\rho_0}-\frac{B_0'}{B_0}+\frac{\partial}{\partial z}\right)u=0, \tag{2.19}$$

$$\frac{Dp}{Dt}+p_0'u-c_0^2\left(\frac{D\rho}{Dt}+\rho_0'u\right)+U_0\frac{\rho_0'}{\rho_0}(c_0^2\rho-\gamma p)=0, \tag{2.20}$$

$$p+\frac{B_0}{\mu}B=0, \tag{2.21}$$

where $D/Dt=\partial/\partial t+U_0\partial/\partial z$ is the material derivative, $c_0^2=\gamma p_0/\rho_0$ is the sound speed and where the un-subscripted quantities are the perturbed quantities and subscript 0 denote the equilibrium quantities. Note u is the perturbed velocity. The magnetic tube is linked to the environment by assuming the pressure perturbation in the environment is negligible, thus it is assumed that the tube is embedded in a quiescent environment, see Roberts & Webb (1978). After Musielak *et al.* (1989) the following variable changes are introduced

$$p_1=\frac{p}{\rho_0},\quad \rho_1=\frac{\rho}{\rho_0},\quad B_1=\frac{B}{B_0}, \tag{2.22}$$

and thus Eq. (2.18) to Eq. (2.21) may be recast into

$$\frac{Du}{Dt}+U_0'u+\left(\frac{\partial}{\partial z}+\frac{\rho_0'}{\rho_0}\right)p_1+(U_0U_0'+g)\rho_1=0, \tag{2.23}$$

$$\frac{D\rho_1}{Dt}-\frac{DB_1}{Dt}+\left(\frac{\rho_0'}{\rho_0}-\frac{B_0'}{B_0}+\frac{\partial}{\partial z}\right)u=0, \tag{2.24}$$

$$\frac{Dp_1}{Dt}-c_0^2\frac{D\rho_1}{Dt}+\left(\frac{p_0'}{\rho_0}-c_0^2\frac{\rho_0'}{\rho_0}\right)u+U_0\frac{\rho_0'}{\rho_0}(1-\gamma)p_1=0, \tag{2.25}$$

$$p_1+v_A^2B_1=0, \tag{2.26}$$

where c_0 and v_A are constants since the atmosphere is assumed to be isothermal. At this point it is necessary to take a limiting assumption in the nature of the bulk flow in order to make the problem tractable.

Assumptions for reduction

For the last term in Eq. (2.23) it can be noted that $U_0U_0'=U_0^2/2H$ and it shall be assumed that

$$\frac{U_0^2}{2H}\ll g, \tag{2.27}$$

for all z. This can be rewritten as

$$U_0^2\ll\frac{2c_0^2}{\gamma}, \tag{2.28}$$

for all z. This may justified given the earlier assumption that $U_0 \ll c_T^2$ for all z. In Eq. (2.25) one can rewrite the D/Dt term as $\partial/\partial t + U_0\partial/\partial z$. Comparing the z derivative term with the other pressure term in Eq. (2.25) and making the assumption that

$$U_0\frac{\partial p_1}{\partial z} \gg U_0\frac{\gamma-1}{H}p_1, \tag{2.29}$$

and if p_1 varies over some length scale L one may take

$$\frac{p_1}{L} \gg \frac{\gamma-1}{H}p_1, \tag{2.30}$$

i.e. $L \ll H$, corresponding to a short wavelength approximation in perturbed quantities. Using the same reasoning the second term in Eq. (2.23) may be neglected. Under these assumptions, substituting in the equilibrium relations, Eq. (2.17), and noting that $p_0'/\rho_0 - c_0^2\rho_0'/\rho_0 = g(\gamma-1)$, one may rewrite the governing equations as

$$\frac{Du}{Dt} + \left(\frac{\partial}{\partial z} - \frac{1}{H}\right)p_1 + g\rho_1 = 0, \tag{2.31}$$

$$\frac{D\rho_1}{Dt} - \frac{DB_1}{Dt} + \left(\frac{\partial}{\partial z} - \frac{1}{2H}\right)u = 0, \tag{2.32}$$

$$\frac{Dp_1}{Dt} - c_0^2\frac{D\rho_1}{Dt} + g(\gamma-1)u + \frac{U_0}{H}(\gamma-1)p_1 = 0. \tag{2.33}$$

$$\frac{Dp_1}{Dt} + v_A^2\frac{DB_1}{Dt} = 0. \tag{2.34}$$

The perturbed magnetic field and density may now be eliminated. Performing the procedure $[c_0^2/v_A^2 \times (2.34) + c_0^2 \times (2.32) + (2.33)]$ yields

$$\left(1 + \frac{c_0^2}{v_A^2}\right)\frac{Dp_1}{Dt} + c_0^2\left(\frac{\partial}{\partial z} - \frac{1}{2H}\right)u + g(\gamma-1)u = 0, \tag{2.35}$$

which may be recast to give the material derivative of the perturbed pressure

$$\frac{Dp_1}{Dt} = -\frac{c_T^2}{c_0^2}\left[c_0^2\left(\frac{\partial}{\partial z} - \frac{1}{2H}\right)u + g(\gamma-1)u\right]. \tag{2.36}$$

Now examining the full time derivative of Eq. (2.31), i.e. D(2.31)/Dt, one finds

$$\frac{D^2u}{Dt^2} + \frac{D}{Dt}\left(\frac{\partial}{\partial z} - \frac{1}{H}\right)p_1 + g\frac{D\rho_1}{Dt} = 0, \tag{2.37}$$

which is

$$\left(\frac{\partial^2 u}{\partial t^2} + 2U_0\frac{\partial^2 u}{\partial t\partial z} + U_0^2\frac{\partial^2 u}{\partial z^2} + \frac{U_0^2}{2H}\frac{\partial u}{\partial z}\right) + \frac{D}{Dt}\frac{\partial p_1}{\partial z} - \frac{1}{H}\frac{Dp_1}{Dt} + g\frac{D\rho_1}{Dt} = 0. \tag{2.38}$$

One sees that

$$\frac{D}{Dt}\frac{\partial p_1}{\partial z} = \frac{\partial^2 p_1}{\partial t\partial z} + U_0\frac{\partial^2 p_1}{\partial z^2}. \tag{2.39}$$

Also one may consider

$$\frac{\partial}{\partial z}\frac{Dp_1}{Dt} = \frac{\partial^2 p_1}{\partial t \partial z} + \frac{U_0}{2H}\frac{\partial p_1}{\partial z} + U_0\frac{\partial^2 p_1}{\partial z^2}. \tag{2.40}$$

Thus, since the assumption $L/H \ll 1$ has been made, it can be seen that

$$\frac{U_0}{2H}\frac{\partial p_1}{\partial z} \ll U_0\frac{\partial^2 p_1}{\partial z^2}, \tag{2.41}$$

then

$$\frac{D}{Dt}\frac{\partial p_1}{\partial z} \approx \frac{\partial}{\partial z}\frac{Dp_1}{Dt}. \tag{2.42}$$

If one makes these assumptions and adds the following $[-g/v_A^2 \times (2.34) - g \times (2.32)]$ one obtains

$$\left(\frac{\partial^2 u}{\partial t^2} + 2U_0\frac{\partial^2 u}{\partial t \partial z} + U_0^2\frac{\partial^2 u}{\partial z^2} + \frac{U_0^2}{2H}\frac{\partial u}{\partial z}\right) + \left(\frac{\partial}{\partial z} - \frac{1}{H} - \frac{g}{v_A^2}\right)\frac{Dp_1}{Dt} - g\left(\frac{\partial}{\partial z} - \frac{1}{2H}\right)u = 0. \tag{2.43}$$

Substituting Eq. (2.36) into Eq. (2.43) it is found that

$$\frac{\partial^2 u}{\partial t^2} + 2U_0\frac{\partial^2 u}{\partial t \partial z} + (U_0^2 - c_T^2)\frac{\partial^2 u}{\partial z^2} + \frac{U_0^2 + c_T^2}{2H}\frac{\partial u}{\partial z} + \frac{c_T^2}{H^2}\left[\frac{c_0^2}{v_A^2}\frac{\gamma - 1}{\gamma^2} + \frac{1}{2} - \frac{1}{2\gamma}\right]u = 0. \tag{2.44}$$

Since $U_0^2 \ll c_T^2$ for all z one may neglect the terms in U_0^2 and rewrite this as

$$\frac{\partial^2 u}{\partial t^2} + 2U_0\frac{\partial^2 u}{\partial t \partial z} - c_T^2\frac{\partial^2 u}{\partial z^2} + \frac{c_T^2}{2H}\frac{\partial u}{\partial z} + \frac{c_T^2}{H^2}\left[\frac{c_0^2}{v_A^2}\frac{\gamma - 1}{\gamma^2} + \frac{1}{2} - \frac{1}{2\gamma}\right]u = 0. \tag{2.45}$$

Thus an equation for the velocity perturbation, u, has been obtained. In similar corresponding studies for wave propagation in stratified, but static, tubes a substitution is made to render the governing equation into Klein-Gordon form, e.g. Rae & Roberts (1982), Musielak *et al.* (1989), Sutmann *et al.* (1998), Roberts (2004). To facilitate a comparison with such studies the following substitution is taken

$$u = Q\left(\frac{B_0}{\rho_0}\right)^{1/2}, \tag{2.46}$$

one sees that Eq. (2.45) reduces to

$$\frac{\partial^2 Q}{\partial t^2} + 2U_0\frac{\partial^2 Q}{\partial t \partial z} + \frac{U_0}{2H}\frac{\partial Q}{\partial t} - c_T^2\frac{\partial^2 Q}{\partial z^2} + \Omega_T^2 Q = 0, \tag{2.47}$$

where

$$\Omega_T^2 = \frac{c_T^2}{H^2}\left(\frac{9}{16} - \frac{1}{2\gamma} + \frac{c_0^2}{v_A^2}\frac{\gamma - 1}{\gamma^2}\right), \tag{2.48}$$

is the longitudinal cutoff frequency. Eq. (2.47) is the governing equation for longitudinal waves in a magnetic flux tube with a background flow subject to the applied conditions.

2.2.3 Formulation of solution by means of Laplace transforms

Returning now to Eq. (2.47), which governs wave propagation in a magnetic tube under isothermal conditions with a background equilibrium flow. To solve Eq. (2.47) analytically Laplace transformations in time are considered (adopting the method outlined by e.g. Sutmann et al. 1998). Since the flux tube is an isothermal medium, c_T and Ω_T are constant. A wave source is introduced into the atmosphere by applying a velocity term at the footpoint of the tube, yielding the relevant boundary condition, $V(t)$, at $z = 0$. The atmosphere is therefore semi-bounded and it is assumed there are no initial velocity perturbations other than at the footpoint. Further, it is assumed there are no wave motions at $z = \infty$. Thus the boundary conditions are given by

$$\lim_{t\to 0,\, z\neq 0} Q(t,z) = 0, \qquad \lim_{t\to 0,\, z\neq 0} \frac{\partial Q}{\partial t} = 0,$$

$$\lim_{z\to 0} Q(t,z) = V(t), \qquad \lim_{z\to\infty} Q(t,z) = 0. \tag{2.49}$$

Thus the homogeneous governing equation, Eq. (2.47), with inhomogeneous boundary conditions, Eq. (2.49), is to be solved by means of Laplace transforms. Let $q(s,z)$ be the Laplace transform in time of $Q(t,z)$ and applying the Laplace transform to Eq. (2.47) one obtains

$$\frac{\partial^2 q(s,z)}{\partial z^2} - \frac{2U_0 s}{c_T^2}\frac{\partial q(s,z)}{\partial z} - \frac{1}{c_T^2}\left(\Omega_T^2 + s^2 + \frac{U_0 s}{2H}\right) q(s,z) = 0. \tag{2.50}$$

It should be recalled that $U_0 = U_0(0)\exp(z/2H)$ and thus one finds that the solution to Eq. (2.50) is likely to be non-trivial. The solution of this equation is first considered by using the mathematical software Maple.

2.2.4 Solution by Maple

Using Maple the solution to Eq. (2.50) may be given by

$$q(z) = A_0 e^{\left(2U_0 sH^2 e^{z/2H} - zc_T^2/4\right)/c_T H} WhittakerM\left(\frac{1}{2} - H, 2H\sqrt{s^2+\Omega_T{}^2}, \frac{4U_0 sHe^{z/2H}}{c_T^2}\right) +$$

$$+A_1 e^{\left(2U_0 sH^2 e^{z/2H} - zc_T^2/4\right)/c_T H} WhittakerW\left(\frac{1}{2} - H, 2H\sqrt{s^2+\Omega_T{}^2}, \frac{4U_0 sHe^{z/2H}}{c_T^2}\right), \tag{2.51}$$

which is in terms of Whittaker functions. Note that the boundary conditions have not yet been applied, such that A_0 and A_1 are as yet undefined. Finding the inverse Laplace transform of Eq. (2.51) analytically is likely to be extremely hard. The exponential nature of the equilibrium flow term provides the complicating factor. A more tractable solution for Eq. (2.50) perhaps could be found by Taylor expanding the exponential nature of the flow, $\exp(z/2H)$, and consider a range of z and value of H such that we may neglect all but the first two terms. Thus, in this limited case, one could rewrite Eq. (2.50) as

$$\frac{\partial^2 q(s,z)}{\partial z^2} - \frac{2U_0(0)s}{c_T^2}\left(1+\frac{z}{2H}\right)\frac{\partial q(s,z)}{\partial z} - \frac{1}{c_T^2}\left[\Omega_T^2 + s^2 + \frac{U_0(0)s}{2H}\left(1+\frac{z}{2H}\right)\right] q(s,z) = 0. \tag{2.52}$$

Maple suggests the solution of this equation is given by

$$q(z) = A_0 e^{-z/2} KummerM\left(\frac{c_T^2 H(4s^2+4\Omega_T^2-1)}{8U_0 s}, \frac{1}{2}, \frac{(U_0(2H+z)s+c_T^2 H)^2}{2c_T^2 U_0 sH}\right) +$$
$$+A_1 e^{-z/2} KummerU\left(\frac{c_T^2 H(4s^2+4\Omega_T^2-1)}{8U_0 s}, \frac{1}{2}, \frac{(U_0(2H+z)s+c_T^2 H)^2}{2c_T^2 U_0 sH}\right). \quad (2.53)$$

Neither of these two solutions is particularly useful since we still need to establish the inverse Laplace transform, which is likely to be non-trivial. Thus progress is made by considering an alternative method for solving Eq. (2.50), namely by means of perturbation methods.

2.2.5 Solution by perturbation methods

The aim of this section is to solve Eq. (2.50) by means of perturbation methods, e.g. Holmes (1995). Perturbation methods allow analytical progress to be made in an otherwise intractable problem. An approximation of the exact solution is sought when a parameter of interest in the problem is small. In this case the parameter in question is the background flow, U_0. Let $U_0(0)/c_T = \varepsilon \ll 1$, such that $\varepsilon e^{z/2H} < 1 \forall z$. Thus the small parameter, ε, has been defined, which forms the basis for the perturbation method. Also let $(\Omega_T^2 + s^2)/c_T^2 \equiv m^2$, $2s/c_T \equiv a$ and $s/2Hc_T \equiv b$. Thus Eq. (2.50) may be rewritten as

$$\frac{\partial^2 q}{\partial z^2} - a\varepsilon e^{z/2H}\frac{\partial q}{\partial z} - (m^2 + b\varepsilon e^{z/2H})q = 0. \quad (2.54)$$

Boundary conditions

The governing equation is subject to the time domain boundary conditions given by Eq. (2.49). Taking the Laplace transform of the last two of these four one obtains

$$\lim_{z\to 0} q(s,z) = v(s), \qquad \lim_{z\to\infty} q(s,z) = 0, \quad (2.55)$$

where $v(s)$ is the Laplace transform of $V(t)$. Noting that the perturbation analysis assumes that $q = q_0 + \varepsilon q_1 + ...$, and thus

$$\lim_{z\to 0} q_0(s,z) = v(s), \qquad \lim_{z\to\infty} q_0(s,z) = 0.$$

$$\lim_{z\to 0} q_1(s,z) = 0, \qquad \lim_{z\to\infty} q_1(s,z) = 0. \quad (2.56)$$

Regular perturbation

Consider this to be a regular perturbation problem, such that we can express $q(s,z)$ as

$$q(s,z) = q_0(s,z) + \varepsilon q_1(s,z) + ..., \quad (2.57)$$

thus substituting into Eq. (2.54) yields

$$(q_0'' + \varepsilon q_1'' + ...) - a\varepsilon e^{z/2H}(q_0' + ...) - (m^2 + b\varepsilon e^{z/2H})(q_0 + \varepsilon q_1 + ...) = 0. \quad (2.58)$$

First consider terms of the order ε^0, such that

$$q_0'' - m^2 q_0 = 0, \tag{2.59}$$

and solving the resulting ordinary differential equation yields

$$q_0 = Ae^{-mz} + Be^{mz}, \tag{2.60}$$

where, A and B are to be determined by the boundary conditions given by Eq. (2.56). For the moment however these shall be left general and the boundary conditions applied later. Next, consider terms of the order ε^1 giving

$$q_1'' - m^2 q_1 = e^{z/2H}(aq_0' + bq_0), \tag{2.61}$$

which, upon the substitution of Eq. (2.60) and it's derivative, yields

$$q_1'' - m^2 q_1 = (bA - amA)e^{z(1/2H-m)} + (bB + amB)e^{z(1/2H+m)}. \tag{2.62}$$

This equation may be now solved for q_1 in terms of the complementary function (CF) and the particular integral (PI). The CF is given by

$$q_1'' - m^2 q_1 = 0, \tag{2.63}$$

which yields

$$q_1 = Ce^{-mz} + De^{mz}, \tag{2.64}$$

where C and D are to be determined by the boundary conditions. For the PI let

$$q_1 = Ee^{z(1/2H-m)} + Fe^{z(1/2H+m)}, \tag{2.65}$$

and upon substitution into Eq. (2.62) one finds that

$$E = \frac{4H^2(bA - amA)}{1 - 4Hm}, \quad F = \frac{4H^2(bB - amB)}{1 + 4Hm}. \tag{2.66}$$

Thus combining the complementary function and the particular integral one obtains

$$\begin{aligned} q_1 &= \mathrm{CF} + \mathrm{PI} \\ &= Ce^{-mz} + De^{mz} + \frac{4H^2(bA - amA)}{1 - 4Hm}e^{z(1/2H-m)} + \frac{4H^2(bB - amB)}{1 + 4Hm}e^{z(1/2H+m)} \end{aligned} \tag{2.67}$$

The boundary conditions may now be applied, such that

$$\lim_{z\to\infty} q_0(s,z) = 0, \quad \text{thus} \quad B = 0, \tag{2.68}$$

$$\lim_{z\to 0} q_0(s,z) = v(s), \quad \text{thus} \quad A = v(s), \tag{2.69}$$

$$\lim_{z\to\infty} q_1(s,z) = 0, \quad \text{thus} \quad D = 0, \tag{2.70}$$

$$\lim_{z\to 0} q_1(s,z) = 0, \quad \text{thus} \quad C = \frac{4H^2 v(s)(am - b)}{1 - 4mH}. \tag{2.71}$$

The general solution for q may now be formed by recalling that $q = q_0 + \varepsilon q_1 + ...$, and one finally obtains

$$q = v(s)e^{-mz}\left(1 + \frac{4\varepsilon H^2(am-b)}{1-4Hm}(1-e^{z/2H})\right). \tag{2.72}$$

The inverse of Eq. (2.72) then remains to be found to provide the general solution to Eq. (2.54). The problem is reformulated in terms of a multiple scales approach in Appendix B, yielding the same result. Thus Eq. (2.72) shows that the solution is given by the static solution plus a corrective term being dependent on the background flow. Setting $U_0 = 0$ returns the static case.

2.2.6 The inverse Laplace transform

The solution to Eq. (2.54) has been shown to be

$$q = v(s)e^{-mz}\left(1 + \frac{\varepsilon 4H^2(am-b)}{1-4Hm}(1-e^{z/2H})\right), \tag{2.73}$$

where $\varepsilon = U_0(0)/c_T$, $m^2 = (\Omega_T^2 + s^2)/c_T^2$, $a = 2s/c_T$ and $b = s/2Hc_T$. Thus one may rewrite $q(s,z)$ as

$$q(s,z) = \tag{2.74}$$
$$v(s)e^{-\sqrt{\Omega_T^2+s^2}z/c_T}\left[1 + \frac{U_0(0)}{c_T}\left(\frac{2s}{c_T}\frac{\sqrt{s^2+\Omega_T^2}}{c_T} - \frac{s}{2Hc_T}\right)\frac{4H^2}{1-\frac{4H}{c_T}\sqrt{s^2+\Omega_T^2}}(1-e^{z/2H})\right],$$

which may be reduced to

$$q(s,z) = v(s)e^{-\sqrt{\Omega_T^2+s^2}z/c_T}\left[1+\lambda s\right], \tag{2.75}$$

with $\lambda = 2U_0(0)H(e^{z/2H}-1)/c_T^2$, which has dimensions of time, see Fig. 2.3. Thus the term λ becomes highly significant since we have shown the solution to be the static solution plus a corrective term dependent on the bulk flow. After Sutmann *et al.* (1998) it is known that

$$e^{-\sqrt{\Omega_T^2+s^2}z/c_T} = e^{-sz/c_T} - \frac{\Omega_T z}{c_T}\mathcal{L}[W(t,z)], \tag{2.76}$$

where $\mathcal{L}$ denotes the Laplace transform and

$$W(t,z) = \frac{J_1(\Omega_T\sqrt{t^2-(z/c_T)^2})}{\sqrt{t^2-(z/c_T)^2}}\mathcal{H}(t-z/c_T), \tag{2.77}$$

where J_1 is a Bessel function. Thus using Eq. (2.75) one has

$$q(s,z) = v(s)\left[e^{-sz/c_T} - \frac{\Omega_T z}{c_T}\mathcal{L}[W(t,z)]\right]\left[1+\lambda(z)s\right]. \tag{2.78}$$

Since $\mathcal{L}[\delta'(t)] = s$, using the *second shift theorem* and the *convolution theorem* in turn yields

$$\begin{aligned} q(s,z) &= \mathcal{L}[V(t-z/c_T)\mathcal{H}(t-z/c_T)] - \frac{\Omega_T z}{c_T}\mathcal{L}[V(t)*W(t,z)] + \\ &+\lambda\mathcal{L}[(V(t-z/c_T)\mathcal{H}(t-z/c_T))*\delta'(t)] - \frac{\Omega_T z\lambda}{c_T}\mathcal{L}[(V(t)*W(t,z))*\delta'(t)], \end{aligned} \tag{2.79}$$

where the prime is represents the first derivative of the delta function with respect to t. This equation is now readily inverted to give

$$Q(t,z) = V(t-z/c_T)\mathcal{H}(t-z/c_T) - \frac{\Omega_T z}{c_T}[V(t)*W(t,z)] + \tag{2.80}$$
$$+\lambda[(V(t-z/c_T)\mathcal{H}(t-z/c_T))*\delta'(t)] - \frac{\Omega_T z\lambda}{c_T}[(V(t)*W(t,z))*\delta'(t)],$$

being an equation describing the evolution of waves in a magnetic flux tube with the presence of a background flow. It should be noted that Eq. (2.80) has been derived for the scaled velocity $Q(t,z)$, and so the original variable u will grow like $e^{z/4H}$ in an isothermal atmosphere, corresponding to an e-folding distance of four scale heights. Thus relatively small velocities, e.g. at the photosphere will be greatly amplified in several scale heights, highlighting the likelihood of shocks and other complicating factors coming into play.

2.2.7 Atmospheric response to various photospheric drivers

In the previous section a general solution to the steady flow problem in terms of a general imposed velocity function, $V(t)$, was derived. In this section the solution for three specific imposed drivers, namely a monochromatic source, a delta-function pulse and a sinusoidal pulse, is considered. The monochromatic source and the sinusoidal pulse (essentially excitation by a piston like motion) provide a plausible model for the representation of the global solar p-modes or the turbulent motions of the convection zone. A further explanation for the observed wave excitation may be turbulent buffeting of the tube by granular motions or by the impact of traveling shocks, which may be represented by the delta-function pulse.

Monochromatic source

Firstly the boundary conditions are to be satisfied by a source of monochromatic acoustic waves, generated continuously with the frequency ω and amplitude V_0. Hence wave propagation in a thin flux tube by a periodic driver is modeled, mimicking the effect, say, of solar global oscillations on vertical steady flux tubes. Thus the required boundary condition is given by

$$V(t) = V_0 e^{-i\omega t}. \tag{2.81}$$

In Eq. (2.80) the first two terms of the general solution are the same as the corresponding static case while the last two terms are new, and are introduced by the background flow. The static case for the magnetic tube has been solved previously by e.g. Musielak & Ulmschneider (2003a), being an extension of the case of a general stratified atmosphere solved by Sutmann *et al.* (1998). The general solution may be thought of as consisting of four terms, which may be denoted as A_1, A_2, A_3 and A_4. The first two (A_1 and A_2) have been dealt with by Sutmann *et al.* (1998) whereas the second two (A_3 and A_4) are entirely new. The solution to the two static terms will now be briefly examined and the main points highlighted. The first term, A_1, is

$$A_1 = V(t-z/c_T)\mathcal{H}(t-z/c_T) = V_0 e^{-i\omega(t-z/c_T)}\mathcal{H}(t-z/c_T). \tag{2.82}$$

The second term is given by

$$A_2 = \frac{-\Omega_T z}{c_T}[V(t) * W(t,z)] = \frac{-\Omega_T z}{c_T}\int_0^t V(t-\tau)W(\tau,z)d\tau,$$
$$= \frac{-\Omega_T z}{c_T}V_0 e^{-i\omega t}\int_0^t e^{i\omega\tau}W(\tau,z)d\tau. \qquad (2.83)$$

The integral term above may be written as $I = I_1 - I_2 = \int_0^\infty ...d\tau - \int_t^\infty ...d\tau$. Looking at I_1 yields

$$I_1 = \int_0^\infty \frac{e^{i\omega\tau}J_1(\Omega_T\sqrt{\tau^2-(z/c_T)^2})}{\sqrt{\tau^2-(z/c_T)^2}}\mathcal{H}(\tau - z/c_T)d\tau. \qquad (2.84)$$

From Sutmann *et al.* (1998) it is known that

$$e^{-\sqrt{\Omega_T^2+s^2}z/c_T} = e^{-sz/c_T} - \frac{\Omega_T z}{c_T}\int_0^\infty e^{-st}\frac{J_1(\Omega_T\sqrt{t^2-(z/c_T)^2})}{\sqrt{t^2-(z/c_T)^2)}}\mathcal{H}(t-z/c_T)dt, \qquad (2.85)$$

and after replacing s with $-i\omega$ one sees that

$$e^{-\sqrt{\Omega_T^2-\omega}\,z/c_T} = e^{i\omega z/c_T} - \frac{\Omega_T z}{c_T}I_1, \qquad (2.86)$$

thus

$$I_1 = \frac{c_T}{\Omega_T z}\left(e^{i\omega z/c_T} - e^{-i\sqrt{\omega^2-\Omega^2}\,z/c_T}\right). \qquad (2.87)$$

Solving for I_2 yields

$$I_2 = \int_t^\infty e^{i\omega\tau}\frac{J_1(\Omega_T\sqrt{\tau^2-(z/c_T)^2})}{\sqrt{\tau^2-(z/c_T)^2)}}\mathcal{H}(\tau-z/c_T)d\tau. \qquad (2.88)$$

Solving for $t \gg z/c_T$, thus $\tau \gg z/c_T$, gives

$$I_2 = \int_t^\infty e^{i\omega\tau}\frac{J_1(\Omega_T\tau)}{\tau}d\tau. \qquad (2.89)$$

It is assumed that t is large (so τ is large) and thus one may expand $J_1(\Omega_T\tau)$ for large arguments, using the expression

$$J_1(\Omega_T\tau) \approx \sqrt{\frac{2}{\pi\Omega_T\tau}}\left(\cos(\Omega_T\tau - 3\pi/4) + O\left(\frac{1}{\tau}\right)\right). \qquad (2.90)$$

Using the exponential representation of the cosine function one may rewrite I_2 as

$$I_2 = \frac{1}{2}\sqrt{\frac{2}{\pi\Omega_T}}(e^{-i3\pi/4}I_a + e^{i3\pi/4}I_b), \quad I_a = \int_t^\infty \frac{e^{i\tau(\omega+\Omega_T)}}{\tau^{3/2}}d\tau, \quad I_b = \int_t^\infty \frac{e^{i\tau(\omega-\Omega_T)}}{\tau^{3/2}}d\tau. \qquad (2.91)$$

The integrals I_a and I_b may be solved by integrating by parts. Sutmann *et al.* (1998) develop an infinite series and retain only the first term, such that

$$I_a = \frac{-1}{t^{3/2}}\frac{e^{it(\omega+\Omega_T)}}{i(\omega+\Omega_T)}, \quad I_b = \frac{-1}{t^{3/2}}\frac{e^{it(\omega-\Omega_T)}}{i(\omega-\Omega_T)}, \qquad (2.92)$$

thus

$$I_2 = \sqrt{\frac{2}{\pi\Omega_T}}\frac{1}{t^{3/2}}\frac{e^{i\omega t}}{\omega^2-\Omega_T^2}(\Omega_T \sin\mu + i\omega\cos\mu), \tag{2.93}$$

with $\mu = \Omega_T t - 3\pi/4$. Thus it can be recalled that

$$\begin{aligned} A_2 = -\frac{\Omega_T z}{c_T}[V(t)*W(t,z)] &= -\frac{\Omega_T z V_0 e^{-i\omega t}}{c_T}(I_1 - I_2), \\ &= -\frac{\Omega_T z V_0 e^{-i\omega t}}{c_T}\left[\frac{c_T}{\Omega_T z}(e^{i\omega z/c_T} - e^{-i\sqrt{\omega^2-\Omega^2}\, z/c_T}) - \right. \\ &\quad \left. -\sqrt{\frac{2}{\pi\Omega_T}}\frac{1}{t^{3/2}}\frac{e^{i\omega t}}{\omega^2-\Omega_T^2}(\Omega_T\sin\mu + i\omega\cos\mu)\right], \\ &= -V_0 e^{-i\omega t}(e^{i\omega z/c_T} - e^{-i\sqrt{\omega^2-\Omega^2}\, z/c_T}) + \\ &\quad + \frac{\Omega_T z V_0}{c_T}\sqrt{\frac{2}{\pi\Omega_T}}\frac{1}{t^{3/2}}\frac{1}{\omega^2-\Omega_T^2}(\Omega_T\sin\mu + i\omega\cos\mu), \end{aligned} \tag{2.94}$$

where $\mu = \Omega_T t - 3\pi/4$. Combining terms A_1 and A_2 yields the general solution for wave propagation in a static magnetic cylinder in a stratified atmosphere.

Attention is now turned to the flow dependent third and fourth terms in Eq. (2.80). The third term is given by

$$A_3 = \lambda[\{V(t - z/c_T)\mathcal{H}(t - z/c_T)\} * \delta'(t)]. \tag{2.95}$$

Since $t \gg z/c_T$

$$V(t - z/c_T)\mathcal{H}(t - z/c_T) = V_0 e^{-i\omega(t - z/c_T)}. \tag{2.96}$$

One may employ a fundamental property of the delta function, which shows that for some arbitrary function, $X(t)$, convoluted with the derivative of the delta function, one obtains the derivative of the function, i.e $X(t) * \delta'(t) = X'(t)$. Thus the third term is

$$A_3 = \lambda[\{V(t - z/c_T)\mathcal{H}(t - z/c_T)\} * \delta'(t)] = -i\lambda V_0 \omega e^{-i\omega(t - z/c_T)} \tag{2.97}$$

The fourth term is given by

$$A_4 = -\frac{z\Omega_T\lambda}{c_T}[\{V(t) * W(t,z)\} * \delta'(t)]. \tag{2.98}$$

The $V(t) * W(t,z)$ term has been previously calculated in working out the second term. Employing the delta function property yields

$$\begin{aligned} A_4 &= V_0\lambda i\omega e^{-i\omega t}\left[e^{i\omega z/c_T} - e^{-i\sqrt{\omega^2-\Omega_T^2}\, z/c_T}\right] + \\ &\quad + \frac{V_0 z\Omega_T\lambda}{c_T}\sqrt{\frac{2}{\pi\Omega_T}}\frac{1}{t^{3/2}}\frac{1}{\omega^2-\Omega_T^2}\left[\Omega_T^2\cos\mu - i\omega\Omega_T\sin\mu - \frac{3}{2}\frac{1}{t}(\Omega_T\sin\mu + i\omega\cos\mu)\right]. \end{aligned} \tag{2.99}$$

Adding the four terms gives the total solution for the monochromatic driver such that

$$Q(t,z) = V_0(1-i\lambda\omega)e^{-i(\omega t+\sqrt{\omega^2-\Omega_T^2}\,z/c_T)} + \frac{V_0 z\Omega_T}{c_T}\sqrt{\frac{2}{\pi\Omega_T}}\frac{1}{t^{3/2}}\frac{1}{\omega^2-\Omega_T^2}\times$$
$$\times\left[\Omega_T\left(1-\lambda i\omega-\frac{3}{2}\frac{\lambda}{t}\right)\sin\mu + i\omega\left(1-\lambda\frac{i\Omega_T^2}{\omega}-\frac{3}{2}\frac{\lambda}{t}\right)\cos\mu\right]. \quad (2.100)$$

The effect of the flow is apparent through the λ term, which has temporal dimensions and thus can be thought of as characteristic time introduced by the flow. Setting $\lambda = 0$ reduces the equation to that of the equivalent static solution given by Musielak & Ulmschneider (2003a). As in the static case the solution is comprised of two parts: the so-called forced oscillations with wave frequency ω, representing the continuous nature of the driver at the footpoint and the free atmospheric oscillations at the cutoff frequency Ω_T, which are shown in Fig. 2.6. The effect of the flow on the forced term may be seen by examining it's real part, which can be shown to be

$$\Re[Q_{Forced}(t,z)] = V_0\sqrt{1+(\omega\lambda)^2}\cos(\xi+\psi), \quad (2.101)$$

where $\xi = \omega t + (\omega^2-\Omega_T^2)^{1/2}\,z/c_T$ and $\psi = \arctan(\lambda\omega)$, see Fig. 2.4. Thus the background flow has increased the amplitude of the forced term and introduced a phase shift. Both these effects are functions of λ, and hence the applied background flow, but interestingly they are dependent also on the wave frequency, ω. The free atmospheric oscillations, represented by the second term in Eq. (2.100), are dominated temporally by the $t^{-3/2}$ term, which results in a decay in time at any given height. The presence of the flow introduces a secondary temporal dependance, given by the $3\lambda/2t$ term. Despite the fact that t is considered to be large, the effect of this term may become significant when considering solar parameters. Furthermore note that in the static case the amplitude of the free oscillations is linear with height, however with the addition of the background flow this is not the case anymore. One may demonstrate these two points by considering the real part of the free oscillations in Eq. (2.100), and rewriting the equation as

$$\Re[Q_{Free}(t,z)] = \frac{V_0 z\Omega_T}{c_T}\sqrt{\frac{2}{\pi\Omega_T}}\frac{1}{t^{3/2}}\frac{1}{\omega^2-\Omega_T^2}\times\left[\Omega_T\sqrt{\left(1-\frac{3\lambda}{2t}\right)^2+(\lambda\Omega_T)^2}\sin(\mu+\alpha)\right], \quad (2.102)$$

where

$$\alpha = \arctan\frac{\Omega_T t}{t/\lambda-3/2}. \quad (2.103)$$

The effect of the flow, therefore, is to alter the amplitude of the free oscillations (relative to the static case) in a non-trivial fashion. The change in amplitude is both a function of time, height and the value of the background flow. Furthermore, the flow introduces a phase shift which equally is dependent on time, height and the magnitude of the flow. It can also be noted that, in contrast to the forced terms, the increase in amplitude and phase shift are not dependent on the wave frequency, ω.

Consider now the special case of a monochromatic driver with a driving frequency matching the tube cut-off, i.e. $\omega = \Omega_T$. Thus the boundary condition is given by

$$V(t) = V_0 e^{-i\Omega_T t}. \tag{2.104}$$

The procedure is much the same such that one considers the general solution to be constructed of four summable terms of the governing equation, each denoted by B_i. The first term, B_1, is given by

$$B_1 = V(t - z/c_T)\mathcal{H}(t - z/c_T) = V_0 e^{-i\Omega_T(t-z/c_T)}\mathcal{H}(t - z/c_T) = V_0 e^{-i\Omega_T(t-z/c_T)}, \tag{2.105}$$

since t will be considered large. The second term, B_2, is given by

$$\begin{aligned} B_2 = \frac{-\Omega_T z}{c_T}[V(t) * W(t,z)] &= \frac{-\Omega_T z}{c_T}\int_0^t V(t-\tau)W(\tau,z)d\tau, \\ &\quad \frac{-\Omega_T z}{c_T}V_0 e^{-i\Omega_T t}\int_0^t e^{i\Omega_T \tau}W(\tau,z)d\tau. \end{aligned} \tag{2.106}$$

The integral term above may be written as $I = I_1 - I_2 = \int_0^\infty ...d\tau - \int_t^\infty ...d\tau$. I_1 may be found directly from the previous section, with ω now replaced with Ω_T, such that

$$I_1 = \frac{c_T}{\Omega_T z}\left(e^{i\Omega_T z/c_T} - 1\right). \tag{2.107}$$

Considering t to be large as before, I_2 can be seen to be

$$I_2 = \frac{1}{2}\sqrt{\frac{2}{\pi\Omega_T}}(e^{-i3\pi/4}I_a + e^{i3\pi/4}I_b), \quad I_a = \int_t^\infty \frac{e^{i2\tau\Omega_T}}{\tau^{3/2}}d\tau, \quad I_b = \int_t^\infty \frac{1}{\tau^{3/2}}d\tau, \tag{2.108}$$

and solving by integration by parts yields

$$I_a = -\frac{e^{12\Omega_T t}}{2it^{3/2}\Omega_T}, \quad I_b = \frac{2}{t^{1/2}} \tag{2.109}$$

Substituting this back into our expression for the second term, B_2, yields

$$\begin{aligned} B_2 &= -V_0 e^{-i\Omega_T(t-z/c_T)} + \\ &\quad + \frac{1}{4}\frac{V_0 z\Omega_T}{c_T}\sqrt{\frac{2}{\pi\Omega_T}}\frac{1}{t^{3/2}}(i\cos\mu - \sin\mu) + \frac{V_0 z\Omega_T}{c_T}\sqrt{\frac{2}{\pi\Omega_T}}\frac{1}{t^{1/2}}(\cos\mu - i\sin\mu). \end{aligned} \tag{2.110}$$

Adding the first and second terms will yields the static case solution for wave propagation in a static magnetic tube, found by Musielak & Ulmschneider (2003a). The flow dependent third term, B_3, is given by

$$\begin{aligned} B_3 = \lambda\left[\{V(t - z/c_T)\mathcal{H}(t - z/c_T)\} * \delta'(t)\right] &= \lambda\left[V_0 e^{-i\Omega_T(t-z/c_T)} * \delta'(t)\right] \\ &= -i\lambda V_0\Omega_T e^{-i\Omega_T(t-z/c_T)}. \end{aligned} \tag{2.111}$$

The fourth term is given by

$$B_4 = -\frac{z\Omega_T\lambda}{c_T}[\{V(t) * W(t,z)\} * \delta'(t)]. \tag{2.112}$$

The term $V(t) * W(t,z)$ has been previously calculated in working out B_2, thus employing the

derivative property of convoluting with the delta function yields

$$B_4 = iV_0\lambda\Omega_T\left[e^{-i\Omega_T(t-z/c_T)} - e^{-i\Omega_T t}\right] - \frac{z\Omega_T\lambda V_0}{c_T}\sqrt{\frac{2}{\pi\Omega_T}}\left[\frac{e^{i\mu}}{t^{3/2}}\left(\frac{1}{4}+i\frac{3}{8\Omega_t t}\right)+\frac{e^{-i\mu}}{t^{1/2}}\left(\frac{1}{2t}+i\Omega_T\right)\right]. \quad (2.113)$$

The final general solution is formed by the summation of the four individual terms giving

$$Q(t,z) = V_0(1-i\lambda\Omega_T)e^{-i\Omega_T t} + \frac{z\Omega_T V_0}{c_T}\sqrt{\frac{2}{\pi\Omega_T}}\left[\frac{e^{i\mu}}{t^{3/2}}\left(\frac{1}{i\Omega_T}-\frac{\lambda}{4}-i\frac{3\lambda}{8\Omega_T t}\right)+\frac{e^{-i\mu}}{t^{1/2}}\left(1-\frac{\lambda}{2t}-i\Omega_T\lambda\right)\right]. \quad (2.114)$$

As discussed in some detail by Sutmann *et al.* (1998) it is necessary to take $t \to \infty$ when $\omega \to \Omega_T$, thus Eq. (2.114) reduces to

$$Q(t,z) = V_0(1-i\lambda\Omega_T)e^{-i\Omega_T t}, \quad (2.115)$$

showing only the forced term remains. In much the same way as in the previous case an amplitude increase and phase shift have been introduced, which may be seen by considering the real part of Eq. (2.115), such that

$$\Re[Q_{Forced}(t,z)] = V_0\sqrt{1+(\Omega_T\lambda)^2}\cos(\Omega_T+\phi), \quad (2.116)$$

where $\phi = \arctan(\lambda\Omega_T)$. The amplitude increase and phase shift are functions of Ω_T rather than ω since the system is being driven at the cutoff frequency.

A more realistic model of the footpoint driver may perhaps be given by a spectrum of longitudinal tubes waves representing turbulent motions in the solar atmosphere. The spectrum can be considered to be the linear superposition of many partial waves with different amplitudes and frequencies. The required boundary condition is given by

$$V(t) = \sum_{n=1}^{N} V_n e^{-i\omega_n t}, \quad (2.117)$$

where V_n and ω_n are the amplitude and frequency of the partial waves. The boundary condition will yield a result that is similar to that presented earlier in this chapter, since each partial wave is essentially a single monochromatic wave, and the result will be the superposition of all such waves. Therefore the solution shall not be presented but see, say, Musielak & Ulmschneider (2003a) Section 3.2, 4.2 for more details.

Delta-function driver

In this section the source is considered to be a single pulse of δ-function form in time. Thus the lower boundary condition at $z = 0$ is

$$V(t) = \bar{V}_0\delta(t). \quad (2.118)$$

The delta function has dimensions $1/T$, consequently the dimensions of $\bar{V}_0$ are not velocity. This may be remedied by using a dimensionless time $\bar{t} = t/P_T$, where $P_T = 2\pi/\Omega_T$. Thus

$$V(t) = \bar{V}_0 \delta(P_T \bar{t}) = \frac{\bar{V}_0}{|P_T|} \delta(\bar{t}) = V_0 \delta(\bar{t}). \tag{2.119}$$

One may adopt a similar strategy as in the previous section, such that the general solution is constructed of four terms, the first two of which are given by Musielak & Ulmschneider (2003a) and the third and fourth are dependent on the applied bulk flow. Briefly reviewing the derivation of the static terms yields

$$C_1 = \bar{V}_0 \delta(\bar{t} P_T - z/c_T) \mathcal{H}(\bar{t} P_T - z/c_T). \tag{2.120}$$

It is known that $\delta(at) = \delta(t)/|a|$ and $\mathcal{H}(at) = \mathcal{H}(t)$. Thus

$$C_1 = V_0 \delta(\bar{t} - z/P_T c_T) \mathcal{H}(\bar{t} - z/P_T c_T). \tag{2.121}$$

Since the interest is generally in large times it is clearly seen that $C_1 = 0$. The second term, C_2, is given by

$$\begin{aligned} C_2 &= -\frac{\Omega_T z}{c_T} [V(t) * W(t,z)], \\ &= \frac{\Omega_T z}{c_T} V_0 \int_0^{\bar{t}} \delta(\bar{t} - \bar{\tau}) W(\bar{\tau} P_T, z) P_T d\bar{\tau}, \\ &= -\frac{\Omega_T z V_0 P_T}{c_T} W(\bar{\tau} P_T, z), \\ &= -\frac{\Omega_T z V_0 P_T}{c_T} W(t,z). \end{aligned} \tag{2.122}$$

The Bessel function contained in the definition of $W(\tau, z)$ may be expanded by considering large times such that

$$C_2 = \frac{-2\pi z V_0}{c_T} \sqrt{\frac{2}{\pi \Omega_T}} \frac{1}{t^{3/2}} \cos\mu, \tag{2.123}$$

where $\mu = \Omega_T t - 3\pi/4$. The third term, C_3, is readilly seen to be zero by considering C_1. The forth term, C_4, is obtained from

$$C_4 = -\frac{z \Omega_T \lambda}{c_T} [\{V(t) * W(t,z)\} * \delta'(t)]. \tag{2.124}$$

The term $V(t) * W(t,z)$ is known, such that

$$C_4 = \frac{2\pi z \lambda V_0}{c_T} \sqrt{\frac{2}{\pi \Omega_T}} \frac{1}{t^{3/2}} \left[\frac{3}{2} \frac{1}{t} \cos\mu + \Omega_T \sin\mu \right]. \tag{2.125}$$

Summing the four separate terms gives the total solution for $Q(t,z)$, yielding

$$Q(t,z) = \frac{-2\pi z V_0}{c_T} \sqrt{\frac{2}{\pi \Omega_T}} \frac{1}{t^{3/2}} \left[\cos\mu - \frac{3}{2} \frac{\lambda}{t} \cos\mu - \lambda \Omega_T \sin\mu \right]. \tag{2.126}$$

Note that the delta function source results in only the free atmospheric oscillations, due to the fact that the pulse is not continuously driven and, in this analysis, has long passed. The oscillations are dominated by the decay in time, given by the $t^{-3/2}$ term and oscillate at the cutoff frequency, Ω_T. The effect of the flow can be emphasised by rewriting Eq. (2.126) in the following form

$$Q(t,z) = \frac{-2\pi z V_0}{c_T}\sqrt{\frac{2}{\pi\Omega_T}}\frac{1}{t^{3/2}} \times \left[\sqrt{\left(1-\frac{3\lambda}{2t}\right)^2 + (\lambda\Omega_T)^2}\cos(\mu-\alpha)\right]. \tag{2.127}$$

Thus the effect of the flow is much the same as for the monochromatic driver. The amplitude is modified in a non-trivial fashion, being a function of time, height and the magnitude of the background flow. A phase shift is also introduced that is also non-trivial in nature.

Sinusoidal pulse driver

The final case to be considered here is a sinusoidal pulse generated at the lower boundary and lasting for one wave period P, where $P = 2\pi/\omega$. Thus the boundary driver is given by

$$V(t) = [\mathcal{H}(t) - \mathcal{H}(t-P)]e^{-i\omega t}. \tag{2.128}$$

As previously the general solution is to be constructed of four summed terms, each denoted by C_i. Since large times are assumed, i.e. $t \gg z/c_T$, one arrives at

$$D_1 = V(t - z/c_T)\mathcal{H}(t - z/c_T) = 0, \tag{2.129}$$

because the two Heaviside functions cancel. The second term is given by

$$\begin{aligned} D_2 = \frac{-\Omega_T z}{c_T}[V(t) * W(t,z)] &= \frac{-\Omega_T z}{c_T}\left[\{V_0 e^{-i\omega t}(\mathcal{H}(t) - \mathcal{H}(t-P))\} * W(t,z)\right], \\ &= \frac{-\Omega_T z}{c_T} V_0 \int_{t-P}^{t} e^{-i\omega(t-\tau)} W(\tau,z)\,d\tau. \end{aligned} \tag{2.130}$$

The integral term in D_2 may be written as $I = I_1 - I_2 = \int_{t-P}^{\infty} ... d\tau - \int_t^{\infty} ... d\tau$. Assuming t is large, upon expanding the Bessel function for large arguments and expressing the resulting cosine function in terms of exponential functions one finds that

$$I = \frac{1}{2}\sqrt{\frac{2}{\pi\Omega_T}}\left[e^{-i3\pi/4} I_a + e^{i3\pi/4} I_b - e^{-i3\pi/4} I_c - e^{i3\pi/4} I_d\right], \tag{2.131}$$

where

$$I_a = \int_{t-P}^{\infty} \frac{e^{i\tau(\omega+\Omega_T)}}{\tau^{3/2}} d\tau, \quad I_b = \int_{t-P}^{\infty} \frac{e^{i\tau(\omega-\Omega_T)}}{\tau^{3/2}} d\tau, \quad I_c = \int_{t}^{\infty} \frac{e^{i\tau(\omega+\Omega_T)}}{\tau^{3/2}} d\tau, \quad I_d = \int_{t}^{\infty} \frac{e^{i\tau(\omega-\Omega_T)}}{\tau^{3/2}} d\tau. \tag{2.132}$$

Evaluating these integrals by parts, retaining only the first term of the resulting infinite series and substituting into the expression for I yields

$$I = \sqrt{\frac{2}{\pi\Omega_T}}\frac{1}{\omega^2 - \Omega_T^2}\left[\frac{i\omega\cos\theta + \Omega_T\sin\theta}{(t-P)^{3/2}} - \frac{i\omega\cos\mu + \Omega_T\sin\mu}{t^{3/2}}\right], \tag{2.133}$$

where $\theta = \Omega_T(t-P) - 3\pi/4$ and $\mu = \Omega_T t - 3\pi/4$. Expanding the term $(t-P)^{-3/2}$ binomially gives

$$\frac{1}{(t-P)^{3/2}} \approx \left(1 + \frac{3}{2}\frac{P}{t}\right), \tag{2.134}$$

and for $t \gg P$ one obtains

$$\frac{1}{(t-P)^{3/2}} \approx \frac{1}{t^{3/2}}. \tag{2.135}$$

Thus D_2 is given by

$$D_2 = \frac{-\Omega_T z V_0}{c_T}\sqrt{\frac{2}{\pi\Omega_T}}\frac{1}{\omega^2-\Omega_T^2}\frac{1}{t^{3/2}}\left[\Omega_T \sin\theta - \Omega_T \sin\mu + i\omega\cos\theta - i\omega\cos\mu\right]. \tag{2.136}$$

The third term, D_3, is zero, which can be deduced by inspection of D_1. For determining D_4 use the same technique is applied as for the other drivers, yielding

$$\begin{aligned} C_4 \;=\; & -\frac{\Omega_T z V_0 \lambda}{c_T}\sqrt{\frac{2}{\pi\Omega_T}}\frac{1}{\omega^2-\Omega_T^2}\frac{1}{t^{3/2}} \times \\ & \times\left[\frac{-3}{2}\frac{1}{t}(\Omega_T\sin\theta - \Omega_T\sin\mu + i\omega\cos\theta - i\omega\cos\mu) + \right. \\ & \left. + \Omega_T^2\cos\theta - \Omega_T^2\cos\mu - i\omega\Omega_T\sin\theta + i\omega\Omega_T\sin\mu\right]. \end{aligned} \tag{2.137}$$

Combining all the four terms gives

$$\begin{aligned} Q(t,z) \;=\; & \frac{-\Omega_T z V_0}{c_T}\sqrt{\frac{2}{\pi\Omega_T}}\frac{1}{\omega^2-\Omega_T^2}\frac{1}{t^{3/2}} \times \\ & \times\left[\left(\Omega_T - \frac{3}{2}\frac{\lambda\Omega_T}{t} - i\lambda\omega\Omega_T\right)\sin\theta - \left(\Omega_T - \frac{3}{2}\frac{\lambda\Omega_T}{t} - i\lambda\omega\Omega_T\right)\sin\mu + \right. \\ & \left. + \left(i\omega - \frac{3}{2}\frac{i\omega\lambda}{t} + \lambda\Omega_T^2\right)\cos\theta - \left(i\omega - \frac{3}{2}\frac{i\lambda\omega}{t} + \lambda\Omega_T^2\right)\cos\mu\right]. \end{aligned} \tag{2.138}$$

As in the case of the delta function source the solution is given by the free oscillations only, since the pulse only was driven for one wave period. The free oscillations decay as $t^{-3/2}$ and are at the cutoff frequency. However, also note that the solution is a function of the pulse frequency. It is interesting to observe the case when $\omega \to \Omega_T$ because, as discussed in Sutmann *et al.* (1998), under these conditions it is necessary to impose the limit $t \to \infty$ and thus we see that there are no free oscillations present. The effect of the flow can be highlighted again by considering the real part of Eq. (2.138), e.g. in the following form

$$\begin{aligned} \Re[Q_{Free}(t,z)] \;=\; & \frac{-\Omega_T z V_0}{c_T}\sqrt{\frac{2}{\pi\Omega_T}}\frac{1}{\omega^2-\Omega_T^2}\frac{1}{t^{3/2}} \times \\ & \times\Omega_T\sqrt{\left(1-\frac{3\lambda}{2t}\right)^2 + (\lambda\Omega_T)^2}\left[\sin(\theta+\alpha) - \sin(\mu+\alpha)\right]. \end{aligned} \tag{2.139}$$

Thus it is found that the effect of the flow, when considering the sinusoidal driver, is to introduce a modification to the amplitude and a phase shift which are both functions of time, height and the magnitude of the background flow.

In much the same way as for the spectrum of longitudinal waves discussed at the end of Section 2.2.7 - Monochromatic source, a more realistic model of a footpoint driver may be given by a wavetrain of such sinusoidal pulses, each with a random period and amplitude. The main result

of which is to allow the free atmospheric oscillations to be continuously re-excited as each pulse generates free oscillations at the cutoff frequency. Thus the free atmospheric oscillations may be maintained for long times and hence, given solar parameters, their interpretation as the 3 min modes observed in the solar atmosphere. In this chapter the focus is on the changes introduced by the flow which is most easily demonstrated for a single sinusoidal pulse.

2.3 Application to the Sun

Taking typical solar parameters, corresponding to the photospheric region, one may apply the equations derived previously to the Sun. The focus is on the changes introduced by the background flow in comparison to the static case. The acceleration due to gravity is taken as $g = 0.275$ km s^{-2} and $\gamma = 5/3$. Then for a sound speed $c_0 = 7.5$ km s^{-1}, a scale height of $H = 122.7$ km, one finds an acoustic cutoff frequency of $\Omega_{AC} = 0.0306$ s^{-1} (where $\Omega_{AC} = c_0/2H$) and a corresponding acoustic cutoff period of $P_{AC} \approx 200$ s. We can express the tube speed, c_T, and the tube cutoff frequency, Ω_T, in terms of the sound speed and plasma beta by means of the following relations

$$c_T = \frac{c_0}{\sqrt{1+\beta\gamma/2}}, \quad \Omega_T = \frac{\Omega_{AC}}{\sqrt{1+\beta\gamma/2}}\sqrt{\frac{9}{4}-\frac{2}{\gamma}+2\beta\frac{\gamma-1}{\gamma}}. \tag{2.140}$$

Thus for $\beta \to 0$ we see that $\Omega_T \approx 1.03\Omega_{AC}$ and for $\beta \gg 0$ we find $\Omega_T \approx 0.98\Omega_{AC}$. Thus the extremes of magnetic configuration yield a very similar frequency range over which longitudinal tube waves and acoustic waves propagate. For the purpose of plotting a plasma beta of $\beta = 0.4$ shall be taken, yielding a cutoff frequency of $\Omega_T = 0.0310$ s^{-1}, which is approximately 1% larger than an acoustic case considered by, say, Sutmann *et al.* (1998). Any application to the solar atmosphere will require consideration of the magnitude of the footpoint flow, $U_0(0)$. In the preceding analysis the background flow was required to remain bounded for all z. This condition is plotted in Fig. 2.2, which shows that for a tube examined at say, $z = 2000$ km, one is severely restricted in the maximum value of the footpoint flow one may adopt. It should be noted that in this example the magnitude of the background flow will increase with height, reaching a value of $U_0 = 1$ km/s at $z = 2000$ km. In Fig. 2.3 the flow timescale λ against height z is plotted. The variation in λ is shown for two different values of the footpoint flow. The dotted line in Fig. 2.3 corresponds to a footpoint flow given by a maximum height of $z = 500$ km (such that $U_0(0) = e^{-500/2H}$), and consequently could only be used to maximum height of $z = 500$ km. The solid line corresponds to a footpoint flow applicable up to $z = 2000$ km.

Forced atmospheric oscillations

The forced atmospheric oscillations given for the monochromatic driver plotted against time are shown in Fig. 2.4. The curve shows the real part of the forced oscillations given by Eq. (2.100) and is plotted for $V_0 = 1$ kms^{-1}, $z = 500$ km, a footpoint flow of $U_0(0) = e^{-500/2H}$ and a driver period of 50 s.

It has been shown that for the case of the continuously driven monochromatic source one obtains the so called forced atmospheric oscillations. Eq. (2.101) demonstrated the real part of the forced oscillations has an amplitude increase and a phase shift when compared with its static counterpart. The percentage difference in amplitude between the static and steady cases is shown in Fig. 2.5. The three curves correspond to propagating wave frequencies of ω=0.13, 0.06, 0.04 s^{-1} (i.e. wave periods of 50, 100, 150 s). For a wave period of 50 s it is seen

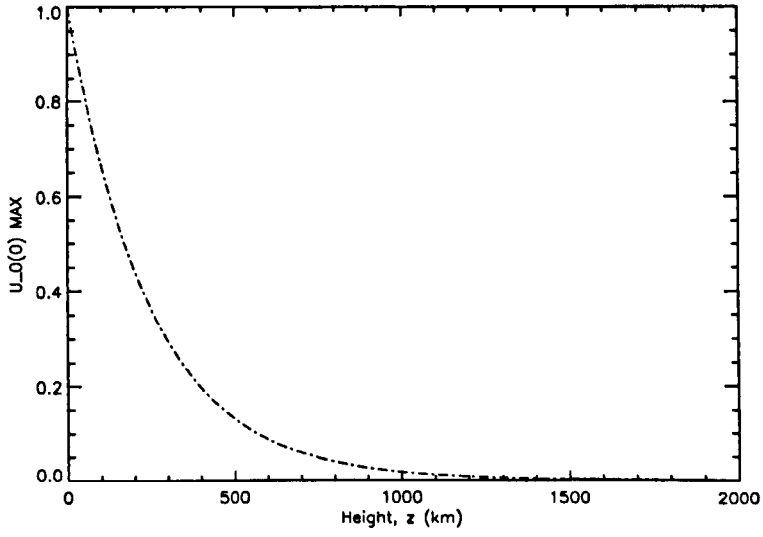

Figure 2.2: The maximum value of footpoint flow, $U_0(0)$, against the maximum height considered.

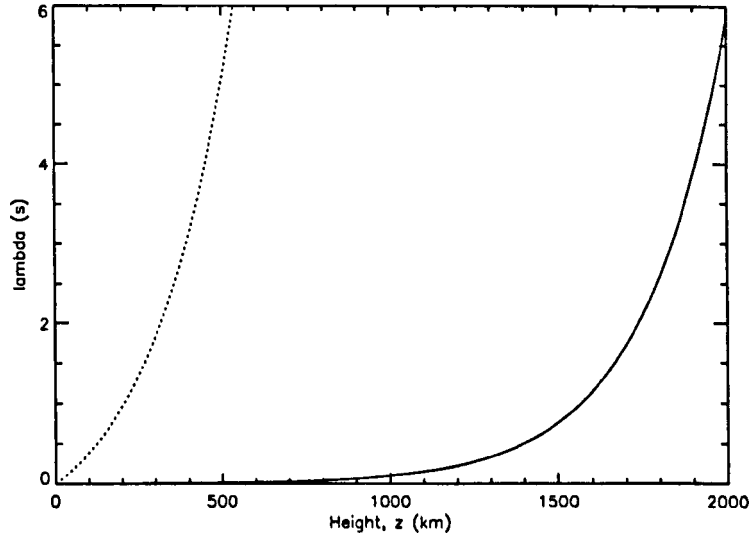

Figure 2.3: The variation of the flow timescale, λ, with height plotted for two magnitudes of footpoint flow, $U_0(0)$. The dotted line corresponds to $z_{max} = 500$, giving $U_0(0) = e^{-500/2H}$. The solid line corresponds to $z_{max} = 2000$.

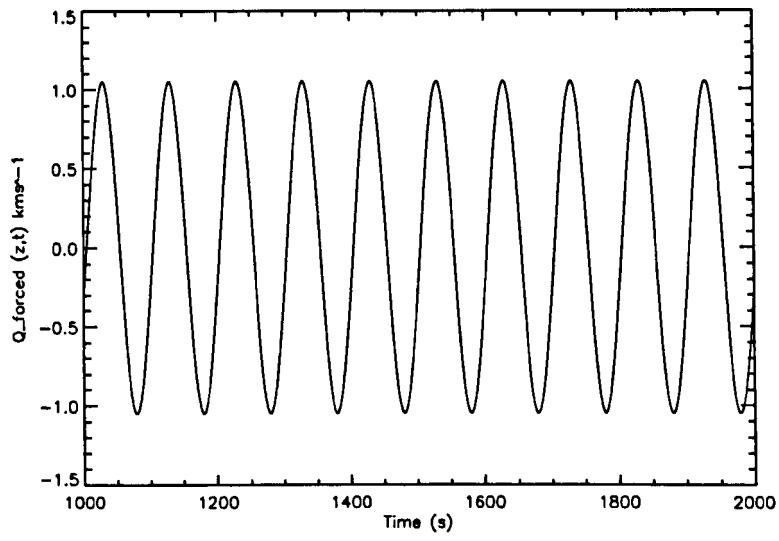

Figure 2.4: The forced atmospheric oscillations for the monochromatic driver against time. Curve plotted for z=500 km, $U_0(0) = e^{-500/2H}$ and a driver period of 50 s.

that the percentage difference in amplitude over the static case rises to the order of 25% at the limit of validity. Since the choice of imposed wave frequency relatively free, one may achieve extremely large percentage differences.

Free atmospheric oscillations

The free atmospheric oscillations given for the monochromatic driver plotted against time are shown in Fig. 2.6. The curve shows the real part of the free oscillations given by Eq. (2.100) and is plotted for $V_0 = 1$ kms^{-1}, $z = 500$ km and a footpoint flow of $U_0(0) = e^{-500/2H}$. The $t^{-2/3}$ dependance is clearly seen.

From the equations presented in Section 2.2.7 it can be seen that the effect of the background flow is to increase the amplitude of the resulting free atmospheric oscillations and to introduce a phase shift. For each of the three drivers considered, the monochromatic source, the delta function source and the sinusoidal pulse, the percentage difference between the amplitude of the free atmospheric oscillations in dynamic case and the static case is the same and is given by

$$\left[\sqrt{1-\frac{3\lambda}{t}+\lambda^2\left(\frac{9}{4t^2}+\Omega_T^2\right)}-1\right]\times 100. \tag{2.141}$$

The percentage increase in amplitude between the dynamic and static case is plotted in Fig. 2.7. Two sets of curves are shown; the leftmost set correspond to a footpoint flow that is applicable up to $z = 500$ km, the rightmost to a footpoint flow valid up to $z = 2000$ km. The solid, dotted and dashed lines correspond to times of $t = 1000, 2000$ and 3000 s respectively. By inspection one may conclude that the amplitude of the free atmospheric oscillations is increased by a maximum of approximately 1.5% for both magnitudes of footpoint flow. Note that if the curves for the larger footpoint flow (i.e. for $z_{max} = 500$ km) were to be extrapolated to higher heights

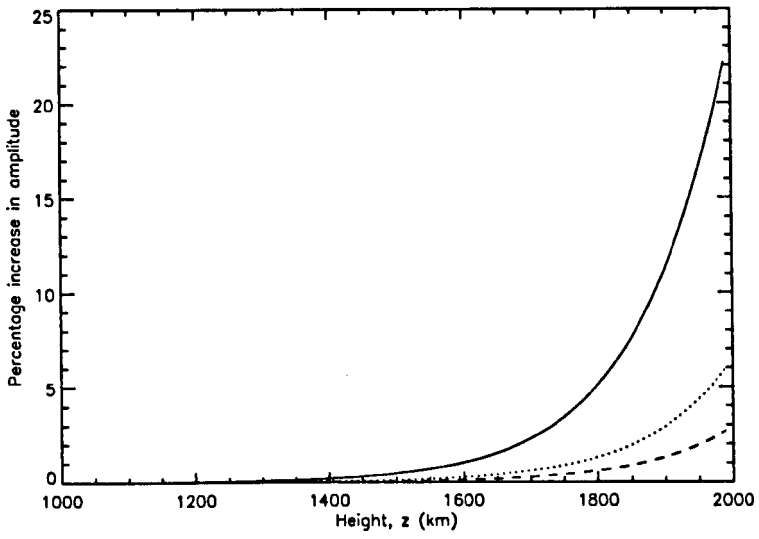

Figure 2.5: The percentage increase in amplitude of the forced atmospheric oscillations between the steady and static flux tubes. The solid, dotted and dashed curves correspond to ω =0.13, 0.06 and 0.04 s^{-1} respectively. All curves are plotted to $z_{max} = 2000$, giving $U_0(0) = e^{-2000/2H}$

then, the percentage increase in amplitude would be considerably larger and could be readily seen in Doppler-shifted spectral lines. However this value of larger footpoint flow may only be used up to the maximum height allowable, i.e. $z = 500$ km.
Further one may examine the percentage increase in amplitude against the magnitude of the footpoint flow, i.e shown in Fig. 2.8. The curve has been plotted for a height of $z = 500$ km and the solid, dashed, dotted and dot-dashed lines correspond to $t = 1000, 2000, 3000$ and 4000 s respectively. The magnitude of $U_0(0)$ ranges from zero to approximately 0.13 km/s, being the maximum permitted for this height. There is approximately 1% increase in amplitude in the dynamic case and that there is a further small increase for larger times. Turning our attention to the introduction of the phase angle, α, by the flow, Fig. 2.9 shows that the phase angle is relatively constant at approximately 1 radian and is practically unaffected by time. The curve has been plotted under the same conditions as the previous figure.

2.4 Conclusions

The propagation of magnetic tube waves in a stratified thin, isothermal flux tube with an internal equilibrium background flow has been studied. The governing equations have been solved by Laplace transforms and perturbation analysis, and been applied for conditions appropriate to the solar atmosphere. It was found that for each of the three footpoint drivers considered, namely a monochromatic source, a delta function pulse and a sinusoidal pulse, that the effect of the flow was to introduce a change in amplitude and phase, with both changes being functions of height, in both the forced and free atmospheric oscillations. The percentage increase in amplitude for the forced terms has been shown to be strongly dependent on the applied wave frequency. For a driving period of 50 s it is shown that the difference over the static case may be up to 25% at the largest heights. Smaller periods will result in even larger differences.

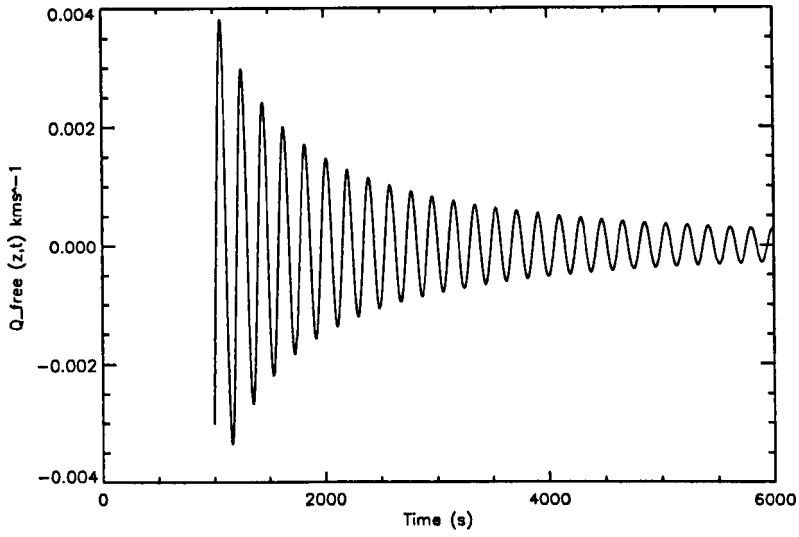

Figure 2.6: The free atmospheric oscillations for the monochromatic driver against time. Curve plotted for z=500 km and $U_0(0) = e^{-500/2H}$.

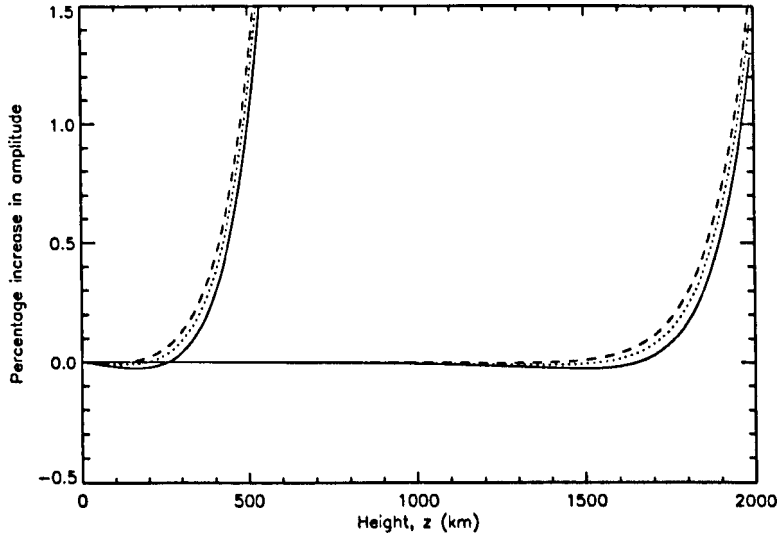

Figure 2.7: The percentage increase in amplitude of the free oscillations between the steady and static cases against height. Two sets of curves are plotted; the leftmost corresponds to a footpoint flow valid up to $z = 500$ km, the rightmost to a footpoint flow valid up to $z = 2000$ km. The solid, dotted and dashed lines correspond to times of $t = 1000, 2000$ and 3000 s respectively.

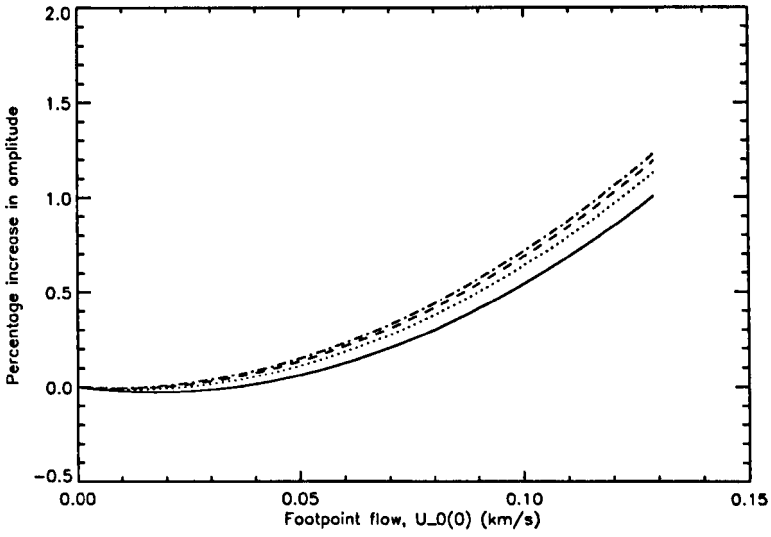

Figure 2.8: The percentage increase in amplitude of the free oscillations between the steady and static cases against footpoint flow. The curve is plotted for $z = 500$ km and the solid, dashed, dotted and dot-dashed lines correspond to $t = 1000, 2000, 3000$ and 4000 s respectively.

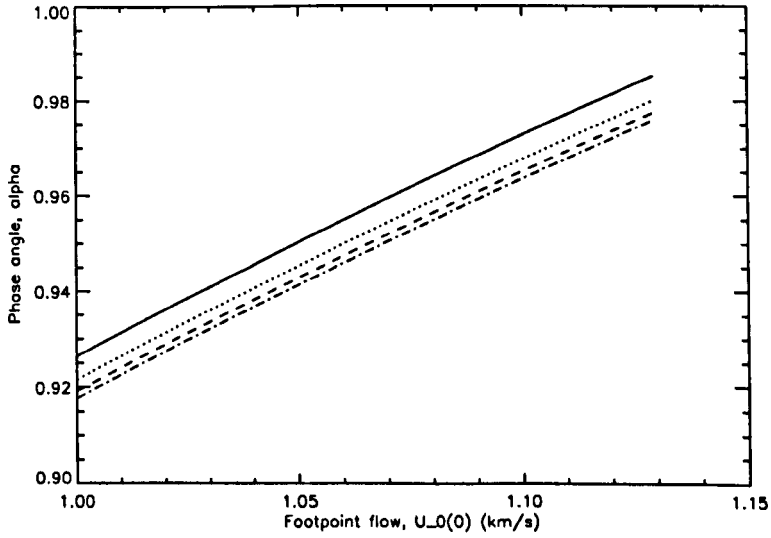

Figure 2.9: The phase angle between against footpoint flow. The curve is plotted for $z = 500$ km and the solid, dashed, dotted and dot-dashed lines correspond to $t = 1000, 2000, 3000$ and 4000 s respectively.

For the free oscillations, the dominant characteristic of the temporal decay at any given height (as $t^{-3/2}$) is relatively unaffected by the bulk flow. For a given footpoint flow it was found that the amplitude will increase with height up to the validity of the analysis. The maximum percentage increase in amplitude is given at the highest z that is analytically still valid and is around 1.5 % when compared to the static case. Although this seems relatively small it must be remembered that we are severely restricted in the magnitude of the footpoint flow we may choose. It can also be noted that the frequency of the free atmospheric oscillations is the same in the steady and static cases. This is perhaps surprising, but it is noted that the background flows of second order and higher have been considered small compared to the characteristic speeds, which is a possible factor. The results presented in this paper may have important observational consequences, especially when flux tube diagnostics are carried out using the tools of magnetic seismology.

3

Transverse wave propagation in steady stratified waveguides

This Chapter studies the propagation of transverse magnetic tube waves in a stratified isothermal flux tube with the presence of an internal equilibrium background flow. The governing differential equation is solved by means of Laplace transforms, and temporal and spatial solutions are developed, with boundary conditions given by various footpoint drivers, namely a monochromatic source, a delta function pulse and a sinusoidal pulse. It is found that for small flows the governing equation for transverse waves is formally similar to that for longitudinal waves. Thus the effect of the background flow is to introduce an increase in amplitude and changes in phase shift when compared with the corresponding static case. When the source is driven continuously the forced atmospheric oscillations are shown to have large percentage differences over the corresponding static case. For the free atmospheric oscillations percentage increases in amplitude of the order of a few percent are found and vary greatly in height but are practically unaltered in time.

3.1 Introduction

The launch of the Hinode satellite in September 2006 has spawned a new era in high-resolution solar observation. Using the high spatial ($\sim$ 150 km) and temporal ($\sim$ 5 s) resolution of the Solar Optical Telescope (SOT) aboard Hinode, De Pontieu *et al.* (2007) report observations that are interpreted as Alfvén waves. Alfvén waves, existing purely because of the magnetic field, have been proposed as an energy transporter that may explain the heating of the corona and the solar wind. De Pontieu *et al.* (2007) found that spicules, which dominate the chromosphere, undergo a oscillatory motion perpendicular to the spicule axis, i.e. in the direction perpendicular to the magnetic field. These transverse motions have been inferred to be Alfvén waves, in the sense that they describe incompressible transverse MHD waves propagating along the magnetic field. They note that the observations could be interpreted as MHD kink modes, if the presence of a stable waveguide exists. They also report that simulations performed show ubiquitous Alfvén waves, with similar properties to the observations. Further they found no evidence for stable waveguides existing in the chromosphere, casting doubt on the applicability of the classical model of a magnetic flux tube in such dynamic events. An alternative explanation of these observations are proposed to be transversal kink oscillations (Erdélyi & Fedun, 2007). Estimates of the energy flux show that Alfvén waves provide enough energy to heat the corona and drive the solar wind. Further Hinode observations reported by Okamoto *et al.* (2007) show Alfvén waves propagating in solar prominences, clouds of cool (10^4 K) plasma supported in the corona, which may also have a role in the heating of the corona.

Thus there is a clear need to investigate transverse oscillations in the light of recent observations. In general a magnetic flux tube may support three types of wave; longitudinal, transverse and torsional waves. Musielak *et al.* (1989) noted that the amount of energy carried by transverse waves is much larger than that carried by longitudinal waves. Spruit & Roberts (1983) have found that the generation of transverse wave is much easier than their longitudinal counterparts. Transverse wave propagation in static tubes has been studied by Spruit (1981), who laid the analytic framework and has been further examined by Musielak & Ulmschneider (2001) and Musielak & Ulmschneider (2003b). A brief summary of studies regarding transverse waves in static flux tubes has been discussed in Section 1.5.2. In this Chapter a background flow shall be introduced into a magnetic flux tube and its effect on the propagation of transverse waves shall be studied.

3.2 Transverse tube waves

This chapter closely follows Hargreaves & Erdélyi (2008). Consider an isolated magnetic flux tube embedded in an isothermal, field free environment, which is in temperature equilibrium with the surroundings. The derivation for transverse waves was first developed by Spruit (1981), the main points of which shall now be discussed, with particular reference given to the introduction of the flow. Given the decomposition of the Lorentz force, the momentum equation can be written in the following form

$$\rho\frac{D\mathbf{v}}{Dt} = -\nabla\left(p+\frac{B^2}{2\mu}\right)+\frac{(\mathbf{B}\cdot\nabla)\mathbf{B}}{\mu}+\rho\mathbf{g}. \tag{3.1}$$

The tube is assumed to be circular and untwisted (such that the kink instability and the propagation of twist by the torsional Alfvén wave may be ignored). A local coordinate system may be adopted along the tube given by $(r,\phi,\mathbf{l})$, where $\mathbf{l}$ is the unit vector along the tube. The tube is untwisted, thus $B_\phi = 0$ and since the tube is thin, B_r is small. In the local coordinate system

the magnetic field may be written as

$$\mathbf{B} = B(r,\phi,\mathrm{l})\hat{\mathbf{l}}, \tag{3.2}$$

where $\hat{\mathbf{l}}$ is the unit vector along the tube in the $\mathbf{l}$ direction. Any arbitrary vector may be decomposed into vectors parallel and perpendicular to the tube axis, such that

$$\mathbf{A} = \mathbf{A}_{\|} + \mathbf{A}_{\perp}, \tag{3.3}$$

where

$$\mathbf{A}_{\|} = (\hat{\mathbf{l}}\cdot\mathbf{A})\hat{\mathbf{l}}, \quad \mathbf{A}_{\perp} = (\hat{\mathbf{l}}\times\mathbf{A})\times\hat{\mathbf{l}}, \tag{3.4}$$

are the components parallel and perpendicular to the tube respectively. Since the Lorentz force is purely perpendicular to the field, and thus to the tube, the parallel component of the momentum equation is given by

$$\rho\left(\frac{D\mathbf{v}}{Dt}\right)_{\|} = (-\hat{\mathbf{l}}\cdot\nabla p + \rho\hat{\mathbf{l}}\cdot\mathbf{g})\hat{\mathbf{l}}. \tag{3.5}$$

Defining $\hat{\mathbf{l}}\cdot\nabla \equiv \partial/\partial l$, being the derivative along the tube, Eq. (3.5) may be rewritten as

$$\rho\left(\frac{D\mathbf{v}}{Dt}\right)_{\|} = (-\frac{\partial p}{\partial l} + \rho\hat{\mathbf{l}}\cdot\mathbf{g})\hat{\mathbf{l}}, \tag{3.6}$$

being the equation of motion for a fluid flowing along a tube at a certain angle to gravity. Defining $\mathbf{k} \equiv \partial\hat{\mathbf{l}}/\partial l$ as the curvature vector (a purely perpendicular quantity with $k_{\|} = 0$) gives

$$(\mathbf{B}\cdot\nabla)\mathbf{B} = \frac{1}{2}\frac{\partial B^2}{\partial l}\hat{\mathbf{l}} + B^2\mathbf{k}. \tag{3.7}$$

Thus the transverse component of the momentum equation can be written as

$$\rho\left(\frac{D\mathbf{v}}{Dt}\right)_{\perp} = -\left(\hat{\mathbf{l}}\times\nabla\left(p+\frac{B^2}{2\mu}\right)\right)\times\hat{\mathbf{l}} + \frac{B^2}{\mu}\mathbf{k} + \rho(\hat{\mathbf{l}}\times\mathbf{g})\times\hat{\mathbf{l}}. \tag{3.8}$$

Since the tube is thin, pressure equilibrium with the surroundings is assumed at all times. In a plane perpendicular to $\mathbf{g}$ the condition of pressure balance

$$p + \frac{B^2}{2\mu} = p_e', \tag{3.9}$$

holds, where $p_e' = p_e(z) + \delta p_e$, with $p_e(z)$ being the external pressure in the absence of the tube and δp_e being the disturbance in external pressure due to the tube's presence. Thus δp_e provides a back-reaction force onto the tube. In fact the back reaction may be treated separately and one can write

$$\nabla\left(p+\frac{B^2}{2\mu}\right) = \nabla p_e = \rho_e\mathbf{g}, \tag{3.10}$$

where ρ_e is the external density. Thus Eq. (3.8) can be written as

$$\rho\left(\frac{D\mathbf{v}}{Dt}\right)_{\perp} = \mathbf{F}_{\perp}, \tag{3.11}$$

where

$$\mathbf{F}_\perp = \frac{B^2}{\mu}\mathbf{k} + (\rho - \rho_e)(\hat{\mathbf{l}} \times \mathbf{g})\hat{\mathbf{l}}, \tag{3.12}$$

is the total force acting perpendicular to the tube axis.

As the tube moves through the external medium the external fluid has to be accelerated out of the way, thus giving rise to a back-reaction force onto the tube. Thus Eq. (3.11) may be rewritten to include the back-reaction force, yielding

$$\rho\left(\frac{D\mathbf{v}}{Dt}\right)_\perp = \mathbf{F}_\perp + \mathbf{F}_{\text{back}}. \tag{3.13}$$

Spruit (1981) assumed the external fluid flow around the tube was potential and incompressible and suggested the back-reaction term to be

$$\mathbf{F}_{\text{back}} = -\rho_e\left(\frac{D\mathbf{v}}{Dt}\right)_\perp, \tag{3.14}$$

which holds for a simple transverse motion of a straight circular flux tube through the external medium. Several authors have subsequently criticised this term and there has been considerable debate in recent years over the exact form the back-reaction should take, see Choudhuri (1990), Cheng (1992), Fan *et al.* (1994), Moreno-Insertis *et al.* (1996) and Osin *et al.* (1999). Osin *et al.* (1999) proposed their own back-reaction term which survives the criticisms leveled at the previous amendments. They suggested $\mathbf{F}_{\text{back}}$ should take the following form

$$\mathbf{F}_{\text{back}} = -\rho_e\left(\frac{D_\perp \mathbf{v}^\perp}{Dt}\right)^\perp, \tag{3.15}$$

which yields the transverse momentum equation

$$(\rho - \rho_e)\left(\frac{D\mathbf{v}}{Dt}\right)_\perp = (\rho v_A^2 - \rho_e v_\parallel^2)\mathbf{k} + 2\rho_e v_\parallel(\boldsymbol{\varpi} \times \hat{\mathbf{l}}) + (\rho - \rho_e)(\hat{\mathbf{l}} \times \mathbf{g})\hat{\mathbf{l}}, \tag{3.16}$$

where $v_\parallel$ is the magnitude of the flow along the tube and $\boldsymbol{\varpi}$ is the angular velocity of a fluid particle. Thus it is clear that when the flow along the tube is small, the differences between the Spruit (1981) back-reaction term and the Osin *et al.* (1999) term are negligible. Thus taking the bulk flow along the tube to be small at all heights yields the transverse momentum equation

$$(\rho - \rho_e)\left(\frac{D\mathbf{v}}{Dt}\right)_\perp = \rho v_A^2\mathbf{k} + (\rho - \rho_e)(\hat{\mathbf{l}} \times \mathbf{g})\hat{\mathbf{l}}, \tag{3.17}$$

which is the same as found by Spruit (1981). Since, for transverse waves, there is no variation in the tube cross section it follows that there are no pressure and density perturbations. Thus p and ρ may be replaced by their equilibrium values, p_0 and ρ_0. In the Cartesian coordinate system let $\hat{\mathbf{l}} = (l_x, 0, l_z)$, and thus the components of Eq. (3.17) in the x and z directions may be written as

$$\left(\frac{D\mathbf{v}}{Dt}\right)_x = -\frac{1}{\rho_0}\frac{\partial p_0}{\partial l}l_x - g l_x l_z + \frac{B^2}{\mu(\rho_0 + \rho_e)}k_x + \frac{\rho_0 - \rho_e}{\rho_0 + \rho_e}g l_x l_z, \tag{3.18}$$

$$\left(\frac{D\mathbf{v}}{Dt}\right)_z = -\frac{1}{\rho_0}\frac{\partial p_0}{\partial l}l_z - g l_z^2 + \frac{B^2}{\mu(\rho_0 + \rho_e)}k_z + \frac{\rho_0 - \rho_e}{\rho_0 + \rho_e}g l_x(1 - l_z^2). \tag{3.19}$$

If the tube is assumed to be nearly vertical, such that $\hat{\mathbf{l}} \approx \hat{\mathbf{z}}$, following Spruit (1981) and Musielak & Ulmschneider (2001) the horizontal displacement of the tube, $\xi(z)$, being a small quantity, may be given in terms of the unit vector $\hat{\mathbf{l}}$, such that

$$l_x = \frac{\partial \xi}{\partial z} = \left(\frac{\partial}{\partial t}\right)^{-1} \frac{\partial v_x}{\partial z}, \quad l_z = 1, \tag{3.20}$$

For the curvature vector one obtains

$$k_x = \frac{\partial^2 \xi}{\partial z^2} = \left(\frac{\partial}{\partial t}\right)^{-1} \frac{\partial^2 v_x}{\partial z^2}, \quad k_z = 0. \tag{3.21}$$

Thus Eq. (3.18) may be rewritten as

$$\frac{\partial}{\partial t}\left(\frac{D\mathbf{v}}{Dt}\right)_x = \left[-\frac{1}{\rho_0}\frac{\partial p_0}{\partial l} - g + \frac{\rho_0 - \rho_e}{\rho_0 + \rho_e} g\right] \frac{\partial v_x}{\partial z} + \frac{B^2}{\mu(\rho_0 + \rho_e)} \frac{\partial^2 v_x}{\partial z^2}. \tag{3.22}$$

The magnetic field in the Cartesian system is given by $\mathbf{B} = B_1(z)\hat{\mathbf{x}} + B_{0z}(z)\hat{\mathbf{z}}$, where $\hat{\mathbf{z}}$ and $\hat{\mathbf{x}}$ are the unit vectors in the z and x direction respectively and the perturbation in the magnetic field in given by B_1. Examining the term containing the magnetic field yields

$$\frac{B^2}{\mu(\rho_0 + \rho_e)} \frac{\partial^2 v_x}{\partial z^2} = \frac{B_{0z}^2}{\mu(\rho_0 + \rho_e)} \frac{\partial^2 v_x}{\partial z^2}, \tag{3.23}$$

since the products of the small perturbed quantities may be ignored. Thus the kink speed, the characteristic speed for the propagation of kink waves, may be defined as

$$c_k = \frac{B_{0z}}{\sqrt{\mu(\rho_0 + \rho_e)}}. \tag{3.24}$$

In much the same manner as for the magnetic field, the total velocity is given by $\mathbf{v} = v_x(z)\hat{\mathbf{x}} + U_0(z)\hat{\mathbf{z}}$, which has introduced the internal background flow. Thus

$$\left(\frac{D\mathbf{v}}{Dt}\right)_x = \frac{\partial v_x}{\partial t} + U_0 \frac{\partial v_x}{\partial z}, \tag{3.25}$$

$$\left(\frac{D\mathbf{v}}{Dt}\right)_z = U_0 \frac{\partial U_0}{\partial z}. \tag{3.26}$$

Thus the x-component of the momentum equation is given by

$$\frac{\partial^2 v_x}{\partial t^2} + U_0 \frac{\partial^2 v_x}{\partial t \partial z} = \left[-\frac{1}{\rho_0}\frac{\partial p_0}{\partial l} - g + \frac{\rho_0 - \rho_e}{\rho_0 + \rho_e} g\right] \frac{\partial v_x}{\partial z} + \frac{B_{0z}^2}{\mu(\rho_0 + \rho_e)} \frac{\partial^2 v_x}{\partial z^2}. \tag{3.27}$$

Attention may now be turned to the vertical component and Eq. (3.19) may be written as

$$\left(\frac{D\mathbf{v}}{Dt}\right)_z = -\frac{1}{\rho_0}\frac{\partial p_0}{\partial z} - g. \tag{3.28}$$

Given Eq. (3.26) this equation becomes

$$U_0 \frac{\partial U_0}{\partial z} = -\frac{1}{\rho_0}\frac{\partial p_0}{\partial z} - g, \tag{3.29}$$

which is the equilibrium equation for fluid flowing along a tube, discussed in the case of longitudinal waves in Chapter 2 and given in Eq. (2.6). Thus the discussion given in Section 2.2.1

holds and, given that the background flow is assumed small, Eq. (3.27) becomes

$$\frac{\partial^2 v_x}{\partial t^2} + U_0 \frac{\partial^2 v_x}{\partial t \partial z} - \frac{\rho_0 - \rho_e}{\rho_0 + \rho_e} g \frac{\partial v_x}{\partial z} - c_k^2 \frac{\partial^2 v_x}{\partial z^2} = 0. \tag{3.30}$$

Noting the fact that

$$\frac{\rho_0 - \rho_e}{\rho_0 + \rho_e} g = -\frac{c_k^2}{2H}, \tag{3.31}$$

where H is the scale height, means Eq. (3.30) may be rewritten as

$$\frac{\partial^2 v_x}{\partial t^2} + U_0 \frac{\partial^2 v_x}{\partial t \partial z} + \frac{c_k^2}{2H} \frac{\partial v_x}{\partial z} - c_k^2 \frac{\partial^2 v_x}{\partial z^2} = 0. \tag{3.32}$$

The substitution $v_x = e^{z/4H} Q$ gives

$$\frac{\partial v_x}{\partial z} = \left(\frac{Q}{4H} + \frac{\partial Q}{\partial z} \right) e^{z/4H}, \quad \frac{\partial^2 v_x}{\partial z^2} = \left(\frac{Q}{16H^2} + \frac{1}{2H} \frac{\partial Q}{\partial z} + \frac{\partial^2 Q}{\partial z^2} \right) e^{z/4H}, \tag{3.33}$$

whereupon substitution into Eq. (3.32) yields

$$\frac{\partial^2 Q}{\partial t^2} + \frac{U_0}{4H} \frac{\partial Q}{\partial t} + U_0 \frac{\partial^2 Q}{\partial t \partial z} - c_k^2 \frac{\partial^2 Q}{\partial z^2} + \Omega_k^2 Q = 0, \tag{3.34}$$

where $\Omega_k^2 = c_k^2 / 16H^2$ is the cutoff frequency associated with transverse kink waves. Examination of Eq. (3.34) shows it is formally similar to Eq. (2.47) in Chapter 2, which is an important result since it shows that both transverse and longitudinal waves with the presence of a small background flow are governed by the same governing equation. Indeed Eq. (3.34) returns exactly the same form as Eq. (2.47) with the substitution $U_0 = 2\bar{U}_0$, albeit with the concomitant changes of frequency and speed. Thus the solutions developed in Section 2.2 may be quoted directly and there is no need to re-derive them.

3.2.1 Solution by Laplace transforms and perturbation methods

Following the discussion in Chapter 2 the Laplace transform of Eq. (3.34) may be taken, giving

$$\frac{\partial^2 q(s,z)}{\partial z^2} - \frac{U_0 s}{c_k^2} \frac{\partial q(s,z)}{\partial z} - \frac{1}{c_T^2} \left(\Omega_k^2 + s^2 + \frac{U_0 s}{4H} \right) q(s,z) = 0, \tag{3.35}$$

where $q(s,z) = \mathcal{L}[Q(t,z)]$ and is subject to the following boundary conditions

$$\lim_{t \to 0,\, z \neq 0} Q(t,z) = 0, \qquad \lim_{t \to 0,\, z \neq 0} \frac{\partial Q}{\partial t} = 0,$$

$$\lim_{z \to 0} Q(t,z) = V(t), \qquad \lim_{z \to \infty} Q(t,z) = 0. \tag{3.36}$$

Solving Eq. (3.35) as regular perturbation problem yields

$$q(s,z) = v(s) \left[e^{-sz/c_k} - \frac{\Omega_k z}{c_k} \mathcal{L}[W(t,z)] \right] [1 + \lambda_k(z) s], \tag{3.37}$$

where

$$W(t,z) = \frac{J_1(\Omega_k \sqrt{t^2 - (z/c_k)^2})}{\sqrt{t^2 - (z/c_k)^2}} \mathcal{H}(t - z/c_k), \tag{3.38}$$

and

$$\lambda_k = \frac{U_0(0)H(e^{z/2H}-1)}{c_k^2}, \tag{3.39}$$

which has been subscripted with k to distinguish it from the term λ used in Chapter 2 for longitudinal waves. Using the second shift and convolution theorems in turns yields

$$\begin{aligned} Q(t,z) &= V(t-z/c_k)\mathcal{H}(t-z/c_k) - \frac{\Omega_k z}{c_k}[V(t)*W(t,z)] + \\ &+\lambda_k[(V(t-z/c_k)\mathcal{H}(t-z/c_k))*\delta'(t)] - \frac{\Omega_k z\lambda_k}{c_k}[(V(t)*W(t,z))*\delta'(t)], \end{aligned} \tag{3.40}$$

being an equation describing the evolution of transverse waves in a magnetic flux tube with the presence of a background flow.

3.2.2 Atmospheric response to various photospheric drivers

Eq. (3.40) may now be solved subject to various footpoint drivers, namely a monochromatic source, a delta-function source and a sinusoidal pulse. Since the governing equation is formally similar to the equation derived in Chapter 2 the solutions may be quoted directly.

Monochromatic Source

The required boundary condition is given by

$$V(t) = V_0 e^{-i\omega t}, \tag{3.41}$$

where ω is the frequency of the driven waves. The solution for the monochromatic driver is given by

$$\begin{aligned} Q(t,z) &= V_0(1-i\lambda_k\omega)e^{-i(\omega t+\sqrt{\omega^2-\Omega_k^2}\,z/c_k)} + \frac{V_0 z\Omega_k}{c_k}\sqrt{\frac{2}{\pi\Omega_k}}\frac{1}{t^{3/2}}\frac{1}{\omega^2-\Omega_k^2}\times \\ &\times\left[\Omega_k\left(1-\lambda_k i\omega-\frac{3}{2}\frac{\lambda_k}{t}\right)\sin\mu + i\omega\left(1-\lambda_k\frac{i\Omega_k^2}{\omega}-\frac{3}{2}\frac{\lambda_k}{t}\right)\cos\mu\right], \end{aligned} \tag{3.42}$$

where $\mu = \Omega_k t - 3\pi/4$. The effect of the background flow is introduced via the λ_k term, which upon setting to zero yields the static solution found by Musielak & Ulmschneider (2003b). The solution is comprised of free and forced atmospheric oscillations. The effect of the flow on the forced term is highlighted by examining the real part, which gives

$$\Re[Q_{Forced}(t,z)] = V_0\sqrt{1+(\omega\lambda_k)^2}\cos(\xi+\psi), \tag{3.43}$$

where $\xi = \omega t + (\omega^2-\Omega_k^2)^{1/2}\,z/c_k$ and $\psi = \arctan(\lambda_k\omega)$. An increase in amplitude and a phase shift have been introduced. Both these effects are dependent on λ_k, and hence the magnitude of the flow and also on the wave frequency, ω. The free atmospheric oscillations are dominated temporally by the $t^{-3/2}$ term. The presence of the flow introduces a secondary temporal dependance, given by the $3\lambda_k/2t$ term. Despite the fact that t is considered to be large, the effect of this term may become significant when solar parameters are considered. The addition of flow

no longer renders the amplitude linear with height. This may be shown by considering the real part of the free oscillations in Eq. (3.42), and rewriting the equation as

$$\Re[Q_{Free}(t,z)] = \frac{V_0 z\Omega_k}{c_k}\sqrt{\frac{2}{\pi\Omega_k}}\frac{1}{t^{3/2}}\frac{1}{\omega^2-\Omega_k^2}\left[\Omega_k\sqrt{\left(1-\frac{3\lambda_k}{2t}\right)^2+(\lambda_k\Omega_k)^2}\sin(\mu+\alpha)\right], \tag{3.44}$$

where

$$\alpha = \arctan\frac{\Omega_k t}{t/\lambda_k - 3/2}. \tag{3.45}$$

Thus there is a change in amplitude and phase that is a function of time, height and the value of the background flow. The increase in amplitude and phase shift of the free atmospheric oscillations are not dependent on the wave frequency, ω.

For the special case of a monochromatic driver with frequency matching the kink cutoff frequency, given by the boundary condition

$$V(t) = V_0 e^{-i\Omega_k t}, \tag{3.46}$$

the solution is given by

$$\begin{aligned} Q(t,z) &= V_0(1-i\lambda_k\Omega_k)e^{-i\Omega_k t} + \\ &+\frac{z\Omega_k V_0}{c_k}\sqrt{\frac{2}{\pi\Omega_k}}\left[\frac{e^{i\mu}}{t^{3/2}}\left(\frac{1}{i\Omega_k}-\frac{\lambda_k}{4}-i\frac{3\lambda_k}{8\Omega_k t}\right)+\frac{e^{-i\mu}}{t^{1/2}}\left(1-\frac{\lambda_k}{2t}-i\Omega_k\lambda_k\right)\right]. \end{aligned} \tag{3.47}$$

It is necessary to take $t \longrightarrow \infty$ when $\omega \longrightarrow \Omega_k$, thus Eq. (3.47) reduces to

$$Q(t,z) = V_0(1-i\lambda_k\Omega_k)e^{-i\Omega_k t}, \tag{3.48}$$

showing only the forced term remains. An amplitude increase and phase shift have been introduced, which may be seen by considering the real part of Eq. (3.48), such that

$$\Re[Q_{Forced}(t,z)] = V_0\sqrt{1+(\Omega_k\lambda_k)^2}\cos(\Omega_T+\phi), \tag{3.49}$$

where $\phi = \arctan(\lambda_k\Omega_k)$. The amplitude increase and phase shift are functions of Ω_k rather than ω since the system is being driven at the cutoff frequency.

Delta-function driver

The required boundary condition in this case is given by

$$V(t) = V_0\delta(\bar{t}), \tag{3.50}$$

where $\bar{t} = t/P_k$, with $P_k = 2\pi/\Omega_k$, being a dimensionless time. The total solution determined in terms of the original time variable, t, is given by

$$Q(t,z) = \frac{-2\pi z V_0}{c_k}\sqrt{\frac{2}{\pi\Omega_k}}\frac{1}{t^{3/2}}\left[\cos\mu - \frac{3}{2}\frac{\lambda_k}{t}\cos\mu - \lambda_k\Omega_k\sin\mu\right]. \tag{3.51}$$

Since the pulse has long passed only the free terms remain, which are dominated by the $t^{-3/2}$ term and oscillate at the cutoff frequency, Ω_k. The effect of the flow can be emphasised by rewriting Eq. (3.51) in the following form

$$Q(t,z) = \frac{-2\pi z V_0}{c_k}\sqrt{\frac{2}{\pi\Omega_k}}\frac{1}{t^{3/2}} \times \left[\sqrt{\left(1-\frac{3\lambda_k}{2t}\right)^2 + (\lambda_k\Omega_k)^2}\cos(\mu-\alpha)\right]. \tag{3.52}$$

Thus the effect is much the same as for the monochromatic driver: the amplitude is modified in a non-trivial fashion, being a function of time, height and the magnitude of the background flow, and a phase shift is introduced.

Sinusoidal pulse driver

The footpoint boundary condition is

$$V(t) = [\mathcal{H}(t) - \mathcal{H}(t-P)]e^{-i\omega t}. \tag{3.53}$$

The total solution in this case is then given by

$$\begin{aligned} Q(t,z) \;=\; & \frac{-\Omega_T z V_0}{c_k}\sqrt{\frac{2}{\pi\Omega_k}}\frac{1}{\omega^2-\Omega_k^2}\frac{1}{t^{3/2}} \times \\ & \times\left[\left(\Omega_k - \frac{3}{2}\frac{\lambda_k\Omega_k}{t} - i\lambda_k\omega\Omega_k\right)\sin\theta - \left(\Omega_k - \frac{3}{2}\frac{\lambda_k\Omega_k}{t} - i\lambda\omega\Omega_k\right)\sin\mu + \right. \\ & \left. + \left(i\omega - \frac{3}{2}\frac{i\omega\lambda_k}{t} + \lambda_k\Omega_k^2\right)\cos\theta - \left(i\omega - \frac{3}{2}\frac{i\lambda_k\omega}{t} + \lambda_k\Omega_k^2\right)\cos\mu\right], \end{aligned} \tag{3.54}$$

where $\theta = \Omega_T(t-P) - 3\pi/4$.
Since the pulse only was driven for one wave period only the free atmospheric oscillations remain. They decay as $t^{-3/2}$ and are at the cutoff frequency. However, also note that the solution is a function of the pulse frequency. It is interesting to observe in the case of $\omega \to \Omega_k$, the limit $t \to \infty$ needs to be imposed and thus there are no free terms present. The effect of the flow can be highlighted once more by considering the real part of Eq. (3.54), e.g. in the following form

$$\begin{aligned} \Re[Q_{Free}(t,z)] \;=\; & \frac{-\Omega_k z V_0}{c_k}\sqrt{\frac{2}{\pi\Omega_k}}\frac{1}{\omega^2-\Omega_k^2}\frac{1}{t^{3/2}} \times \\ & \times\Omega_k\sqrt{\left(1-\frac{3\lambda_k}{2t}\right)^2 + (\lambda_k\Omega_k)^2}\,[\sin(\theta+\alpha) - \sin(\mu+\alpha)]. \end{aligned} \tag{3.55}$$

The effect therefore is the same as for the previous drivers.

3.3 Application to the Sun

It is interesting to examine the nature of the kink speed, c_k, in terms of the tube speed for longitudinal waves, c_T, and the sound speed, c_0. To this end the c_k can be rewritten as in terms of the Alfvén speed such that

$$c_k^2 = \frac{v_A^2}{1+\rho_e/\rho_0}, \tag{3.56}$$

and employing the fact that

$$v_A^2 = \frac{2c_0^2}{\gamma\beta}, \tag{3.57}$$

and the condition of horizontal pressure balance yields the expression

$$c_k^2 = \frac{c_0^2}{\gamma(\beta+1/2)}. \tag{3.58}$$

Thus for $\gamma = 5/3$ in the zero β limit $c_k/c_0 \approx 1.1$ and in the case of $\beta \to \infty$, $c_k/c_0 \to 0$. Employing Eq. (2.140) one may eliminate the sound speed to give c_k in terms of the tube speed, c_T, yielding

$$c_k^2 = \frac{c_T^2(2+\gamma\beta)}{\gamma(1+2\beta)}. \tag{3.59}$$

Thus in the zero β limit $c_k/c_T \approx 1.1$ whereas for $\beta \to \infty$, $c_k/c_T \approx 0.7$. In cases other than the low-β plasma transverse tube waves travel slower than longitudinal tube waves. Relations may also be developed for the corresponding cutoff frequencies. Since $\Omega_k = c_k/4H$ and $\Omega_{AC} = c_0/2H$ one finds

$$\Omega_k = \frac{\Omega_{AC}}{2\sqrt{\gamma(\beta+1/2)}}, \tag{3.60}$$

and by employing Eq. (2.140) once more one obtains

$$\Omega_K = \frac{\Omega_T}{2}\sqrt{\frac{2+\gamma\beta}{\gamma(1+2\beta)}}\left(\frac{9}{4} - \frac{2}{\gamma} + 2\beta\frac{\gamma-1}{\gamma}\right)^{-1/2}. \tag{3.61}$$

Thus in the zero β limit $\Omega_k/\Omega_{AC} \approx 0.55$ and $\Omega_k/\Omega_T \approx 0.53$. Thus the kink cutoff is approximately half that of both the tube and sound speed in this limit. For $\beta \to \infty$, $\Omega_k/\Omega_{AC} \to 0$ and for $\beta \gg 0$, $\Omega_k/\Omega_T \approx 0.4/\sqrt{\beta}$, and thus decreases when the plasma β is increased. The cutoff frequency for tube waves varies little from the acoustic cutoff in the small and large β limits, whereas the range of frequencies that allow propagation for transverse waves is at least twice as large. It should be recalled that waves may propagate for $\omega > \Omega_k$ or else they are evanescent.

The solar parameters taken are the same as in Chapter 2, such that $g = 0.275$ km s^{-2} and $\gamma = 5/3$. Then for a sound speed $c_0 = 7.5$ km s^{-1}, a scale height of $H = 122.7$ km, yields an acoustic cutoff frequency of $\Omega_{AC} = 0.031$ s^{-1}. The plasma $\beta = 0.4$ which yields a kink speed of $c_k = 6.1$ km s^{-1} and a cutoff frequency of $\Omega_k = 0.012$ s^{-1}, giving $\Omega_k/\Omega_T = 0.4$. The preceding analysis has assumed that the background flow is small at all heights. Since the flow is exponentially increasing with z the magnitude of the footpoint flow, $U_0(0)$, needs to be carefully considered. This point has been discussed in Chapter 2 and highlighted in Fig. 2.2. The equilibrium flow introduces the term λ_k which has the dimensions of time and is given by Eq. (3.39). In Fig. 3.1, λ_k against z is plotted for two values of $U_0(0)$, the first curve corresponds to $U_0(0) = e^{-500/H}$ and the second $U_0(0) = e^{-2000/H}$. The general form of λ_k is the same as in the longitudinal case, since it is strongly dependent on the exponential nature of the flow, however it is seen that lower values are returned at all heights. This is due to the fact that for transverse waves the flow term is half than for longitudinal waves despite c_k being slightly smaller than an equivalent c_T.

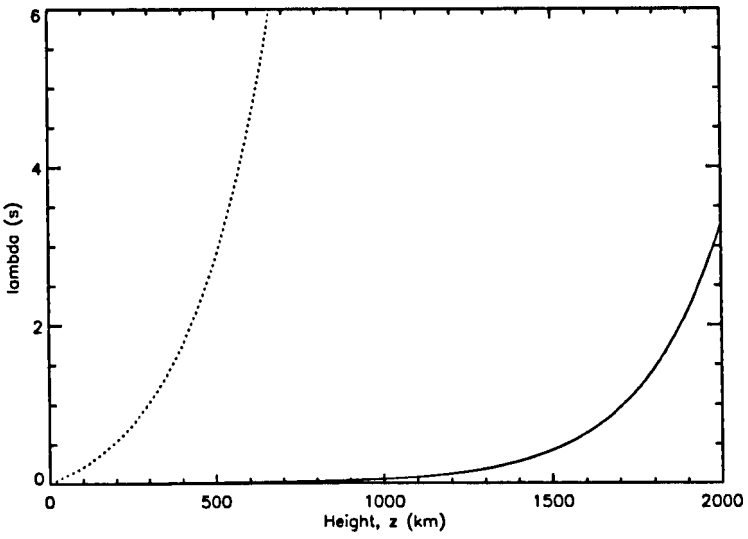

Figure 3.1: The variation of the flow timescale, λ_k, with height plotted for two magnitudes of footpoint flow, $U_0(0)$. The dotted line corresponds to $z_{max} = 500$, giving $U_0(0) = \exp(-500/2H)$. The solid line corresponds to $z_{max} = 2000$.

Forced atmospheric oscillations

For the case of the continuously driven monochromatic source, the forced atmospheric oscillations are obtained. Eq. (3.43) shows the real part of the forced oscillations has an amplitude increase and a phase shift when compared with its static counterpart. The percentage difference in amplitude between the static and steady cases is shown in Fig. 3.2 plotted for a footpoint flow magnitude of $U_0(0) = e^{-2000/H}$. The three curves correspond to propagating wave frequencies of ω=0.13, 0.06, 0.04 s^{-1} (i.e. wave periods of 50, 100, 150 s). For a wave period of 50 s it is seen that the percentage difference in amplitude over the static case is of the order 8% at the limit of validity. This is somewhat lower than for longitudinal waves and is expected since the corresponding values of $\lambda_k(z)$ are lower for the transverse case. Also note that smaller driving frequencies will result in substantially greater percentage differences.

Free atmospheric oscillations

For each of the three drivers considered the percentage difference between the amplitude of the free atmospheric oscillations in dynamic case and the static case is the same and is given by

$$\left[\sqrt{1-\frac{3\lambda_k}{t}+\lambda_k^2\left(\frac{9}{4t^2}+\Omega_k^2\right)}-1\right]\times 100. \tag{3.62}$$

The percentage increase in amplitude between the dynamic and static case is plotted in Fig. 3.3. Two sets of curves are shown; the leftmost set correspond to a footpoint flow that is applicable up to $z = 500$ km, the rightmost to a footpoint flow valid up to $z = 2000$ km. The solid, dotted and dashed lines correspond to times of $t = 1000, 2000$ and 3000 s respectively. Fig. 3.3 shows the interesting result that the amplitude actually decreases before the exponential nature of λ_k dominates. The leftmost set of curves ($z_{\max} = 500$ km) show a maximum percentage increase of the order 1.5% at the $z \approx 1000$ km. However it should be noted that this is beyond

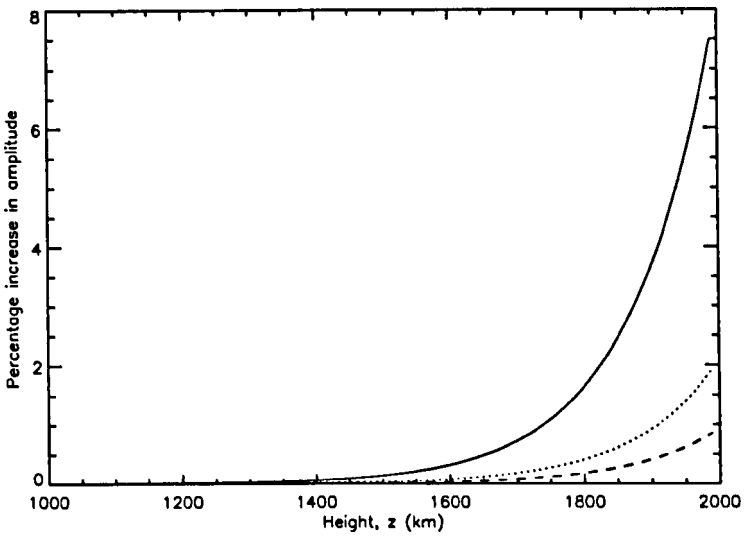

Figure 3.2: The percentage increase in amplitude of the forced atmospheric oscillations between the steady and static flux tubes. The solid, dotted and dashed curves correspond to ω =0.13, 0.06 and 0.04 s^{-1} respectively. All curves are plotted to z_{max} = 2000, giving $U_0(0) = e^{-2000/2H}$

the limit of validity, thus up to $z = 500$ km the trend shows a small reduction in amplitude in comparison to the static case. For the rightmost set of curves ($z_{\max} = 2000$ km) a similar trend is shown. In fact this effect is seen in the longitudinal case but it is extremely small. Further one may examine the percentage increase in amplitude against the magnitude of the footpoint flow, i.e shown in Fig. 3.4. The curve has been plotted for a height of $z = 500$ km and the solid, dashed, dotted and dot-dashed lines correspond to $t = 1000, 2000, 3000$ and 4000 s respectively. The magnitude of $U_0(0)$ ranges from zero to approximately 0.13 km/s, being the maximum permitted for this height. It can be seen that there is a small decrease in amplitude over the range of permitted footpoint flow values, although the percentage difference increases with time. Fig. 3.5 examines the phase angle, α, introduced by the flow, and shows that the phase angle is relatively constant at approximately 0.3 radians and is practically unaffected by time. The curve has been plotted under the same conditions as the Fig. 3.4.

3.4 Conclusions

The propagation of transverse kink waves in a stratified thin, isothermal flux tube with an internal small equilibrium background flow has been studied. The governing equations have been solved by Laplace transforms and perturbation analysis, and been applied for conditions appropriate to the solar photosphere. It is found that the governing equation for transverse waves is formally similar to that for longitudinal waves. This is an interesting and important result, although is perhaps expected since transverse and longitudinal waves are governed by the same KG equation in the static case. The difference between the two governing equations arises due to the magnitude of the flow terms and the obvious change in characteristic speed and frequency. Thus the results mirror those found in Chapter 2, but with some interesting differences. Since the relative size of λ_k is smaller than λ found in the longitudinal case, the magnitude of

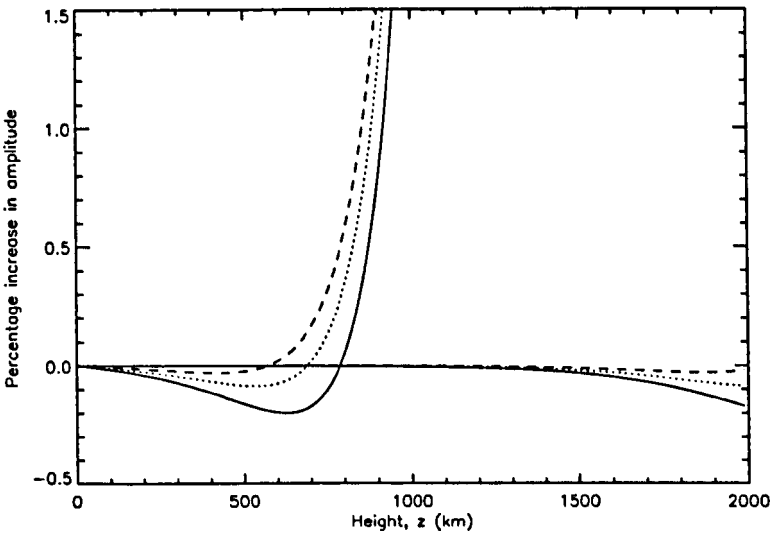

Figure 3.3: The percentage increase in amplitude of the free oscillations between the steady and static cases against height. Two sets of curves are plotted; the leftmost corresponds to a footpoint flow valid up to $z = 500$ km, the rightmost to a footpoint flow valid up to $z = 2000$ km. The solid, dotted and dashed lines correspond to times of $t = 1000, 2000$ and 3000 s respectively.

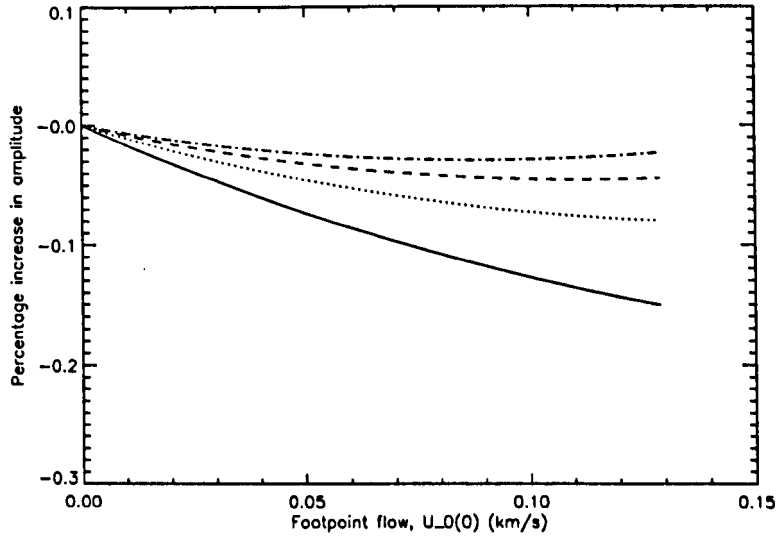

Figure 3.4: The percentage increase in amplitude of the free oscillations between the steady and static cases against footpoint flow. The curve is plotted for $z = 500$ km and the solid, dashed, dotted and dot-dashed lines correspond to $t = 1000, 2000, 3000$ and 4000 s respectively.

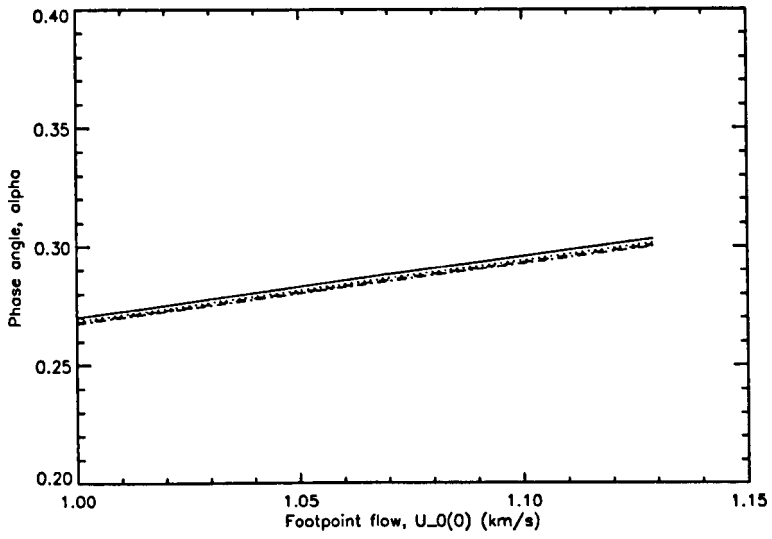

Figure 3.5: The phase angle between against footpoint flow. The curve is plotted for $z = 500$ km and the solid, dashed, dotted and dot-dashed lines correspond to $t = 1000, 2000, 3000$ and 4000 s respectively.

the percentage differences is generally smaller. For the forced atmospheric oscillations the percentage increase is strongly dependent on the driving frequency and given a driving period of 50 *s* it is shown that the difference over the static case may be up to 8%. Smaller periods will result in even larger differences. For a footpoint flow of $U_0(0) = e^{-500/2H}$ (i.e. valid up to z=500 km) the free atmospheric oscillations show a small reduction in amplitude in comparison to the static case. At the limit of validity this difference is of the order -0.2%. At greater heights the exponential nature of the flow terms dominate and there is an increase in the amplitude, which will become large at appreciable heights. This however no longer assumes the flow is small at all heights. Thus for the free oscillations the effect of the small internal background flow has a somewhat negligible effect on the transverse wave characteristics.

4

Longitudinal MHD waves in stratified and viscous plasmas

The propagation of slow magnetohydrodynamic waves in vertical thin flux tubes embedded in a vertically stratified plasma in the presence of viscosity is shown to be governed by the Klein-Gordon-Burgers (KGB) equation, which is solved in two limiting cases assuming an isothermal medium in hydrostatic equilibrium surrounded by a quiescent environment. The results presented can be applied to, e.g., study the propagation of slow magnetohydrodynamic waves generated by footpoint motion, such as the granular buffeting in thin magnetic photospheric tubes. When the variation in the reduced velocity occurs over typical lengths much larger than the gravitational scale height, the KGB equation can be reduced to a KG equation which shows a wake oscillating with the frequency reduced by viscosity and the solution has no spatial or temporal decay when considering normal mode solutions. However, in the other limiting case, i.e., typical variations in the reduced velocity occur over characteristic lengths much smaller than the gravitational scale height, waves have a temporal and spatial decay. Applications to solar atmospheres are also considered and it is shown that the effect of viscosity is negligible for realistic photospheric values.

4.1 Introduction

It has been seen that magnetic field in solar and stellar atmospheres tends not to be diffuse but, instead, to concentrate in small cylindrical magnetic flux tubes or magnetic loops. Further we have seen that the magnetic field can be, as a first approximation, considered to be axial. Such structures are a perfect medium for MHD wave propagation. If the tube is sufficiently thin so that the radial variations can be neglected to leading order, one can apply the so-called thin flux tube approximation resulting in a much simpler mathematical analysis, e.g. Roberts & Webb (1978), Ferriz-Mas *et al.* (1989b). In this Chapter the propagation of linear longitudinal waves in a non-ideal (viscous) plasma is studied. All previous studies assumed waves propagating in an ideal medium, though it is widely recognized that the medium in which these waves can propagate is dissipative. The effect of non-adiabacity on the propagation of waves in stratified media solar plasmas was explored by Roberts (1983). Roberts argues that the cutoff frequencies actually are changed in the photosphere due to the stratification and the modes observed by, e.g. Giovanelli *et al.* (1978), De Pontieu *et al.* (2003b) are, in fact, non-adiabatic acoustic modes propagating along a slender magnetic flux tube. This idea was further exploited in detail by De Pontieu *et al.* (2004), De Pontieu *et al.* (2005). The effect of viscosity as the dissipative mechanism upon wave propagation in stratified waveguides has not yet been addressed. Viscosity is the measure of resistance to flow, or friction, in a fluid. In many textbook treatments of viscosity (e.g Priest, 1982) the viscous force appears in the momentum equation, see Eq. (1.26), in the following form

$$\mathbf{F}_\nu = \rho\nu\left(\nabla^2\mathbf{v} + \frac{1}{3}\nabla(\nabla\cdot\mathbf{v})\right), \tag{4.1}$$

where ν is the kinematic coefficient of viscosity, here assumed constant. However Eq. (4.1) is a simplification of the more general viscous force described by the Braginskii viscosity tensor (Braginskii, 1965). The quantity $\omega_i\tau_i$, where ω_i is the ion cyclotron frequency and τ_i is the mean collisional time between the ions, provides an important distinction in the discussion of the viscous force. For $\omega_i\tau_i \gg 1$ the full five-termed tensorial representation of viscosity needs to be employed, e.g Erdélyi & Goossens (1995). In this chapter however, the inequality $\omega_i\tau_i \ll 1$ is taken, such that the viscosity tensor may be assumed isotropic and Eq. (4.1) can be employed. For ρ in kg m^{-3} and temperature in K and for a fully ionised hydrogen plasma the viscosity is given by (Spitzer, 1962)

$$\nu = 2.21\times10^{-16}\frac{T^{5/2}}{\rho\ln\Lambda}\quad (\mathrm{m^2 s^{-1}}), \tag{4.2}$$

where $\ln\Lambda$ is a plasma parameter (the Coulomb logarithm), being weakly dependent on both temperature and pressure and is of the order 10-20. In this chapter the effect of dissipation (i.e. viscosity) on the propagation of waves in a thin magnetic flux tube filled with a vertically stratified plasma is investigated. Throughout the derivation it will be assumed, for the sake of simplicity, that the medium, in hydrostatic equilibrium, is isothermal and the temporal variation in the pressure outside the tube is the largest temporal scale in the problem. The mathematical derivation describing the propagation of longitudinal magnetoacoustic waves and it's solution will be presented in detail.

4.2 Governing equations

This section will closely follow Ballai, Erdélyi & Hargreaves (2006). Consider an isolated magnetic tube embedded in a magnetic free compressible and isothermal medium. It is supposed

that the coordinate system is such that the z-axis is parallel to the gravitational acceleration vector, i.e. $\mathbf{g} = -g\hat{\mathbf{z}}$. The tube is considered to be thin, with circular cross-section, $A(z)$, and in thermal equilibrium with its environment. Waves propagate in a plasma described by the pressure, $p(z)$ and density $\rho(z)$ and is permeated by a longitudinal magnetic field $B(z)$. The equilibrium of the tube is prescribed by the hydrostatic equilibrium

$$\frac{dp_0}{dz} = -\rho_0 g, \tag{4.3}$$

where the quantities with an index 0 describe the equilibrium state and the lateral pressure balance $p_0 + B_0^2/2\mu = p_e$, with p_e being the kinetic (thermal) pressure of the environment. We suppose oscillations with wavelengths comparable to the gravitational scale-height, H, which for an isothermal medium is a constant quantity. Since the equilibrium configuration is isothermal, the scale-height outside the tube will also be H. We suppose the z-dependence of the equilibrium quantities are given as

$$\begin{aligned} p_0(z) &= p_0(0)e^{-z/H}, \quad \rho_0(z) = \rho_0(0)e^{-z/H}, \\ B_0(z) &= B_0(0)e^{-z/2H}, \quad A_0(z) = A_0(0)e^{z/2H}, \end{aligned} \tag{4.4}$$

describing a barometric atmosphere. With these particular choices, the sound speed $(\gamma p_0/\rho_0)^{1/2}$, the Alfvén speed $B_0/(\mu\rho_0)^{1/2}$ and the cusp speed $c_T = c_0 v_A/(c_0^2 + v_A^2)^{1/2}$ are all constant quantities. Eq. (4.4) also verifies that the dependence of the magnetic field and the cross-section of the tube are such that the magnetic flux in the tube is always conserved.
The linear perturbation of the equilibrium state is governed by the system of equations

$$\frac{\partial}{\partial t}(\rho_0 A + \rho A_0) + \frac{\partial}{\partial z}(\rho_0 A_0 u) = 0, \tag{4.5}$$

$$\rho_0 \frac{\partial u}{\partial t} + \frac{\partial p}{\partial z} + \rho g = \frac{4}{3}\nu\rho_0 \frac{\partial^2 u}{\partial z^2}, \tag{4.6}$$

$$\frac{\partial p}{\partial t} + u\frac{dp_0}{dz} = c_0^2\left(\frac{\partial \rho}{\partial t} + u\frac{\partial \rho_0}{\partial z}\right), \tag{4.7}$$

where u is the component of the velocity along the z-axis. These equations must be supplemented by two equations which describe the conservation of the magnetic flux and the conservation of total pressure (the sum of the kinetic and magnetic pressure) inside the tube is balanced at the boundary by the external kinetic pressure, p_e. These two conditions are expressed as

$$B_0 A + B A_0 = 0, \quad p + \frac{B_0}{\mu}B = p_e. \tag{4.8}$$

In Eq. (4.6) ν is the coefficient of kinematic viscosity (here considered as a constant quantity). Taking the time derivative of Eq. (4.6) and employing Eq. (4.3) and Eq. (4.7) yields

$$\rho_0 \frac{\partial^2 u}{\partial t^2} + \left[\frac{\partial}{\partial z} + \frac{g}{c_0^2}\right]\frac{\partial p}{\partial t} - \frac{g^2\rho_0 u}{c_0^2} - g\frac{\partial \rho}{\partial z}u - \frac{4}{3}\nu\rho_0\frac{\partial^2}{\partial z^2}\left[\frac{\partial u}{\partial t}\right]. \tag{4.9}$$

Examining the time derivative of the condition of pressure balance and employing the conservation of magnetic flux gives

$$\frac{\partial p}{\partial t} = \frac{\partial p_e}{\partial t} + \frac{B_0^2}{\mu A_0}\frac{\partial A}{\partial t}. \tag{4.10}$$

Thus it is readily shown that

$$\frac{\partial p}{\partial t} = \frac{c_T^2}{v_A^2}\frac{\partial p_e}{\partial t} - \frac{c_T^2}{A_0}\frac{\partial}{\partial z}[\rho_0 A_0 u] + \frac{c_T^2 \rho_0 g u}{c_0^2} + c_0^2 \frac{\partial \rho_0}{\partial z} u. \tag{4.11}$$

Given the equilibrium conditions

$$\frac{A_0'}{A_0} = \frac{1}{2H}, \quad \frac{\rho_0'}{\rho_0} = \frac{-1}{H}, \tag{4.12}$$

where the prime indicates the derivative in the z-direction, and the substitution of Eq. (4.11) into Eq. (4.9) one finds, after some algebra, that

$$\frac{\partial^2 u}{\partial t^2} - c_T^2 u'' + \frac{c_T^2}{2H}u' + \left[\frac{c_T^2}{2H^2} - \frac{g c_T^2}{2H c_0^2} + \frac{g^2 c_T^2}{c_0^4} - \frac{g c_T^2}{H c_0^2} - \frac{g^2}{c_0^2} + \frac{g}{H}\right] u - \\ -\frac{4}{3}\nu\left[\frac{\partial u}{\partial t}\right]'' = -\frac{1}{\rho_0}\frac{c_T^2}{v_A^2}\frac{\partial}{\partial t}\left[p_e' + \frac{g}{c_0^2}p_e\right]. \tag{4.13}$$

Substituting the well known reduced speed

$$u(t,z) = e^{z/4H} Q(t,z), \tag{4.14}$$

into Eq. (4.13) yields the inhomogeneous Klein-Gordon-Burgers (KGB) equation

$$\frac{\partial^2 Q}{\partial t^2} - c_T^2 \frac{\partial^2 Q}{\partial z^2} + \Omega_T^2 Q - \frac{4}{3}\nu\frac{\partial}{\partial t}\left(\frac{1}{16H^2} + \frac{1}{2H}\frac{\partial}{\partial z} + \frac{\partial^2}{\partial z^2}\right) Q = \\ -\frac{e^{-z/4H}}{\rho_0(z)}\left(\frac{c_T}{v_A}\right)^2 \frac{\partial}{\partial t}\left(\frac{\partial p_e}{\partial z} + \frac{g}{c_0^2}p_e\right), \tag{4.15}$$

where Ω_T^2 is given by

$$\Omega_T^2 = \left(\frac{9}{4} - \frac{2}{\gamma}\right)\Omega_{AC}^2 - \left(\frac{3}{2} - \frac{2}{\gamma}\right)^2 \frac{\beta\gamma}{\beta\gamma + 2}\Omega_{AC}^2, \tag{4.16}$$

with $\Omega_{AC} = c_0/2H$ is the acoustic cutoff frequency, and $\beta = 2\mu p_0/B_0^2$ is the plasma-beta. Eq. (4.15) fully describes the dynamics of a linear perturbation propagating along the magnetic field in a magnetically isolated, expanding, stratified and viscous tube. The derivation presented above has been constructed using the area of the tube and then employing a condition of flux conservation. It should be noted that the governing equation may be formulated by using a similar process to that presented in Chapter 2, in which the area is not considered. This is readily achievable and the method is outlined in Appendix C.

It is interesting to note that for $\gamma = 5/3$ the magnetic field increases the cutoff frequency (compared to the acoustic cutoff frequency) if $\beta \leq 1.5$. If the last term in the left-hand side of Eq. (4.15) is neglected (ideal medium) we recover the governing equation given by Rae & Roberts (1982). If, in addition, we suppose that waves propagate in an ideal medium surrounded by a quiescent environment (i.e. the temporal variation of the external pressure is the longest temporal scale in the problem), we obtain the KG equation

$$\frac{\partial^2 Q}{\partial t^2} - c_T^2 \frac{\partial^2 Q}{\partial z^2} + \Omega_T^2 Q = 0. \tag{4.17}$$

The subject of the present study is the propagation of slow MHD waves in a viscous plasma embedded in a quiescent environment. For this model, the KGB equation reduces to

$$\frac{\partial^2 Q}{\partial t^2} - c_T^2 \frac{\partial^2 Q}{\partial z^2} + \Omega_T^2 Q - \frac{4}{3}\nu \frac{\partial}{\partial t}\left(\frac{1}{16H^2} + \frac{1}{2H}\frac{\partial}{\partial z} + \frac{\partial^2}{\partial z^2}\right) Q = 0. \tag{4.18}$$

Recall that the general properties of the Klein-Gordon equation were discussed in Section 1.5. Now let us turn our attention to properties and solutions of the KGB equation. In what follows we are going to solve Eq. (4.18) in two limiting cases. The two cases simplify the governing equation and allow analytical progress to be made. In the first case it is assumed that Q varies on a scale that is much larger than the scale height, and in the second Q is taken to vary over scales much smaller than the scale height.

4.3 Variation in Q occurs over length scales much larger than the scale height

In this first case, the two terms including the spatial derivatives in the viscous term are much smaller than the first term and may be neglected. Thus the KGB equation describing longitudinal wave propagation in a viscous thin flux tube in a quiescent environment can be reduced to

$$\frac{\partial^2 Q}{\partial t^2} - c_T^2 \frac{\partial^2 Q}{\partial z^2} + \Omega_T^2 Q - \frac{\nu}{12H^2}\frac{\partial Q}{\partial t} = 0. \tag{4.19}$$

In order to have a first glimpse of the behaviour of the solution of Eq. (4.19), let us carry out a normal mode analysis. For the function $Q(t,z)$ we suppose a dependence of the form $\exp[i(\omega t - kz)]$. This leads us to the dispersion relation

$$\omega^2 + \frac{i\nu\omega}{12H^2} - k^2 c_T^2 - \Omega_T^2 = 0, \tag{4.20}$$

where the second term describes the contribution due to viscosity. Supposing a temporarily decaying wave, waves will damp provided $\Im(\omega)$ is a positive quantity. Solving the dispersion relation, Eq. (4.20), for ω we find that waves cannot damp temporally, moreover waves will propagate provided the condition

$$\nu < 24H^2\sqrt{k^2 c_T^2 + \Omega_T^2}, \tag{4.21}$$

is satisfied. Under photospheric conditions the scale height, H, is of the order 10^2 km and the tube cutoff, Ω_T, is of the order 10^{-2} s^{-1}, given the coefficient of viscosity is of the order 10^{-3} km^{2}s^{-1}, it is clear that the condition Eq. (4.21) is easily satisfied.
Supposing a spatially damped wave (i.e. complex wave vector but now ω is real), the dispersion relation can be recast as

$$k^2 = \frac{\omega^2 - \Omega_T^2}{c_T^2} + i\frac{\nu\omega}{12H^2 c_T^2}, \tag{4.22}$$

and waves will decay if the imaginary part of k is negative. Assuming mainly propagating waves ($k_r \gg k_i$) we obtain

$$k_i \approx \frac{\nu\omega}{24H^2 c_T \sqrt{\omega^2 - \Omega_T^2}}, \tag{4.23}$$

which is clearly a positive quantity, therefore we conclude that in the limit when the characteristic variation in $Q(t,z)$ is larger than the gravitational scale height waves will have neither spatial damping nor temporal one. Employing the aforementioned normal mode analysis we can derive the characteristic speeds of these waves, i.e. phase and group speed. Using Eq. (4.20) the phase speed is found as

$$v_{ph} = \frac{\omega}{k} = -\frac{i\nu}{24H^2 k} \pm \sqrt{c_T^2 + \frac{1}{k^2}\left(\Omega_T^2 - \frac{\nu^2}{4 \times 12^2 H^4}\right)}, \tag{4.24}$$

where $\pm$ denotes upward/downward propagating waves. Assuming a real wave number, waves with larger wavelengths will propagate faster provided $\nu < 24H^2\Omega_T$. The group speed can be obtained as

$$v_g = \frac{\partial\omega}{\partial k} = \frac{kc_T^2}{\sqrt{k^2 c_T^2 + \Omega_T^2 - \frac{\nu^2}{4\times 12^2 H^4}}}, \tag{4.25}$$

which, for real or complex wave number approaching infinity, will tend to c_T, similar to the ideal case (see, for example, Rae & Roberts, 1982). Eq. (4.25) shows that the more viscous the medium is the larger the group speed is.

Eq. (4.19) is again a telegrapher-type equation and it can be reduced to a KG equation by introducing the transformation

$$Q(t,z) = q(t,z)e^{\nu t/24H^2}. \tag{4.26}$$

(this transformation in essence is similar to the introduction of a transformation of the type $Q(t,z) = q(t,z)\exp(\lambda t)$ in Eq. (4.19), and, the parameter λ is chosen such that the resulting equation does not contain first order derivatives in time). With this transformation the equation of wave propagation in a viscous plasma is given by

$$\frac{\partial^2 q}{\partial t^2} - c_T^2 \frac{\partial^2 q}{\partial z^2} + \left(\Omega_T^2 - \frac{\nu^2}{24^2 H^4}\right) q = 0, \tag{4.27}$$

and describes a wave propagating with the group speed c_T followed by a wake whose frequency is *reduced* by viscosity (when compared to the ideal counterpart). The solution of this equation (written for the original function, $Q(t,z)$) can be given according to the type of the initial and/or boundary condition in one of the forms given by Eq. (1.84) and Eq. (1.88) with Ω_T replaced by $\sqrt{\Omega_T^2 - \nu^2/(24^2H^4)}$ and the solution is multiplied by $\exp[\nu t/24H^2]$. The solution of this equation shows a decaying behavior for $t < t_a = 24H^2/\nu$. For photospheric conditions, the solution will decay for times less than 6.4×10^8 s since the launch of the wave, i.e. for a slow wave propagating with a speed of 6 km s^{-1}, waves will amplify for distances larger than 17 AU. In reality, the time dependence of the Bessel functions in the solutions ensures the temporal decay of the solution.

Eq. (4.27) may be solved subject to the following temporal boundary conditions

$$\lim_{t\to 0,\ z\neq 0} Q(t,z) = 0, \qquad \lim_{t\to 0,\ z\neq 0} \frac{\partial Q}{\partial t} = 0,$$

$$\lim_{z\to 0} Q(t,z) = V(t), \qquad \lim_{z\to\infty} Q(t,z) = 0, \tag{4.28}$$

where $V(t)$ is an imposed velocity driver at the footpoint of the tube. Since the form of Eq. (4.27) is the same as that solved by Sutmann *et al.* (1998) (and examined in detail in parts of Chapter 2) their results may be directly reproduced here. Thus the general solution is

$$q(t,z) = V\left(t-\frac{z}{c_T}\right)\mathcal{H}\left(t-\frac{z}{c_T}\right) + \int_0^t V(t-\tau)W(\tau,z)d\tau, \tag{4.29}$$

where $\mathcal{H}(t-z/c_T)$ is the Heaviside unit step function and $W(\tau,z)$ is given by

$$W(z,\tau) = -\frac{\Omega_{T\nu}z}{c_T}\frac{J_1\left[\Omega_{T\nu}\sqrt{\tau^2-z^2/c_T^2}\right]}{\sqrt{\tau^2-z^2/c_T^2}}\mathcal{H}\left(\tau-\frac{z}{c_T}\right), \tag{4.30}$$

with

$$\Omega_{T\nu} = \left(\Omega_T^2 - \frac{\nu^2}{2^2H^4}\right)^{\frac{1}{2}}, \tag{4.31}$$

being the reduced tube cut-off frequency in the viscous medium. Thus we see that the final general solution in terms of the original function $Q(t,z)$ may be written as

$$Q(t,z) = e^{\nu t/24H^2}\left[V\left(t-\frac{z}{c_T}\right)\mathcal{H}\left(t-\frac{z}{c_T}\right) + \int_0^t V(t-\tau)W(\tau,z)d\tau\right]. \tag{4.32}$$

This equation may be readily solved for various types of velocity driver such as a monochromatic driver [$V(t) = V_0e^{-i\omega t}$], a delta-function pulse [$V(t) = V_0\delta(\Omega_{T\nu}t/2\pi)$] or a sinusoidal pulse [$V(t) = V_0(\mathcal{H}(t) - \mathcal{H}(t-P))e^{-i\omega t}$].

4.3.1 Solving for various footpoint drivers

It has been shown that for the case of the variation in $Q(t,z)$ occurring over length scales that are much larger than the scale height, H, the propagation of waves in the viscous medium is governed by a Klein-Gordon equation with a reduced frequency, when compared to its ideal counterpart. The general solution has been formulated subject to the temporal boundary conditions given by Eq. (4.28). The general solution may now be solved for three specific drivers by specifying the imposed velocity function, $V(t)$. The three drivers are the same three considered in Chapters 2 and 3, namely a monochromatic source, a delta-function source and a sinusoidal pulse. Given the form of the general solution it is possible, after the substitution of c_T and $\Omega_{T\nu}$, to quote the results given by Sutmann *et al.* (1998) directly. Indeed, the detailed derivations for the three drivers have been examined in Chapter 2, in a slightly different context, when examining the presence of a background flow in the flux tube. Setting the flow terms to zero in the derivations presented in Section 2.2.7 gives the derivations appropriate for this section, albeit with the need to substitute the appropriate frequencies.

Monochromatic source

The boundary condition is to be satisfied by a source of monochromatic acoustic waves, driven with a frequency ω and amplitude V_0. Thus the required boundary condition is given by

$$V(t) = V_0 e^{-i\omega t}. \tag{4.33}$$

The solution may be quoted directly to give

$$Q(t,z) = \tag{4.34}$$
$$e^{\nu t/24H^2}\left[V_0 e^{-i(\omega t+\sqrt{\omega^2-\Omega_{T\nu}^2}\, z/c_T)} + \frac{V_0 z\Omega_{T\nu}}{c_T}\sqrt{\frac{2}{\pi\Omega_{T\nu}}}\frac{1}{t^{3/2}}\frac{1}{\omega^2-\Omega_{T\nu}^2}[\Omega_{T\nu}\sin\mu + i\omega\cos\mu]\right],$$

where now $\mu = \Omega_{T\nu}t - 3\pi/4$. Thus it can be seen that in the case when Q varies over scales much larger than H the solution for a monochromatic driver differs only in the nature of the cutoff frequency (now a function of viscosity) and the fact that there is an exponential multiplier. The solution consists of the familiar free and forced atmospheric oscillations. The forced oscillations now represent propagating ($\omega > \Omega_{T\nu}$) or evanescent waves ($\omega < \Omega_{T\nu}$), and to not decay in time since they are driven continuously by the source. The free oscillations show decay in time as $t^{-3/2}$ (as long as the exponential multiplying term does not dominate) and are at the cutoff frequency $\Omega_{T\nu}$.

Delta-function driver

The source considered is a single pulse of δ-function form in time. Thus the boundary condition is given by

$$V(t) = \bar{V}_0\delta(t). \tag{4.35}$$

The dimensions of $\bar{V}_0$ are not velocity since the δ-function has dimensions of T^{-1}. This is remedied by considering a dimensionless time given by $\bar{t} = \Omega_{T\nu}t/2\pi$ (see Section 2.2.7 for details). The solution for $Q(t,z)$ is then given by

$$Q(t,z) = e^{\nu t/24H^2}\left[\frac{-2\pi z V_0}{c_T}\sqrt{\frac{2}{\pi\Omega_{T\nu}}}\frac{1}{t^{3/2}}\cos\mu\right], \tag{4.36}$$

where $V_0 = \Omega_{T\nu}\bar{V}_0/2\pi$. Since the source is a delta-function pulse no forced terms are present and only the free oscillations remain which exhibit similar behaviour as discussed above.

Sinusoidal pulse driver

The final case to be considered is that of a sinusoidal pulse at the footpoint of the tube lasting for one wave period, P, with $P = 2\pi/\omega$. The boundary condition is thus

$$V(t) = V_0[\mathcal{H}(t) - \mathcal{H}(t-P)]e^{-i\omega t}. \tag{4.37}$$

The final solution for $Q(t,z)$ for the sinusoidal driver is given by

$$Q(t,z) = \tag{4.38}$$
$$e^{\nu t/24H^2}\left[\frac{-\Omega_{T\nu}zV_0}{c_T}\sqrt{\frac{2}{\pi\Omega_{T\nu}}}\frac{1}{\omega^2-\Omega_{T\nu}^2}\frac{1}{t^{3/2}}\left[\Omega_{T\nu}\sin\theta-\Omega_{T\nu}\sin\mu+i\omega\cos\theta-i\omega\cos\mu\right]\right],$$

where $\theta = \Omega_{T\nu}(t-P)-3\pi/4$. Since the pulse lasts for one period only, and large times are considered for the analytic solution, only the free oscillations remain, which are of a similar form. Musielak & Ulmschneider (2003a) show how a wavetrain of random sinusoidal pulses can sustain the free oscillations in the atmosphere for long time periods. Since they are at the cutoff frequency, for the viscous case $\Omega_{T\nu}$, it is of interest to see under what conditions viscosity causes appreciable differences from the ideal case. This shall be examined in Section 4.5, but first the second case, in which Q varies over scales much smaller than H, shall be studied in detail.

4.4 Variation in Q occurs over length scales much smaller than the scale height

In this second case the KGB equation is reduced to

$$\frac{\partial^2 Q}{\partial t^2}-c_T^2\frac{\partial^2 Q}{\partial z^2}+\Omega_T^2 Q-\frac{4}{3}\nu\frac{\partial^3 Q}{\partial t\partial z^2}=0. \tag{4.39}$$

Normal mode analysis is carried out by supposing the ansatz $Q(t,z)\sim\exp[i(\omega t-kz)]$. Eq. (4.39) yields the dispersion relation

$$\omega=\pm\sqrt{k^2c_T^2+\Omega_T^2-\frac{4\nu^2k^4}{9}}+\frac{2i\nu k^2}{3}, \tag{4.40}$$

where the second term in the dispersion relation describes the damping of these modes. Since the imaginary part of the frequency is positive, waves in this limit will have a temporal decay. Supposing a complex wavenumber, for mainly propagating waves, the imaginary part is given by

$$k_i\approx-\frac{2\nu\omega}{c_T}\sqrt{\frac{\omega^2-\Omega_T^2}{9c_T^4+16\nu^2\omega^2}}, \tag{4.41}$$

which is a negative quantity, and therefore waves in this limit will have spatial damping. Waves will propagate if the viscosity coefficient satisfies the condition

$$\nu<\frac{3}{2k^2}\sqrt{k^2c_T^2+\Omega_T^2}. \tag{4.42}$$

Comparing to the case presented in the previous section, now the damping rate depends on k (waves with larger wavelength will damp stronger than those with smaller wavelength) and a positive imaginary frequency means that waves have temporal damping. Computing the phase and group speed of the damped modes (the real part of the dispersion relation), the phase speed of waves is larger for smaller wavelengths; the maximum group speed is not c_T (as in the ideal case) but is zero and this value is obtained when $k\to 0$. When $k\to\infty$ the real part of the group speed tends to $-\infty$. Here we have neglected the imaginary part of the group speed since for a

wave number of $\sim(10^{-10}, 10^{-4})$ m^{-1} the ratio between the real part and the imaginary part of the group speed is of the order of $10^5 - 10^6$.

4.4.1 Spatial boundary conditions

Let us now consider the KGB equation subject to the same boundary conditions as given by Eq. (1.79), i.e.

$$Q\,|_{t=0} = f(z), \quad \left.\frac{\partial Q}{\partial t}\right|_{t=0} = g(z), \quad -\infty < z < \infty. \tag{4.43}$$

After applying a Laplace transform to Eq. (4.39), the ODE describing the propagation of waves is given by

$$\frac{d^2\Psi(s,z)}{dz^2} - m_1^2\Psi(s,z) = \frac{\upsilon}{c_T^2 + \upsilon s}\frac{d^2 f(z)}{dz^2} - \frac{g(z)}{c_T^2 + \upsilon s} - \frac{sf(z)}{c_T^2 + \upsilon s}, \tag{4.44}$$

where

$$\Psi(s,z) = \mathcal{L}[Q(t,z)] = \int_0^\infty Q(t,z)e^{-st}dt, \quad m_1^2 = \frac{s^2 + \Omega_T^2}{c_T^2 + s\upsilon}, \tag{4.45}$$

and where $\upsilon = 4\nu/3$. The solution of this differential equation which is bounded at $\pm\infty$, from Eq. (1.82), is

$$\Psi(s,z) = \frac{1}{2m_1(c_T^2 + s\upsilon)}\left[\int_{-\infty}^{z}\left(g(\eta) + sf(\eta) - \upsilon\frac{d^2 f(\eta)}{d\eta^2}\right)e^{-m_1(z-\eta)}d\eta + \int_z^\infty\left(g(\eta) + sf(\eta) - \upsilon\frac{d^2 f(\eta)}{d\eta^2}\right)e^{-m_1(\eta - z)}d\eta\right]. \tag{4.46}$$

Taking into account the expression of m_1, it becomes necessary to find the inverse Laplace transform of the following quantities

$$I_1 = \frac{1}{\sqrt{(s^2 + \Omega_T^2)(c_T^2 + s\upsilon)}}\exp\left(-z\sqrt{\frac{s^2 + \Omega_T^2}{c_T^2 + s\upsilon}}\right), \tag{4.47}$$

and

$$I_2 = \frac{s}{\sqrt{(s^2 + \Omega_T^2)(c_T^2 + s\upsilon)}}\exp\left(-z\sqrt{\frac{s^2 + \Omega_T^2}{c_T^2 + s\upsilon}}\right). \tag{4.48}$$

The inverse Laplace transform is found by considering the Bromwich integral given by

$$X(t,z) = \frac{1}{2\pi i}\lim_{\beta\to\infty}\int_{\alpha - i\beta}^{\alpha + i\beta} F(s,z)e^{st}ds, \tag{4.49}$$

where where the integration is performed along the vertical line $\Re(s) = \gamma$ in the complex plane such that γ is greater than the real part of all singularities of $F(s,z)$. This ensures that the contour path is in the region of convergence. For more on the inverse Laplace transform see, e.g. the textbooks Schiff (1999), Wunsch (2005).

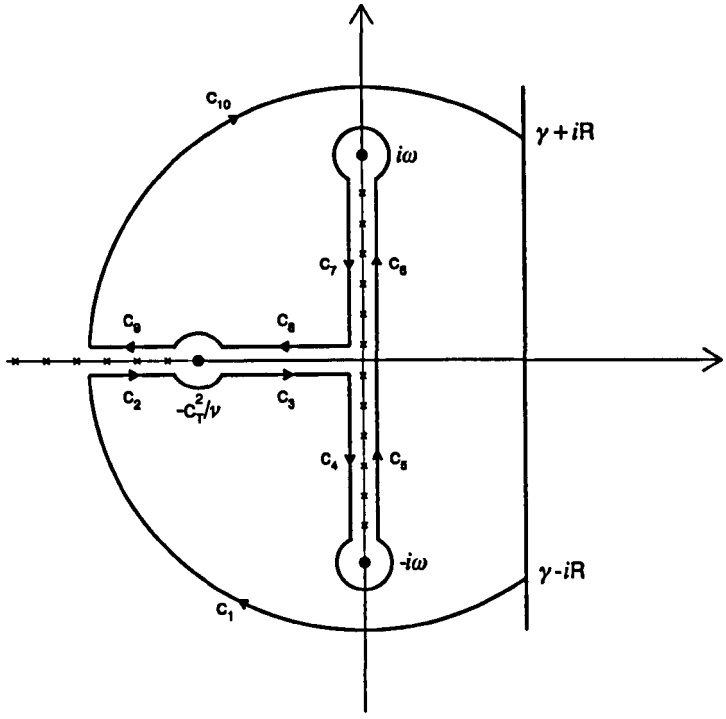

Figure 4.1: The integration contour and the branch cuts for the inverse Laplace transforms of the quantities Eq. (4.47) and Eq. (4.48). The branch cuts are shown by crosses.

Considering the complex s-plane, the transforms we have to calculate are given by the Bromwich integrals

$$I_1 = \frac{1}{2\pi i\sqrt{\upsilon}} \int_{\gamma-i\infty}^{\gamma+i\infty} \frac{e^{ts}}{\sqrt{(s^2+\Omega_T^2)(c_T^2/\upsilon+s)}} \exp\left(-\frac{z}{\sqrt{\upsilon}}\sqrt{\frac{s^2+\Omega_T^2}{c_T^2/\upsilon+s}}\right) ds, \tag{4.50}$$

and

$$I_2 = \frac{1}{2\pi i\sqrt{\upsilon}} \int_{\gamma-i\infty}^{\gamma+i\infty} \frac{se^{ts}}{\sqrt{(s^2+\Omega_T^2)(c_T^2/\upsilon+s)}} \exp\left(-\frac{z}{\sqrt{\upsilon}}\sqrt{\frac{s^2+\Omega_T^2}{c_T^2/\upsilon+s}}\right) ds. \tag{4.51}$$

Let us consider the first transform, the second one can be calculated in an similar way as presented here. The integrand in I_1 contains two branch cuts, one is running on the real axis from $s = -c_T^2/\upsilon$ to $-\infty$ and the other one is running on the imaginary axis in between $\pm i\Omega_T$ (in principle, we could have the symmetric branch cuts but it can be shown that in this case the inverse Laplace transform cannot be defined as there will be impossible to choose such a $\Re(s) = \gamma$ in the complex s-plane so that all singularities lie on the left of the line at $\Re(s) = \gamma$). The integration contour is deformed as in Fig. 4.1, and the Bromwich integral transforms into a contour integral over the closed contour C. According to the Fig. 4.1, the contour integral comprises the line integrals $C_1, C_2, \ldots C_{10}$, plus the integration around the infinitesimally small circles around $\pm i\Omega_T$ and $-c_T^2/\upsilon$. The contributions along the arcs C_1 and C_{10} vanish as the radius of the arcs (R) tends to infinity. This result is a direct consequence of Jordan's lemma. On C_2 we change the variable such that $s = \eta e^{-i\pi}$, i.e.

$$s+\frac{c_T^2}{\upsilon}=\left(\eta-\frac{c_T^2}{\upsilon}\right)e^{-i\pi}. \tag{4.52}$$

The integral transforms into

$$\int_{C_2}F(s)e^{ts}=-i\int_{\infty}^{c_T^2/\upsilon}\frac{e^{-t\eta}}{\sqrt{(\eta^2+\Omega_T^2)(\eta-c_T^2/\upsilon)}}\exp\left(-i\frac{z}{\sqrt{\upsilon}}\sqrt{\frac{\eta^2+\Omega_T^2}{\eta-c_T^2/\upsilon}}\right)d\eta. \tag{4.53}$$

On C_3 the new variable is $s=\eta e^{-i\pi}$ with $s+\frac{c_T^2}{\upsilon}=\left(\frac{c_T^2}{\upsilon}-\eta\right)$ so the integral becomes

$$\int_{C_3}F(s)e^{ts}=-\int_{c_T^2/\upsilon}^{0}\frac{e^{-t\eta}}{\sqrt{(\eta^2+\Omega_T^2)(c_T^2/\upsilon-\eta)}}\exp\left(-\frac{z}{\sqrt{\upsilon}}\sqrt{\frac{\eta^2+\Omega_T^2}{c_T^2/\upsilon-\eta}}\right)d\eta. \tag{4.54}$$

In a similar way, we can define a new variable for all remaining integration paths

$$\text{along } C_4,\quad s=\eta e^{-i\pi/2},\ s-i\Omega_T=(\Omega_T+\eta)e^{3i\pi/2},\ s+i\Omega_T=(\Omega_T-\eta)e^{i\pi/2}, \tag{4.55}$$

$$\text{along } C_5,\quad s=\eta e^{-i\pi/2},\ s-i\Omega_T=(\Omega_T+\eta)e^{i\pi/2},\ s+i\Omega_T=(\Omega_T-\eta)e^{-i\pi/2}. \tag{4.56}$$

$$\text{along } C_6,\quad s=\eta e^{i\pi/2},\ s-i\Omega_T=(\Omega_T-\eta)e^{-i\pi/2},\ s+i\Omega_T=(\Omega_T+\eta)e^{i\pi/2}, \tag{4.57}$$

$$\text{along } C_7,\quad s=\eta e^{i\pi/2},s-i\Omega_T=(\Omega_T-\eta)e^{3i\pi/2},\ s+i\Omega_T=(\Omega_T+\eta)e^{i\pi/2}, \tag{4.58}$$

$$\text{along } C_8,\quad s=\eta e^{i\pi},\ s+c_T^2/\upsilon=c_T^2/\upsilon-\eta, \tag{4.59}$$

$$\text{along } C_9,\quad s=\eta e^{i\pi},\ s+c_T^2/\upsilon=(\eta-c_T^2/\upsilon)e^{i\pi}. \tag{4.60}$$

Upon substituting these relations into the integrals and after simplifying one obtains

$$\int_{C_3}=-\int_{C_8}, \tag{4.61}$$

$$\int_{C_4}+\int_{C_5}=\frac{1}{\pi\sqrt{\upsilon}}\int_0^{\Omega_T}\frac{e^{-it\eta}}{\sqrt{(\Omega_T^2-\eta^2)(c_T^2/\upsilon-i\eta)}}\cosh\left(\frac{z}{\sqrt{\upsilon}}\sqrt{\frac{\Omega_T^2-\eta^2}{c_T^2/\upsilon-i\eta}}\right)d\eta, \tag{4.62}$$

$$\int_{C_6}+\int_{C_7}=\frac{1}{\pi\sqrt{\upsilon}}\int_0^{\Omega_T}\frac{e^{it\eta}}{\sqrt{(\Omega_T^2-\eta^2)(c_T^2/\upsilon+i\eta)}}\cosh\left(\frac{z}{\sqrt{\upsilon}}\sqrt{\frac{\Omega_T^2-\eta^2}{c_T^2/\upsilon+i\eta}}\right)d\eta, \tag{4.63}$$

$$\int_{C_9}=i\int_{c_T^2/\upsilon}^{\infty}\frac{e^{-t\eta}}{\sqrt{(\Omega_T^2+\eta^2)(\eta-c_T^2/\upsilon)}}\exp\left(-i\frac{z}{\sqrt{\upsilon}}\sqrt{\frac{\Omega_T^2+\eta^2}{\eta-c_T^2/\upsilon}}\right)d\eta. \tag{4.64}$$

Adding all these integrals together, the integrals along the arcs C_3 and C_8 cancel while the integrals along C_2 and C_9 will result in

$$\int_{C_2\cup C_9} = \frac{1}{\pi\sqrt{\upsilon}}\int_{c_T^2/\upsilon}^{\infty} \frac{e^{-t\eta}\cos\frac{z}{\sqrt{\upsilon}}\sqrt{\frac{\eta^2+\Omega_T^2}{\eta-c_T^2/\upsilon}}}{\sqrt{(\eta^2+\Omega_T^2)(\eta-c_T^2/\upsilon)}}d\eta. \tag{4.65}$$

Summing up the integrals along the branch cut on the imaginary axis we obtain that

$$\int_{C_4\cup C_5\cup C_6\cup C_7} = \frac{1}{\pi\sqrt{\upsilon}}\frac{\partial}{\partial z}\int_{-\Omega_T}^{\Omega_T}\frac{e^{-i\eta t}}{\Omega_T^2-\eta^2}\sinh\left(\frac{z}{\sqrt{\upsilon}}\sqrt{\frac{\Omega_T^2-\eta^2}{c_T^2/\upsilon-i\eta}}\right)d\eta. \tag{4.66}$$

Next we have to calculate the value of the integral around the singular points $\pm i\Omega_T$ and $-c_T^2/\upsilon$. When performing the integrals around the singular points on the imaginary axis we introduce a new variable such that $s = \pm i\Omega_T + \varepsilon e^{i\theta}$ and the variable θ varies from $-\pi/2$ to $3\pi/2$ for $s = i\Omega_T$ and $-3\pi/2$ to $\pi/2$ at $s = -i\Omega_T$. In both cases, the radius of the circle, ε, tends to zero. It can be shown that both integrals tend to zero when the radius of the circles surrounding the singular points tend to zero. At the singularity on the real axis, we introduce a new variable such that $s = -c_T^2/\upsilon + \varepsilon e^{i\theta}$ and the integrals are evaluated such that θ varies from $-\pi$ to 0 for the arc below the singularity and 0 to π for the arc above the singularity. Taking the radius of the circle infinitesimally small, both integrals tend to zero. Finally, the inverse Laplace transform of I_1 takes the form

$$\begin{aligned} I_1 = \frac{1}{\pi\sqrt{\upsilon}}\Bigg[&\int_{c_T^2/\upsilon}^{\infty}\frac{e^{-t\eta}}{\sqrt{(\eta^2+\Omega_T^2)(\eta-c_T^2/\upsilon)}}\cos\left(\frac{z}{\sqrt{\upsilon}}\sqrt{\frac{\eta^2+\Omega_T^2}{\eta-c_T^2/\upsilon}}\right)d\eta + \\ &\times\frac{\partial}{\partial z}\int_{-\Omega_T}^{\Omega_T}\frac{e^{-i\eta t}}{\Omega_T^2-\eta^2}\sinh\left(\frac{z}{\sqrt{\upsilon}}\sqrt{\frac{\Omega_T^2-\eta^2}{c_T^2/\upsilon-i\eta}}\right)d\eta\Bigg]. \end{aligned} \tag{4.67}$$

Applying the described method for I_2 we obtain that

$$\begin{aligned} I_2 = -\frac{1}{\pi\sqrt{\upsilon}}\Bigg[&\int_{c_T^2/\upsilon}^{\infty}\frac{\eta e^{-t\eta}}{\sqrt{(\eta^2+\Omega_T^2)(\eta-c_T^2/\upsilon)}}\cos\left(\frac{z}{\sqrt{\upsilon}}\sqrt{\frac{\eta^2+\Omega_T^2}{\eta-c_T^2/\upsilon}}\right)d\eta - \\ &\frac{\partial}{\partial z}\int_{-\Omega_T}^{\Omega_T}\frac{\eta e^{-i\eta t}}{\Omega_T^2-\eta^2}\sinh\left(\frac{z}{\sqrt{\upsilon}}\sqrt{\frac{\Omega_T^2-\eta^2}{c_T^2/\upsilon-i\eta}}\right)d\eta\Bigg]. \end{aligned} \tag{4.68}$$

Taking the two values of the inverse Laplace transform, the solution of the KGB equation is

$$Q(t,z) = \frac{1}{2}\int_{-\infty}^{\infty}\left(g(z') - \upsilon\frac{d^2f(z')}{dz'^2}\right)\mathcal{L}_1 dz' - \frac{1}{2}\int_{-\infty}^{\infty} f(z')\mathcal{L}_2 dz', \tag{4.69}$$

where

$$\mathcal{L}_1 = \frac{1}{\pi\sqrt{\upsilon}}\int_{c_T^2/\upsilon}^{\infty}\frac{e^{-t\eta}\cos\left(\frac{z-z'}{\sqrt{\upsilon}}\sqrt{\frac{\eta^2+\Omega_T^2}{\eta-c_T^2/\upsilon}}\right)}{\sqrt{(\eta^2+\Omega_T^2)(\eta-c_T^2/\upsilon)}}d\eta, \tag{4.70}$$

and

$$\mathcal{L}_2 = -\frac{1}{\pi\sqrt{\upsilon}}\int_{c_T^2/\upsilon}^{\infty} \frac{\eta e^{-t\eta}\cos\left(\frac{z-z'}{\sqrt{\upsilon}}\sqrt{\frac{\eta^2+\Omega_T^2}{\eta-c_T^2/\upsilon}}\right)}{\sqrt{(\eta^2+\Omega_T^2)(\eta-c_T^2/\upsilon)}}d\eta, \tag{4.71}$$

where we have used the properties $\cos(-z) = \cos(z)$ and $\sinh(-z) = -\sinh(z)$.

4.4.2 Temporal boundary conditions

If the initial conditions are given as a temporal function, i.e. a prescribed form of $Q(t,z)$ when $z = 0$ then the solution of the KGB equation is changed. Supposing that a wave source is introduced at the footpoint of the tube, such that the boundary conditions may be expressed as per Eq. (1.87), i.e

$$\lim_{t\to 0,\, z\neq 0} Q(t,z) = 0, \qquad \lim_{t\to 0,\, z\neq 0} \frac{\partial Q}{\partial t} = 0,$$

$$\lim_{z\to 0} Q(t,z) = V(t), \qquad \lim_{z\to\infty} Q(t,z) = 0, \tag{4.72}$$

Taking Laplace transforms of Eq. (4.39) and applying the boundary conditions yields

$$\frac{\partial^2\Psi(s,z)}{\partial z^2} - m_1^2\Psi(s,z) = 0, \tag{4.73}$$

where $\Psi(s,z) = \mathcal{L}[Q(t,z)]$ and $m_1 = (s^2+\Omega_T^2)/(c_T^2+\upsilon s)$. Eq. (4.73) is readily solved to yield

$$\Psi(s,z) = \Psi_0(s)e^{-m_1 z} + \Psi_1(s)e^{m_1 z}. \tag{4.74}$$

Since it is required that the solution be bounded at infinity it is necessary to take $\Psi_1(s) = 0$, thus the inverse Laplace transform of

$$F(s,z) = exp\left[\frac{-z}{\sqrt{\upsilon}}\sqrt{\frac{s^2+\Omega_T^2}{c_T^2/\upsilon+s}}\right], \tag{4.75}$$

is sought by means of the Bromwich integral, Eq. (4.49). Examining $F(s)$ shows branch points at $s = \pm i\Omega_T$ and $s = -c_T^2/\upsilon$, allowing the branch cuts shown in Fig. 4.1 to be taken. The inverse Laplace transform is in a similar manner to previously, such that the following variable changes are made

$$\text{along } C_2, \quad s = \lambda e^{-i\pi},\ s+\frac{c_T^2}{\upsilon} = (\lambda - \frac{c_T^2}{\upsilon})e^{-i\pi}, \tag{4.76}$$

$$\text{along } C_4, \quad s = \lambda e^{-i\pi/2},\ s - i\Omega_T = (\Omega_T+\lambda)e^{3i\pi/2},\ s+i\Omega_T = (\Omega_T-\lambda)e^{i\pi/2}, \tag{4.77}$$

$$\text{along } C_5, \quad s = \lambda e^{-i\pi/2},\ s - i\Omega_T = (\Omega_T+\lambda)e^{i\pi/2},\ s+i\Omega_T = (\Omega_T-\lambda)e^{-i\pi/2}. \tag{4.78}$$

$$\text{along } C_6, \quad s = \lambda e^{i\pi/2},\ s - i\Omega_T = (\Omega_T-\lambda)e^{-i\pi/2},\ s+i\Omega_T = (\Omega_T+\lambda)e^{i\pi/2}, \tag{4.79}$$

$$\text{along } C_7, \quad s=\lambda e^{i\pi/2}, s-i\Omega_T=(\Omega_T-\lambda)e^{3i\pi/2},\ s+i\Omega_T=(\Omega_T+\lambda)e^{i\pi/2}, \tag{4.80}$$

$$\text{along } C_9, \quad s=\lambda e^{i\pi},\ s+c_T^2/\upsilon=\left(\lambda-c_T^2/\upsilon\right)e^{i\pi}. \tag{4.81}$$

As in the previous inverse Laplace calculation it is clear that the integrals along the contours C_3 and C_8 will cancel and the integrals around the small circles at the branch points will tend to zero. Combining the contour integrals yields

$$\int_{C_2}+\int_{C_9}=-2i\int_{c_T^2/\upsilon}^{\infty}e^{-\lambda t}\sin\left[\frac{z}{\sqrt{\upsilon}}\sqrt{\frac{\Omega_T^2+\lambda^2}{\lambda-c_T^2/\upsilon}}\right], \tag{4.82}$$

$$\int_{C_4}+\int_{C_5}=-2i\int_{0}^{\Omega_T}e^{-i\lambda t}\sinh\left[\frac{z}{\sqrt{\upsilon}}\sqrt{\frac{\Omega_T^2-\lambda^2}{c_T^2/\upsilon-i\lambda}}\right], \tag{4.83}$$

$$\int_{C_6}+\int_{C_7}=-2i\int_{0}^{\Omega_T}e^{i\lambda t}\sinh\left[\frac{z}{\sqrt{\upsilon}}\sqrt{\frac{\Omega_T^2-\lambda^2}{c_T^2/\upsilon+i\lambda}}\right]. \tag{4.84}$$

The latter two of these integrals, Eq. (4.83) and Eq. (4.84), may be combined to give

$$\int_{C_4\cup C_5\cup C_6\cup C_7}=-2i\int_{-\Omega_T}^{\Omega_T}e^{-i\lambda t}\sinh\left[\frac{z}{\sqrt{\upsilon}}\sqrt{\frac{\Omega_T^2-\lambda^2}{c_T^2/\upsilon-i\lambda}}\right]. \tag{4.85}$$

Thus, defining $W(t,z)=\mathcal{L}^{-1}[F(s,z)]$, one obtains

$$W(t,z)=-\frac{1}{\pi}\int_{c_T^2/\upsilon}^{\infty}e^{-\lambda t}\sin\left[\frac{z}{\sqrt{\upsilon}}\sqrt{\frac{\Omega_T^2+\lambda^2}{\lambda-c_T^2/\upsilon}}\right]-\frac{1}{\pi}\int_{-\Omega_T}^{\Omega_T}e^{-i\lambda t}\sinh\left[\frac{z}{\sqrt{\upsilon}}\sqrt{\frac{\Omega_T^2-\lambda^2}{c_T^2/\upsilon-i\lambda}}\right]. \tag{4.86}$$

Recall Eq. (4.74) taken with $\Psi_1=0$ and after defining $\Psi_0(s)=\mathcal{L}[V(t)]$, where $V(t)$ is the temporal footpoint driver given by the boundary conditions, one obtains

$$\Psi(s,z)=\mathcal{L}[V(t)]\mathcal{L}[W(t,z)]. \tag{4.87}$$

Applying the convolution theorem yields

$$\Psi(s,z)=\mathcal{L}\left[\int_0^t V(t-\tau)W(\tau,z)d\tau\right]. \tag{4.88}$$

Given that $Q(t,z)=\mathcal{L}^{-1}[\Psi(s,z)]$ the solution of the KGB equation can be expressed as

$$Q(t,z)=\int_0^t V(t-\tau)W(\tau,z)d\tau, \tag{4.89}$$

where

$$\begin{aligned}W(\tau,z) \;=\; & -\frac{1}{\pi}\int_{c_T^2/\upsilon}^{\infty}e^{-\tau\lambda}\sin\left(\frac{z}{\sqrt{\upsilon}}\sqrt{\frac{\lambda^2+\Omega_T^2}{\lambda-c_T^2/\upsilon}}\right)d\lambda- \\ & \frac{1}{\pi}\int_{-\Omega_T}^{\Omega_T}e^{-i\tau\lambda}\sinh\left(\frac{z}{\sqrt{\upsilon}}\sqrt{\frac{\lambda^2+\Omega_T^2}{c_T^2/\upsilon-i\lambda}}\right)d\lambda.\end{aligned} \tag{4.90}$$

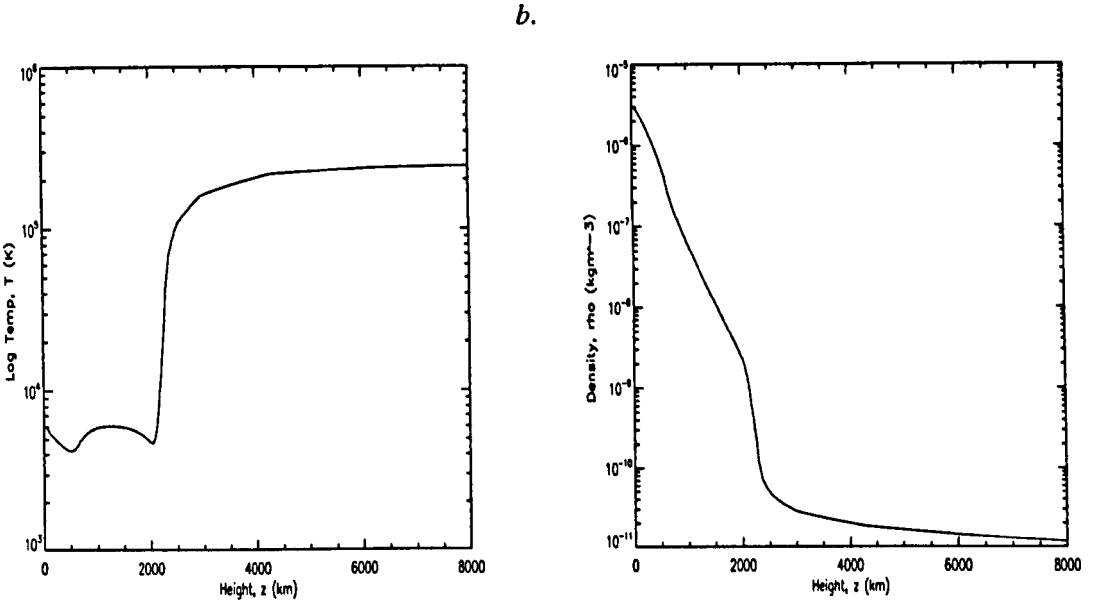

Figure 4.2: Temperature and density as a function of height based on the VALIIIc model; a)temperature against height b) density against height.

4.5 Application to the Sun

In order to evaluate the effect of viscosity it is worth examining the value of the kinematic coefficient of viscosity that may be expected in the solar atmosphere. In Fig. 4.2 the temperature and density profiles for the VALIIIc (Vernazza *et al.*, 1981) have been plotted. These profiles may be used to calculate the coefficient of viscosity at corresponding temperatures and pressures as given by Eq. (4.2), where $\ln\Lambda$ is given by (e.g. Ballai, 2003)

$$\ln\Lambda = 8\ln 10 + \frac{3}{2}\ln\left(\frac{T}{10^6}\right) - \frac{1}{2}\ln\left(\frac{n}{10^9}\right), \tag{4.91}$$

where T is the temperature in K and n is the number density in cm^{-3}. The viscosity profile calculated from these two equations is shown in Fig. 4.3, which shows that for the photospheric region the value of the viscosity coefficient is extremely small. Even given deviations from the VALIIIc model a value in the order of 10^{-3} is unlikely to be exceeded. Thus is it clear that the effect of viscosity on photospheric tubes will be negligible. For the case where the propagation in Q occurs over scales much larger than the scale height, it has been shown that the propagation is governed by a KG equation with the reduced cutoff frequency, $\Omega_{T\nu}$. It is worth examining however what value of viscosity is needed to show appreciable effects on the cutoff frequency and correspondingly the cutoff period, $P_{T\nu} = 2\pi/\Omega_{T\nu}$, where $\Omega_{T\nu}$ is given by Eq. (4.31). The cutoff period is plotted against viscosity in Fig. 4.4, which shows that $P_{T\nu}$ can be increased from the order of 3 mins to 5 mins if the viscosity is increased to the order of 80 $\mathrm{km}^2\mathrm{s}^{-1}$. This represents an increase of 4-5 orders of magnitude of the value of the expected viscosity coefficient for photospheric regions and thus is somewhat unrealistic. It highlights however that, in regions where the viscosity is enhanced for some reason, an increase in the cutoff period is expected. Fig. 4.4 has been plotted for similar values as in the previous chapters, corresponding to the photospheric region.

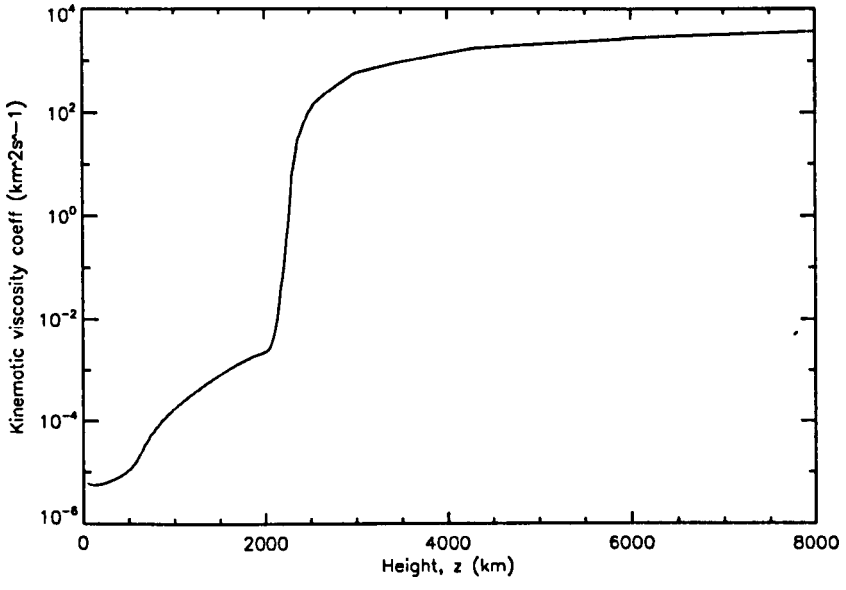

Figure 4.3: Viscosity coefficient against height, based on the VALIIIc model.

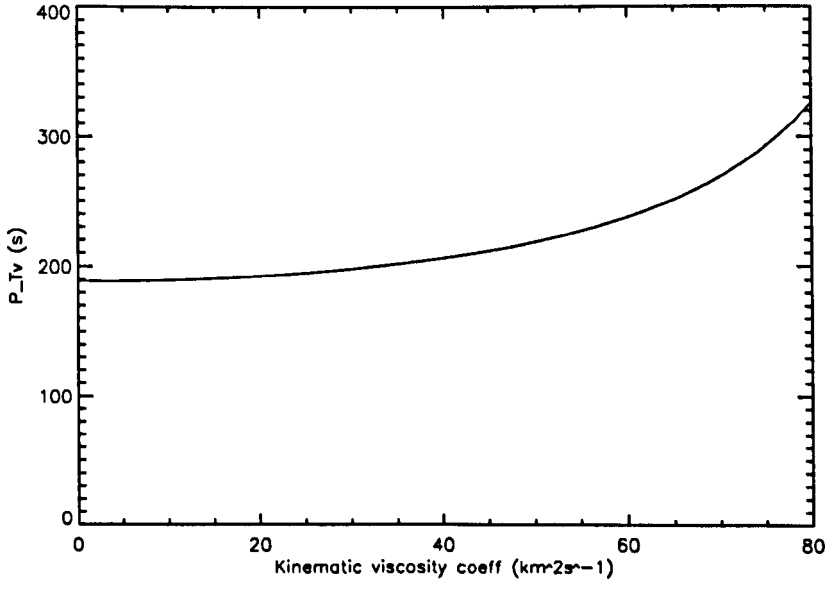

Figure 4.4: Change in cutoff period, P_{Tv}, versus viscosity coefficient.

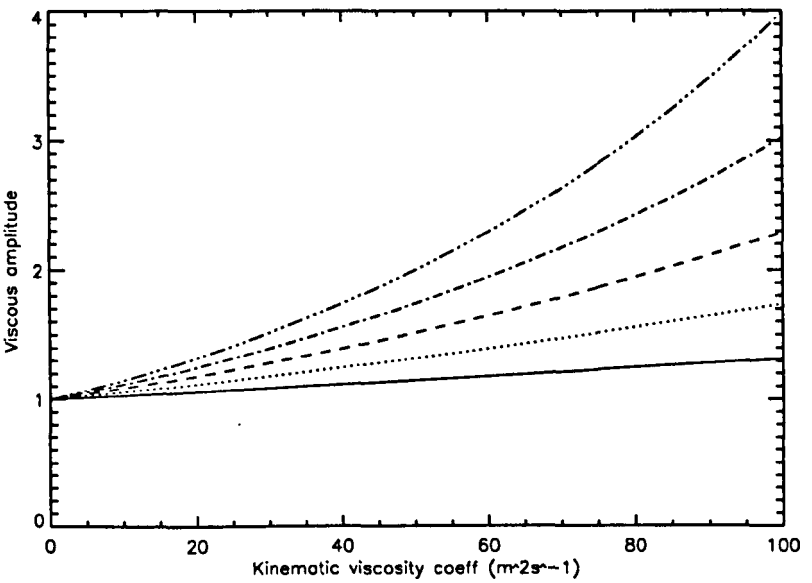

Figure 4.5: The exponential multiplier versus viscosity for times $t = 1000$ s (solid line) to $t = 5000$ s (dash-dot-dot-dot line).

Another interesting difference in the viscous case as compared to the ideal case is the introduction of the exponential multiplying term $e^{\nu t/24H^2}$. This is shown in Fig. 4.5 which has been plotted for the same photospheric values as in the previous plots and shows curves for 5 different times. Fig. 4.5 shows that the amplitude could be increase by a factor of 4 if large viscosities are taken (in the order of 80 km^2s^{-1}) and for large times. Even given the unrealistically large viscosity chosen the effect on the amplitude of such disturbances is not large. Indeed, although it may seem that the amplitude will increase indefinitely with increasing time, it is clear from Eq. (4.34), Eq. (4.36) and Eq. (4.38) that the $t^{-3/2}$ term will prevent such an increase occouring.
The equations presented in the second case (variation in Q much smaller than H) have not been applied to the solar atmosphere. Solutions and applications have been left for future work.

4.6 Conclusions

We have developed a model for analyzing the propagation of slow MHD modes in a vertical thin flux tube with a vertical stratification in the presence of viscous dissipation. The evolution of these waves is described by the Klein-Gordon-Burgers (KGB) equation written for the reduced velocity, Q. Restricting ourself to a simplified model in which the temporal response of the environment is the largest temporal scale in the problem we solved the KGB equation in two limiting cases (a) when spatial variation in the reduced velocity occur over typical length scales much larger than the gravitational scale height and (b) when the changes in Q occur over distances much shorter than the gravitational scale height. According to the variation scale of Q, the slow wave propagating in the dissipative plasma has different attenuation, in Section 4.3, after employing normal mode analysis, we obtained that slow waves do not have spatial or temporal damping, while in the second (Section 4.4) case we found a temporal and spatial decay. The impulsive excitation, say, of slow waves in Section 4.3 results in a wave front prop-

agating in opposite directions followed by a wake which oscillate with a frequency decreased by the viscosity, i.e. in this case the viscosity acts on the wake only. Detailed solutions have been developed for three initial drivers. In Section 4.4 it is not so straightforward to decompose the motion into a leading front and a wake. The solutions presented here are given in a general form, indeed it may be possible to solve these equations for a particular initial driver (e.g. monochromatic source, delta-function etc.) but this is likely to be extremely hard to achieve analytically. Progress would be made by considering numerical solutions to these equations, but such an undertaking is not attempted in this Thesis and is left for future work.

It is clear that although the consideration of the effect of viscosity on wave propagation in stratified flux tubes has led to some interesting mathematics, its applicability to the solar atmosphere is somewhat limited. The value of the coefficient of kinematic viscosity is too small to have any appreciable effect on the viscous cutoff frequency, Ω_{Tv}, presented in Section 4.3. However it is also clear that the effect of dissipative effects in the solar atmosphere may become important. Indeed the introduction of magnetic diffusivity as the dissipative coefficient may have a significant effect. This topic is returned to in greater detail in Chapter 6.

5

Transverse MHD waves in stratified and viscous plasmas

The propagation of transverse MHD waves in vertical thin flux tubes embedded in a vertically stratified plasma in the presence of viscosity is shown to be governed by the KGB equation, which is solved in two limiting cases assuming an isothermal medium in hydrostatic equilibrium surrounded by a quiescent environment. It is found that the effect of viscosity on transverse waves is less than that for longitudinal waves. When the variation in the reduced velocity occurs over typical lengths much larger than the gravitational scale height, the KGB equation can be reduced to a Klein-Gordon equation which yields a wake oscillating with the frequency reduced by viscosity and the solution has no spatial or temporal decay. However, in the other limiting case, i.e., typical variations in the reduced velocity occur over characteristic lengths much smaller than the gravitational scale height, waves have a temporal and spatial decay. Applications to solar atmospheres are also considered.

5.1 Introduction

This Chapter extends the ideas from the previous Chapter such that the effect of viscosity on the propagation of transverse waves in thin flux tubes embedded in a vertically stratified plasma is studied. In Chapter 4 the introduction viscosity resulted in the formation of a KGB equation and consequently it is of interest as to what form the governing equation for transverse waves shall take. Will it be of the same form? Can we apply the same results? Is the effect of viscosity of greater or lesser significance in the transverse case? It is questions such as these that this Chapter will address.

5.2 Governing equations

In this chapter we mainly follow Hargreaves & Erdélyi (2008). We assume the tube is situated in a field-free, hydrostatic, isothermal and quiescent medium. The tube is assumed thin, vertical, free from twists, having a circular cross section and in temperature equilibrium with its surroundings. We neglect any distortions from a circular cross section by considering the average physical values inside the tube over the cross section. The axis of the equilibrium tube is given by the z-axis and thus the gravity vector is given by $\mathbf{g} = -g\hat{\mathbf{z}}$. A local cylindrical co-ordinate frame may also be introduced, $(r, \phi, \mathbf{l})$ where $\mathbf{l}$ is the vector along the tube. Since the tube is untwisted and assumed thin then the magnetic field is thus given by $\mathbf{B}_0 = B_0(r, \phi, \mathbf{l})\hat{\mathbf{l}}$, where the hat denotes the unit vector. Note also that for the equilibrium tube $\hat{\mathbf{l}} = \hat{\mathbf{z}}$. Since the environment is field-free the horizontal pressure balance is given by

$$p_0 + \frac{B_0^2}{2\mu} = p_e, \tag{5.1}$$

where p_0 and p_e are the gas pressures inside and outside the tube respectively. Since we are concerned with transverse tube waves, we note there is no variation in the cross section and thus density and pressure perturbations are neglected and we consider the equilibrium values, ρ_0 and p_0 respectively. The equation of motion is given by Eq. (1.26) with the term $\mathbf{F}_g = \rho_0 g$ and $\mathbf{F}_v$ given by Eq. (4.1), which can be simplified by taking $\nabla \cdot \mathbf{v} = 0$, describing the fact the medium inside the tube is incompressible. Thus the equation of motion for a viscous fluid may be written as

$$\rho_0 \frac{D\mathbf{v}}{Dt} = -\nabla\left(p_0 + \frac{B_0^2}{2\mu}\right) + \frac{1}{\mu}(\mathbf{B}_0 \cdot \nabla)\mathbf{B}_0 + \rho_0 \mathbf{g} + \rho_0 \nu \nabla^2 \mathbf{v}, \tag{5.2}$$

where ν is the coefficient of viscosity. Following Spruit (1981) we see that any arbitrary vector may be split into a component parallel and perpendicular to the tube axis, $\mathbf{a} = \mathbf{a}_\parallel + \mathbf{a}_\perp$ with $\mathbf{a}_\parallel = (\hat{\mathbf{l}} \cdot \mathbf{a})\hat{\mathbf{l}}$ and $\mathbf{a}_\perp = (\hat{\mathbf{l}} \times \mathbf{a}) \times \hat{\mathbf{l}}$. The full equation of motion may be decomposed into components in directions parallel and perpendicular to the tube axis. The parallel component of the equation of motion, supplemented with equations of continuity and energy, comprise the governing equations for longitudinal wave studies, which have been dealt with in the previous Chapter. Here we consider the transverse component which is given by

$$\rho_0 \left(\frac{D\mathbf{v}}{Dt}\right)_\perp = \hat{\mathbf{l}} \times \left[\rho_0 \mathbf{g} - \nabla\left(p_0 + \frac{B_0^2}{2\mu}\right)\right] \times \hat{\mathbf{l}} + \frac{B_0^2}{2\mu}\mathbf{k} + \mathbf{F}_{back} + \rho_0 \nu (\nabla^2 \mathbf{v})_\perp, \tag{5.3}$$

where the vector $\mathbf{k}$ is the curvature vector, perpendicular to the tube axis and having a magnitude of R^{-1}, where R is the radius of curvature. Note we have included the $\mathbf{F}_{back}$ term in Eq. (5.3). The back-reaction force was discussed at some length in Chapter 3. In this context

it is clear that since we are considering transverse motions only ($\mathbf{v}_{\parallel} = 0$) we may employ the original back-reaction term given by

$$\mathbf{F}_{back} = -\rho_e \left(\frac{D\mathbf{v}}{Dt}\right)_{\perp}, \tag{5.4}$$

which is correct for a simple transverse motion of a straight flux tube through the external medium.

Assuming horizontal pressure balance and taking the external medium to be one of hydrostatic equilibrium ($\nabla p_e = \rho_e \mathbf{g}$) we may rewrite the transverse equation of motion as

$$(\rho_0 + \rho_e)\left(\frac{D\mathbf{v}}{Dt}\right)_{\perp} = \rho_0 v_A^2 \mathbf{k} + (\rho_0 - \rho_e)[\hat{\mathbf{l}} \times \mathbf{g}] \times \hat{\mathbf{l}} + \rho_0 \nu (\nabla^2 \mathbf{v})_{\perp}. \tag{5.5}$$

We suppose that the tube is oriented almost vertically and assume that the horizontal displacement of matter relative to the exact equilibrium position, $\xi(z)$, is small. If the vertical displacements are also small then we may write

$$\left(\frac{D\mathbf{v}}{Dt}\right)_{\perp} = \left(\frac{D\mathbf{v}}{Dt}\right)_{x} = \frac{\partial v_x}{\partial t}, \tag{5.6}$$

where $v_x(t,z)$ is the linear transverse perturbed velocity and also

$$(\nabla^2 \mathbf{v})_{\perp} = \frac{\partial^2 v_x}{\partial z^2}. \tag{5.7}$$

Writing $\hat{\mathbf{l}} = (l_x, l_y, l_z)$ allows us to rewrite Eq. (5.5) as

$$\frac{\partial v_x}{\partial t} = \frac{\rho_0}{\rho_0 + \rho_e} v_A^2 k_x - \frac{\rho_0 - \rho_e}{\rho_0 + \rho_e} l_x l_z g + \frac{\rho_0}{\rho_0 + \rho_e} \nu \frac{\partial^2 v_x}{\partial z^2}. \tag{5.8}$$

Following Spruit (1981) we may write the the components of the unit vector $\hat{\mathbf{l}}$ and the curvature vector $\mathbf{k}$ as

$$l_x = \frac{\partial \xi}{\partial z} = \left(\frac{\partial}{\partial t}\right)^{-1} \frac{\partial v_x}{\partial z}, \quad l_z = 1, \tag{5.9}$$

and

$$k_x = \frac{\partial^2 \xi}{\partial z^2} = \left(\frac{\partial}{\partial t}\right)^{-1} \frac{\partial^2 v_x}{\partial z^2}, \quad k_z = 0. \tag{5.10}$$

Thus we write Eq. (5.8) as

$$\frac{\partial v_x}{\partial t} = \frac{\rho_0}{\rho_0 + \rho_e} v_A^2 \left(\frac{\partial}{\partial t}\right)^{-1} \frac{\partial^2 v_x}{\partial z^2} + \frac{\rho_0 - \rho_e}{\rho_0 + \rho_e} \left(\frac{\partial}{\partial t}\right)^{-1} \frac{\partial v_x}{\partial z} g + \frac{\rho_0}{\rho_0 + \rho_e} \nu \frac{\partial^2 v_x}{\partial z^2}, \tag{5.11}$$

and noting that $c_k^2 = \rho_0 v_A^2/(\rho_0 + \rho_e)$ being the kink speed (essentially the Alfvén speed for transverse tube waves) along with $g(\rho_e - \rho_0)/(\rho_0 + \rho_e) = c_k^2/2H$ (where H is the pressure scale height) we find

$$\frac{\partial^2 v_x}{\partial t^2} - c_k^2 \frac{\partial^2 v_x}{\partial z^2} + \frac{c_k^2}{2H} \frac{\partial v_x}{\partial z} - \frac{c_k^2}{v_A^2} \nu \frac{\partial^3 v_x}{\partial t \partial z^2} = 0. \tag{5.12}$$

To eliminate the first order derivative we adopted the following well known transformation

$$v_x(t,z) = e^{z/4H} Q(t,z), \tag{5.13}$$

giving

$$\frac{\partial^2 Q}{\partial t^2} - c_k^2 \frac{\partial^2 Q}{\partial z^2} + \Omega_k^2 Q - \frac{c_k^2}{v_A^2} \nu \frac{\partial}{\partial t}\left[\frac{1}{16H^2} Q + \frac{1}{2H}\frac{\partial Q}{\partial z} + \frac{\partial^2 Q}{\partial z^2}\right] = 0, \tag{5.14}$$

where $\Omega_k = c_k/4H$, being the cutoff frequency for transverse tube waves, hereafter called the kink cutoff frequency. Thus from Eq.(5.14) we see that a linear perturbation propagating transversely along the magnetic field in a magnetically isolated, stratified, viscous, and expanding tube is also governed by homogeneous Klein-Gordon-Burgers (KGB) equation. If we consider the internal medium to be ideal then we return to a wave equation in the Klein-Gordon form, see Hasan & Kalkofen (1999), Musielak & Ulmschneider (2001, 2003b). It is interesting at this point to compare the derived wave equation for transverse waves in a viscous medium with those for longitudinal waves derived in Chapter 4. We see that the equations are formally similar except for the propagation speed, the form of the cutoff frequency. The main difference arises in the form of the viscous term. For longitudinal waves the viscous term was preceded by a 4/3 term that arose from the fact that the medium is compressible. For transverse waves, which are incompressible, there is no contribution from this term and thus the effect of viscosity is consequently smaller. However there is an additional difference introduced by the c_k^2/v_A^2 term, which is a term that is dependent on the densities inside and outside the tube, since

$$\frac{c_k^2}{v_A^2} = \frac{\rho_0}{\rho_0 + \rho_e}. \tag{5.15}$$

This term will have a magnitude less than unity, highlighting the fact that the effect of viscosity is less pronounced for transverse waves propagating in a stratified atmosphere. We now consider the governing wave equation in two limiting cases.

5.3 Case 1: Variation in Q occurs over length scales much larger than H

Under this condition we see that the KGB equation describing transverse waves in a viscous flux tube may be reduced to

$$\frac{\partial^2 Q}{\partial t^2} - c_k^2 \frac{\partial^2 Q}{\partial z^2} + \Omega_k^2 Q - \frac{c_k^2}{v_A^2} \frac{\nu}{16H^2} \frac{\partial Q}{\partial t} = 0. \tag{5.16}$$

In much the same way as in the previous Chapter the nature of this equation may be examined by employing normal mode analysis by supposing a dependance of $Q(t,z)$ of the form $\exp[i(\omega t - kz)]$, where ω and k are the frequency and wavenumber respectively. This gives the dispersion relation

$$\omega^2 + \frac{i\nu c_k^2 \omega}{16H^2 v_A^2} - c_k^2 k^2 - \Omega_k^2 = 0, \tag{5.17}$$

where we note the second term is the contribution by viscosity. Suppose now we have a temporarily decaying wave, it is clear that the waves will damp if the imaginary part of ω is a positive quantity. We see from solving Eq. (5.17) for ω that $\Im(\omega)$ is always a negative quantity, thus waves may not damp temporarily. Further we note that the wave will propagate if the real part of ω exists and thus waves will propagate provided

$$\nu < 32H^2\frac{v_A^2}{c_k^2}\sqrt{c_k^2k^2+\Omega_k^2}. \tag{5.18}$$

Suppose now a spatially damped wave, we note waves will decay if $\Im(k) < 0$ and the dispersion relation may be written as

$$k^2 = \frac{\omega^2-\Omega_k^2}{c_k^2} + i\frac{\nu\omega}{16H^2v_A^2}. \tag{5.19}$$

Assuming mainly propagating waves, such that the magnitude of the real part of the wavenumber is much larger than that of the imaginary part ($|k_r| \gg |k_i|$), we find

$$k_i \approx \frac{\nu c_k\omega}{32H^2v_A^2\sqrt{\omega^2-\Omega_k^2}}, \tag{5.20}$$

being a positive quantity, thus in this limit we note there is no temporal or spatial damping. Considering the speeds of such waves we find the phase speed is given by

$$v_{ph} = \frac{\omega}{k} = -\frac{i\nu c_k^2}{32H^2kv_A^2} \pm \sqrt{c_k^2+\frac{1}{k^2}\left(\Omega_k^2-\frac{\nu^2c_k^4}{4\times16^2H^4v_A^4}\right)}, \tag{5.21}$$

with the $\pm$ sign denoting upward/downward propagating waves. The group speed is given by

$$v_g = \frac{\partial\omega}{\partial k} = \frac{kc_k^2}{\sqrt{c_k^2k^2+\Omega_k^2-\frac{\nu^2c_k^4}{4\times16^2H^2v_A^2}}}. \tag{5.22}$$

Reconsidering Eq. (5.16) we note it is a "telegrapher-type" and can be reduced into Klein-Gordon (KG) form with the following transformation

$$Q(t,z) = \exp\left(\frac{c_k^2}{32v_A^2}\frac{\nu}{H^2}t\right)q(t,z), \tag{5.23}$$

where the form of the transform results in an equation without first-order derivatives in time. Employing this transformation we find that equation for wave propagation in the case where the variation in Q is much larger than H is given by

$$\frac{\partial^2q}{\partial t^2} - c_k^2\frac{\partial^2q}{\partial z^2} + \left[\Omega_k^2 - \frac{c_k^4\nu^2}{32^2v_A^4H^4}\right]q = 0. \tag{5.24}$$

Thus the resulting KG equation describes waves propagating at the group speed c_k^2 followed by an oscillating wake, the frequency of which is reduced by the presence of the viscosity when compared to its ideal counterpart. In comparison to the corresponding equation for longitudinal wave propagation in a viscous plasma we see the reduction differs by a factor of c_k^4/v_A^4 and the extra 4/3 present in the longitudinal case. Eq. (5.24) may be solved subject to the following initial and boundary conditions

$$\lim_{t\to0,\, z\neq0} Q(t,z) = 0, \qquad \lim_{t\to0,\, z\neq0}\frac{\partial Q}{\partial t} = 0,$$

$$\lim_{z\to0} Q(t,z) = V(t), \qquad \lim_{z\to\infty} Q(t,z) = 0, \tag{5.25}$$

where $V(t)$ is an imposed velocity driver at the footpoint of the tube. Since the form of Eq. (4.27) is the same as that solved by Sutmann *et al.* (1998) we may reproduce their results directly here. Thus the general solution is

$$q(t,z) = V\left(t-\frac{z}{c_k}\right)\mathcal{H}\left(t-\frac{z}{c_k}\right)+\int_0^t V(t-\tau)W(\tau,z)d\tau, \tag{5.26}$$

where $\mathcal{H}(t-z/c_k)$ is the Heaviside unit step function and $W(\tau,z)$ is given by

$$W(\tau,z) = -\frac{\Omega_{kv}z}{c_k}\frac{J_1\left[\Omega_{kv}\sqrt{\tau^2-z^2/c_k^2}\right]}{\sqrt{\tau^2-z^2/c_k^2}}\mathcal{H}\left(\tau-\frac{z}{c_k}\right), \tag{5.27}$$

with

$$\Omega_{kv} = \left(\Omega_k^2-\frac{c_k^4\nu^2}{32^2v_A^4H^4}\right)^{\frac{1}{2}}, \tag{5.28}$$

being the reduced kink cut-off frequency in the viscous medium. It can readily be seen that the final general solution in terms of the original function $Q(t,z)$ may be written as

$$Q(t,z) = e^{c_k^2\nu t/32v_A^2H^2}\left[V\left(t-\frac{z}{c_k}\right)\mathcal{H}\left(t-\frac{z}{c_k}\right)+\int_0^t V(t-\tau)W(\tau,z)d\tau\right]. \tag{5.29}$$

This equation may be readily solved for various types of velocity driver.

5.3.1 Solving for various footpoint drivers

The governing Klein-Gordon equation may now be solved for the three drivers considered, namely a monochromatic source, a delta-function source and a sinusoidal pulse source.

Monochromatic source

The boundary condition is to be satisfied by a source of monochromatic acoustic waves, driven with a frequency ω and amplitude V_0. Thus the required boundary condition is given by

$$V(t) = V_0e^{-i\omega t}. \tag{5.30}$$

The solution may be quoted directly to give

$$\begin{aligned} Q(t,z) &= e^{c_k^2\nu t/32v_A^2H^2}\left[V_0e^{-i(\omega t+\sqrt{\omega^2-\Omega_{kv}^2}\,z/c_Tk)}+\right. \\ &\left.+\frac{V_0z\Omega_{kv}}{c_k}\sqrt{\frac{2}{\pi\Omega_{kv}}}\frac{1}{t^{3/2}}\frac{1}{\omega^2-\Omega_{kv}^2}\left[\Omega_{kv}\sin\mu+i\omega\cos\mu\right]\right], \end{aligned} \tag{5.31}$$

where now $\mu = \Omega_{kv}t-3\pi/4$. The solution is the sum of the free atmospheric oscillations (propagating from Ω_{kv}, otherwise evanescent) and the free oscillations (decay as $t^{3/2}$ and are at the cutoff frequency). The solution is multiplied by the $e^{c_k^2\nu t/32v_A^2H^2}$ term the exact behaviour of which will depend on the size of the viscous coefficient.

Delta-function driver

The source considered is a single pulse of δ-function form in time. Thus the boundary condition is given by

$$V(t) = \bar{V}_0 \delta(t). \tag{5.32}$$

The solution for $Q(t,z)$ is then given by

$$Q(t,z) = e^{c_k^2 \nu t/32 v_A^2 H^2} \left[\frac{-2\pi z V_0}{c_k} \sqrt{\frac{2}{\pi \Omega_{kv}}} \frac{1}{t^{3/2}} [\cos \mu] \right], \tag{5.33}$$

where $V_0 = \Omega_{kv} \bar{V}_0 / 2\pi$. Only the free terms remain since the analysis is carried out for $t \gg z/c_k$.

Sinusoidal pulse driver

The final case to be considered is that of a sinusoidal pulse at the footpoint of the tube lasting for one wave period, P, with $P = 2\pi/\omega$. The boundary condition is thus

$$V(t) = [\mathcal{H}(t) - \mathcal{H}(t-P)] e^{-i\omega t}. \tag{5.34}$$

The final solution for $Q(t,z)$ for the sinusoidal driver is given by

$$Q(t,z) = \tag{5.35}$$
$$e^{c_k^2 \nu t/32 v_A^2 H^2} \left[\frac{-\Omega_{kv} z V_0}{c_k} \sqrt{\frac{2}{\pi \Omega_{kv}}} \frac{1}{\omega^2 - \Omega_{kv}^2} \frac{1}{t^{3/2}} [\Omega_{kv} \sin\theta - \Omega_{kv} \sin\mu + i\omega \cos\theta - i\omega \cos\mu] \right],$$

where $\theta = \Omega_{kv}(t-P) - 3\pi/4$. For the sinusoidal pulse only the free oscillations remain. A random wavetrain of such pulses can be shown to be sustainable in the solar atmosphere and such the magnitude of the cutoff frequency modified by viscosity is important. This shall be examined later in the chapter but first the second limiting case is considered.

5.4 Case 2: Variation in Q occurs over length scales much smaller than H

Secondly we consider the case where the variation in Q occurs over length scales that are much smaller than the gravitational scale height, H. We note that Eq. (5.14) reduces to

$$\frac{\partial^2 Q}{\partial t^2} - c_k^2 \frac{\partial^2 Q}{\partial z^2} + \Omega_k^2 Q - \frac{c_k^2}{v_A^2} \nu \frac{\partial^3 Q}{\partial t \partial z^2} = 0. \tag{5.36}$$

Employing normal mode analysis as in the previous section reveals the dispersion relation

$$\omega = i \frac{k^2 \nu c_k^2}{2 v_A^2} \pm \sqrt{c_k^2 k^2 + \Omega_k^2 - \frac{\nu^2 c_k^4 k^4}{4 v_A^4}}, \tag{5.37}$$

where the first term represents the damping term. The imaginary part of the frequency is therefore positive and we note that the waves will thus display a temporal decay. We can also note that waves will propagate (i.e. $\Re(\omega)$ exists) if the condition

$$\nu < \frac{2v_A^2}{k^2 c_k^2}\sqrt{c_k^2 k^2 + \Omega_k^2}, \tag{5.38}$$

is satisfied. Supposing now a complex wavenumber but a real ω (i.e. a spatially damped wave), for mainly propagating waves the imaginary part of the wavenumber may be given by

$$k_i = -\frac{\nu\omega}{2c_k}\sqrt{\frac{\omega^2 - \Omega_k^2}{v_A^4 + \nu^2\omega^2}}, \tag{5.39}$$

which is a negative quantity and thus it can be concluded that waves in this limit are spatially damped.

5.4.1 Spatial boundary conditions

Let us now consider the KGB equation subject to the same boundary conditions as in the previous chapter, i.e.

$$Q\,|_{t=0} = f(z), \quad \left.\frac{\partial Q}{\partial t}\right|_{t=0} = g(z), \quad -\infty < z < \infty. \tag{5.40}$$

After applying a Laplace transform to Eq. (5.36), the ODE describing the propagation of waves is given by

$$\frac{d^2\Psi(s,z)}{dz^2} - m_2^2\Psi(s,z) = \frac{\nu}{v_A^2 + \nu s}\frac{d^2 f(z)}{dz^2} - \frac{v_A^2 g(z)}{v_A^2 c_k^2 + c_k^2 \nu s} - \frac{v_A^2 s f(z)}{v_A^2 c_k^2 + c_k^2 \nu s}, \tag{5.41}$$

where

$$\Psi(s,z) = \mathcal{L}[Q(t,z)] = \int_0^\infty Q(t,z)e^{-st}dt, \quad m_2^2 = \frac{v_A^2}{c_k^2 \nu}\left(\frac{s^2 + \Omega_k^2}{v_A^2/\nu + s}\right). \tag{5.42}$$

Eq. (5.41) may be solved in exactly the same way as presented in Section 4.4.1, such that we have the same result except that ν is replaced with $c_k^2\nu/v_A^2$. Thus one obtains

$$Q(t,z) = \frac{1}{2}\int_{-\infty}^{\infty}\left(g(z') - \frac{c_k^2\nu}{v_A^2}\frac{d^2 f(z')}{dz'^2}\right)\mathcal{L}_1 dz' - \frac{1}{2}\int_{-\infty}^{\infty} f(z')\mathcal{L}_2 dz', \tag{5.43}$$

where

$$\mathcal{L}_1 = \frac{v_A}{\pi c_k\sqrt{\nu}}\int_{v_A^2/\nu}^{\infty}\frac{e^{-t\eta}\cos\left(\frac{v_A(z-z')}{c_k\sqrt{\nu}}\sqrt{\frac{\eta^2+\Omega_T^2}{\eta - v_A^2/\nu}}\right)}{\sqrt{(\eta^2+\Omega_T^2)(\eta - v_A^2/\nu)}}d\eta, \tag{5.44}$$

and

$$\mathcal{L}_2 = -\frac{v_A}{\pi c_k\sqrt{\nu}}\int_{v_A^2/\nu}^{\infty}\frac{\eta e^{-t\eta}\cos\left(\frac{v_A(z-z')}{c_k\sqrt{\nu}}\sqrt{\frac{\eta^2+\Omega_T^2}{\eta - v_A^2/\nu}}\right)}{\sqrt{(\eta^2+\Omega_T^2)(\eta - v_A^2/\nu)}}d\eta. \tag{5.45}$$

5.4.2 Temporal boundary conditions

We now consider the solution Eq. (5.36) subject to the same temporal boundary conditions given in Eq. (5.25). Taking Laplace transforms we see that

$$\frac{\partial^2\psi(s,z)}{\partial z^2} - m_2^2\psi(s,z) = 0. \tag{5.46}$$

The solution of this ODE is readily seen to be

$$\psi(s,z) = \psi_0(s)e^{-mz} + \psi_1(s)e^{mz}, \tag{5.47}$$

where we may discard the ψ_1 term since we require a solution that is bounded at infinity. Thus we are seeking to find the inverse Laplace transform (see previous chapter for details)

$$\begin{aligned}\mathcal{L}^{-1}\left[\exp\left(\frac{-zv_A}{c_k\sqrt{\nu}}\sqrt{\frac{s^2+\Omega_k^2}{v_A^2/\nu+s}}\right)\right] &= -\frac{1}{\pi}\int_{v_A^2/\nu}^{\infty} e^{-\lambda t}\sin\left(\frac{zv_A}{c_k\sqrt{\nu}}\sqrt{\frac{\Omega_k^2+\lambda^2}{\lambda^2-v_A^2/\nu}}\right)d\lambda \\ &\quad -\frac{1}{\pi}\int_{-\Omega_k}^{\Omega_k} e^{-i\lambda t}\sinh\left(\frac{zv_A}{c_k\sqrt{\nu}}\sqrt{\frac{\Omega_k^2-\lambda^2}{v_A^2/\nu-i\lambda}}\right)d\lambda \\ &= W(t,z). \end{aligned} \tag{5.48}$$

Thus we see that the general solution for waves propagating in a viscous medium in the case where the variation in Q occurs over lengths scales much smaller that H is given by

$$Q(t,z) = \int_0^t V(t-\tau)W(\tau,z)d\tau. \tag{5.49}$$

5.5 Conclusions

It was shown in Section 4.5 that the coefficient of kinematic viscosity in the solar photosphere is extremely small, and thus will have a limited effect on the wave propagation. In the case when the variation in Q is much smaller than the scale height, it has been shown that wave propagation is governed by a KG equation with the reduced cutoff frequency $\Omega_{k\nu}$ and an exponential multiplier $e^{c_k^2\nu t/32v_A^2H^2}$. The cutoff period, $P_{k\nu} = 2\pi/\Omega_{k\nu}$, is shown in Fig. 5.1, which shows that the period may be increased from around 8 mins to around 9.5 mins, if the viscosity is increased to the order of 100 $\mathrm{km^2s^{-1}}$. This represents an increase of 5 orders of magnitude from expected photospheric values of viscosity. The percentage increase of cutoff period in the transverse case is smaller than in the corresponding longitudinal case due to the fact that the viscous term is effectively smaller in the transverse case by a factor of $4c_k^2/3v_A^2$. Fig. 5.2 illustrates this fact further by showing a multiplying factor of at most 1.2 for the highest viscosities and times as compared to approximately 4 in the longitudinal case. As previously discussed, however, any large increase in time is prevented by the $t^{-3/2}$ term present in Eq. (5.31), Eq. (5.33) and Eq. (5.35).

This chapter has demonstrated the effect of viscosity on transverse wave propagation in stratified atmospheres. It is shown that the governing equation for transverse waves is formally similar to that for longitudinal waves, with differences arising in the relative size of the viscous term. Transverse waves are less effected by viscosity than their longitudinal counterparts, the viscous term being at most 3/4 of that in the longitudinal case and possibly less. The governing equation was solved in two limiting cases corresponding to the variation of the velocity function Q compared to the scale height, H. In the first case it is shown that kink waves have no spatial or temporal damping, while the opposite is true in the second case. Detailed solutions have been developed in Section 5.3 which show that the atmospheric response is dependent on the viscosity in terms of both amplitude and frequency. In the second case (Section 5.4) it is not

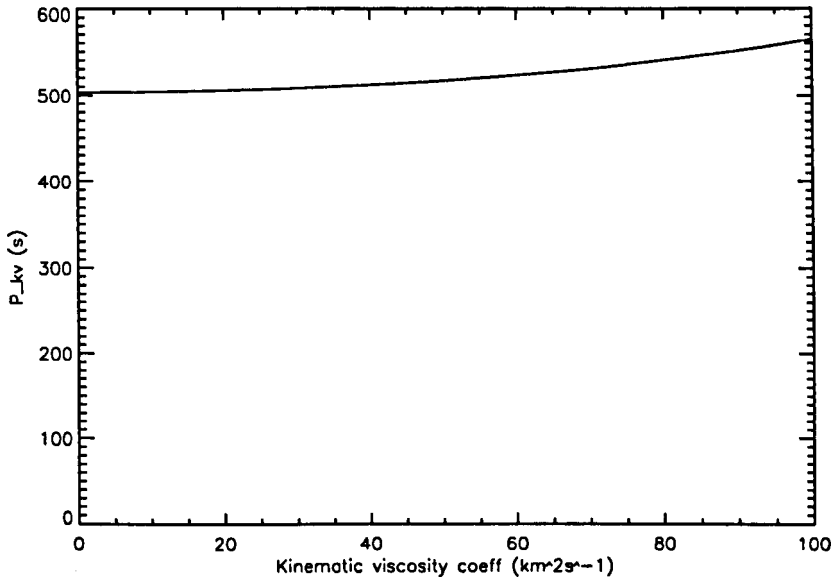

Figure 5.1: Change in cutoff period, P_{kv}, plotted against the viscosity coefficient.

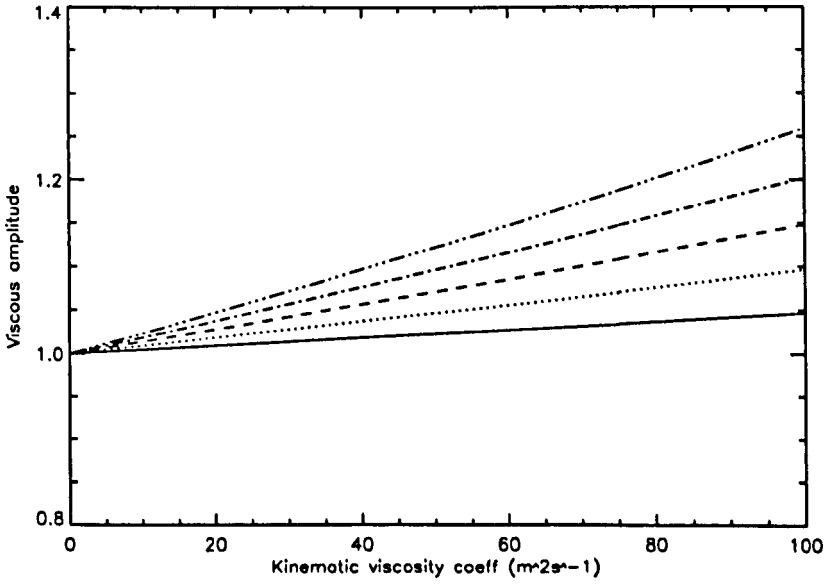

Figure 5.2: The exponential multiplier versus viscosity coefficient for times $t = 1000$ s (solid line) to $t = 5000$ s (dash-dot-dot-dot line).

so straightforward to provide such a conclusion since the resulting equations are considerably more complex.

It has been shown that in both cases the effect of viscosity on the propagation of transverse waves is less than in a corresponding longitudinal case. For the case when Q varies over scales smaller than H it was demonstrated that for realistic photospheric values the effect of viscosity is negligible. The coefficient of viscosity is required to raise by approximately 5 orders of magnitude before any appreciable change in the cutoff period is registered.

6 Conclusions

6.1 Overview of Thesis

This Thesis concentrates on the effect of flow and of the dissipative effect of viscosity on the characteristics of wave propagation in thin stratified flux tubes. The study has involved the derivation of the governing equations for both longitudinal and transverse waves and has attempted to solve them with regards to various footpoint drivers. The study of flow and viscosity has introduced realistic solar features into previous models of stratified flux tubes which have only dealt with the static and ideal cases. A theoretical examination of these aspects has been performed, which has then been applied to the solar atmosphere, although equating the results directly with observations is limited by the assumptions taken in order to allow an analytical treatment. The analysis is performed under the assumption of the thin flux tube equations and that the atmosphere is isothermal. For flux tubes in the solar atmosphere spatial variations and temperature effects are likely to become important.
The first half of the Thesis deals with wave propagation in a stratified flux tube with the presence of a background flow. Chapter 2 deals with longitudinal wave propagation and Chapter 3 investigates transverse wave propagation. In both cases the governing equations, derived for an isothermal atmosphere and under the assumption that the flow is small, are found to be formally similar. A general solution is derived by use of Laplace transforms and perturbation methods and solved for three specific drivers. The changes introduced by the flow compared to the corresponding static cases are highlighted and examined under relevant solar parameters. The second half of the Thesis investigated the effect of dissipation by viscosity on wave propagation in stratified static flux tubes. For an isothermal atmosphere the governing equations were derived and discussed in detail for two regimes of supposed velocity wavelength. Solutions were developed in each. Analysis was performed for longitudinal waves (Chapter 4) and for transverse waves (Chapter 5). The main results of the thesis are discussed in the next section.

6.2 Summary of results

Chapter 2 studied propagation of longitudinal tube waves in a stratified thin, isothermal flux tube with an internal equilibrium background. Laplace transforms and perturbation analysis

were used to solve the derived governing equation, and an application was made to photospheric conditions. It was found that for each of the three footpoint drivers considered, that the effect of the flow was to introduce a change in amplitude and phase, with both changes being functions of height. This applied to both the forced and free atmospheric oscillations. The percentage increase in amplitude for the forced terms was been shown to be strongly dependent on the applied wave frequency. For a driving period of 50 s it was shown that the difference over the static case may be up to 25% at the largest heights, with larger differences possible. The free oscillations are dominated by the temporal decay at any given height and this is relatively unaffected by the bulk flow. For a given footpoint driver it was found that the amplitude will increase with height up to the validity of the analysis. The maximum value was found to be around 1.5 %, but it should be recalled that the magnitude of the flow is restricted.

Chapter 3 extended the ideas presented in Chapter 2 for longitudinal waves to consider the propagation of transverse kink waves with an internal field-aligned background flow. A similar analysis was performed and it was found that the governing equation for transverse waves is formally similar to that for longitudinal waves. The results, therefore, echo those found in Chapter 2, but with some interesting differences. The flow introduces a term λ_k, the size of which is smaller than λ found in the longitudinal case. Since the introduced amplitude differences over the static case are dependent on this term, the effect of the flow is smaller in the transverse case. For the forced atmospheric oscillations the percentage increase is strongly dependent on the driving frequency and differences over the static case may be up to 8%, but higher differences may be achieved if smaller periods are considered. The free atmospheric oscillations show some interesting changes in amplitude, in which the amplitude may be reduced under certain conditions. The effect however is small and it is concluded that the small internal background flow has no major effect on the transverse wave characteristics under solar conditions.

In Chapter 4 a model for analyzing the propagation of slow MHD modes in a vertical thin flux tube with vertical stratification in the presence of viscous dissipation was developed. The equation governing the evolution of such waves was found to be of KGB form and analytical progress was made by considering solutions in two limiting cases. The first assumed that the variation in the perturbed velocity was much larger than the scale height, while the second assumed that the variation was much smaller. The dispersion relations were found for each case. In the first case it was possible to reduce the governing equation into KG form, where the viscosity manifested itself as a reduction in the cutoff frequency. Thus solutions were found for three footpoint drivers, namely a monochromatic source, a delta-function pulse and a sinusoidal pulse. When an application was made to the solar photosphere it becomes clear that the value of the coefficient of kinematic viscosity is too small to have any appreciable effect on the viscous cutoff frequency. The value of the viscosity coefficient would be required to increase by several orders of magnitude to register any appreciable effect on evolution of the waves. In the second case analytical solutions were found that did not lend themselves to simple treatment.
Chapter 5 demonstrated the effect of viscosity on transverse wave propagation in stratified atmospheres. The governing equation for transverse waves is formally similar to that for longitudinal waves, with differences arising in the relative size of the viscous term. Transverse waves are less effected by viscosity than their longitudinal counterparts, the viscous term being at most 3/4 of that in the longitudinal case. Much like in the longitudinal study the governing equation was solved in two limiting cases. It was shown that in both cases the effect of viscosity on the propagation of transverse waves is less than in a corresponding longitudinal case. For the case when Q varies over scales smaller than H it was demonstrated that for realistic

photospheric values the effect of viscosity is negligible.

6.3 Outlook

This Thesis studies wave propagation in stratified atmospheres and focuses on two major aspects, that of the introduction of a background flow and the effect of viscosity. The analysis has been performed under the assumption of the thin flux tube equations. This provides the work with three obvious extensions.

- Instead of taking the thin tube equations, the work of Terra-Homem *et al.* (2003) could be extended, which studied a background flow in a straight magnetic in cylindrical coordinates, to include gravity. They found that the flow has a marked effect on the dispersion relations and the conditions under which waves may propagate. The dispersion relations that could be derived would be of considerable interest. It is probable that this undertaking would be extremely difficult, and perhaps even impossible unless under restricted conditions, such as treating the flow as a small quantity which has been a requirement of this work.
- The thin flux tube model works well for a single isolated tube where the tube has room to expand before running into its neighbours. The model is much less applicable in regions where there are many tubes jostling next to each other, as may be expected in crowded cell boundaries. Thus a much more complicated model is required to deal with such a situation, one where progress is likely to be made numerically.
- It would also be interesting to attempt to derive the governing equations for the flow work along the lines of the derivation outlined in Roberts (2006), in which the KG equation was derived by scalings which extract the slow mode. This method, if tractable, would allow the derivation to be free of the assumption of isothermality, and thus allowing the characteristic speeds to be functions of height. This would give interesting and important results with far greater applicability to the solar atmosphere.

Chapters 2 and 3 have analytically studied 1-D wave propagation in tubes with a background flow. It would be of interest to attempt a similar study numerically to back up the solutions found in this Thesis. It should be recalled that the analysis was performed under the assumption that the flow was small at all heights, leading to restrictions on the magnitude of the footpoint flow. However the percentage differences (over the static case) in amplitude were found to be strongly dependant on the flow, such that extrapolating to large heights would give large percentage differences. A numerical study would show how far (if at all) the analytical solutions could be extended. This could have important consequences for observations.

Attention is now turned to the second half of the Thesis, namely the study into wave propagation with the introduction of viscosity. Chapters 4 and 5 included sections in which analysis was performed where the velocity perturbation varied over scales much smaller than the scale height. The solutions for temporal and spatial boundary conditions were found to have complicated integral forms that were not amenable to much further analytical study. Possible progress could be made, however, by considering these equations numerically and solving them for various footpoint drivers. Further the general governing equations, regardless of the variation in Q could be solved in terms of standing wave solutions rather than propagating waves. This would be another interesting study and important extension.

A further extension and generalisation of this work would be to consider the introduction of other dissipative coefficients, such as thermal conductivity or magnetic diffusivity. The thermal conduction appears in the energy equation as the loss function, $\mathcal{L}$. Potentially the more interesting dissipative coefficient is the electrical conductivity (σ), or its inverse, the electrical

resistivity (σ^{-1}), and hence the magnetic diffusivity ($\eta = 1/\mu\sigma$). This coefficient may be taken as isotropic only in the lower solar atmosphere when the condition $\omega_e\tau_e \gg 1$ may be applied, where ω_e is the electron gyrofrequency and τ_e is the electron collisional time. The inclusion of the diffusivity term in the induction equation describes the decay of the magnetic field. The magnetic diffusivity coefficient, η, is given by (Spitzer, 1962)

$$\eta = 10^9 T^{-3/2} \quad \mathrm{m^2/s}, \tag{6.1}$$

where T is the temperature. For conditions relevant to the solar photosphere the value of η may be many orders of magnitude greater than the corresponding coefficient of viscosity. An analysis that includes diffusivity will be less simple to derive but it is expected (Ballai, 2008 - private communication) that a similar equation, be it KG or KGB, as found in Chapters 4 and 5 will be produced. If this is the case then the considerably larger dissipative coefficient will have a marked effect on the wave propagation characteristics, and thus may have important consequences for the solar atmosphere.

A further interesting, if somewhat abstract and technical, study would be to consider the formal inclusion of the dissipative coefficients (viscosity, magnetic diffusivity etc.) in the derivation of the thin flux tube equations. This would be achieved by a reexamination of the work of say Roberts & Webb (1978) or Ferriz-Mas (1989a,b) to include such dissipative coefficients. This would provide more insight into the limitations and applicability of the thin flux tube equations in this non-ideal case.

6.4 Concluding Remarks

This Thesis provides some insight into the vastly complicated and fascinating realm of solar atmospheric physics. The aspects it has studied, namely steady flows and dissipative effects, are important in building up realistic models of the solar atmosphere. It is hoped that this Thesis has shed new light on these topics and may allow future development in this area of study.

A

Thin flux tube equations

The starting point for the discussion of the thin flux tube equations is the MHD equations for an ideal, inviscid and perfectly conducting gas, derived in Section 1.2.1, where $\mathbf{F}_g = \rho\mathbf{g}$ and $\mathbf{F}_\mu = 0$ in the momentum equation. The gravity vector is given by $\mathbf{g} = -g\mathbf{e}_3$, where here $\mathbf{e}_3$ denotes the unit vector in the z-direction. The thin flux tube equations were first derived by Roberts & Webb (1978). The system of equations is thus

$$\frac{\partial \rho}{\partial t} + \nabla \cdot (\rho \mathbf{v}) = 0, \tag{A-1}$$

$$\rho\left(\frac{\partial \mathbf{v}}{\partial t} + (\mathbf{v}\cdot\nabla)\mathbf{v}\right) = -\nabla p + \mathbf{j}\times\mathbf{B} + \rho\mathbf{g}, \tag{A-2}$$

$$\frac{\partial \mathbf{B}}{\partial t} = \nabla \times (\mathbf{v}\times\mathbf{B}), \tag{A-3}$$

$$\frac{\partial p}{\partial t} + \mathbf{v}\cdot\nabla p = \frac{\gamma p}{\rho}\left(\frac{\partial \rho}{\partial t} + \mathbf{v}\cdot\nabla\rho\right), \tag{A-4}$$

$$p = \frac{k}{\hat{m}}\rho T, \tag{A-5}$$

$$\nabla\cdot\mathbf{B} = 0, \tag{A-6}$$

$$\mathbf{j} = \frac{\nabla\times\mathbf{B}}{\mu}. \tag{A-7}$$

To consider axis-symmetric motions in an intense, vertical, untwisted flux tube, a cylindrical coordinate system is taken. It is assumed that there is no azimuthal dependance, such that variables are dependent on r, z and t only. Expanding each variable in its Maclaurin series about $r = 0$ and retaining only the zeroth order terms ($r = 0$) takes the tube to be thin, i.e the lateral scale is much less than the vertical scale. A small parameter may be introduced, such that $r = \varepsilon R$, with $\varepsilon \ll 1$ and R order unity. Thus

$$\frac{\partial}{\partial r} = \frac{1}{\varepsilon}\frac{\partial}{\partial R}. \tag{A-8}$$

The Maclaurin series for an arbitrary function, $f(x)$, expanded about $r = 0$ is given by

$$f(x) = f(0) + xf'(0) + \frac{x^2}{2!}f''(0) + ..., \tag{A-9}$$

where the primes indicates the first derivative, second derivative and so on. Expanding the pressure, p, in terms of its Maclaurin series about $r = 0$ yields

$$\begin{aligned} p(r,z,t) &= p(r=0,z,t) + r\frac{\partial p}{\partial r}(r=0,z,t) + O(\varepsilon^2), \\ &= p(t,z) + \varepsilon R p_1, \end{aligned} \tag{A-10}$$

where $p_1 = (\partial p/\partial r)_{r=0}$ showing p_1 is a function of z and t only. A correspondingly similar equation for density may be readily obtained. For the magnetic field it can be seen that $\mathbf{B} = (B_r, 0, B_z) = B_r\mathbf{e}_1 + B_z\mathbf{e}_3$, where $\mathbf{e}_1$ is the unit vector in the radial direction and $\mathbf{e}_3$ is the unit vector in the z-direction. The expansion of the magnetic field yields

$$\begin{aligned} \mathbf{B}(r,z,t) &= \mathbf{B}(r=0,z,t) + r\frac{\partial \mathbf{B}}{\partial r}(r=0,z,t) + O(\varepsilon^2), \\ &= (0,0,B_z(t,z)) + \varepsilon R(b_1,0,b_2), \end{aligned} \tag{A-11}$$

where $b_1 = (\partial B_r/\partial r)_{r=0}$ and $b_2 = (\partial B_z/\partial r)_{r=0}$, with b_1, b_2 therefore being functions of z and t only. The B_r is removed from the first term in the above equation due to the fact axis-symmetric motions are considered, thus its inclusion would invalidate either this condition or the solenoidal condition. A corresponding relation for the velocity vector $\mathbf{v}$ may be derived. Considering the zeroth order state (i.e as $\varepsilon \to 0$), $\mathbf{B}$, $\mathbf{v}$, p and ρ assume axial values. The equations of continuity, momentum, induction, energy, the ideal gas law and the solenoidal condition shall be dealt with in turn.

A.1 The MHD equations

A.1.1 Continuity

The equation of continuity is given by Eq.(A-1). Neglecting squares of the small parameter, i.e. $O(\varepsilon^2)$, it can be seen that the $\rho\mathbf{v}$ term may be given by

$$\begin{aligned} \rho\mathbf{v} &= [\rho + r\rho_1][(0,0,v_z(t,z)) + r(v_1,0,v_2)], \\ &= [\rho + r\rho_1][rv_1\mathbf{e}_1 + (v_z + rv_2)\mathbf{e}_3]. \end{aligned} \tag{A-12}$$

For an arbitrary vector $\mathbf{A}$, with no azimuthal dependance the divergence is given by

$$\nabla\cdot\mathbf{A} = \frac{1}{r}\frac{\partial}{\partial r}(rA_r) + \frac{\partial A_z}{\partial z}. \tag{A-13}$$

Using Eq. (A-13) to consider the radial component, $\mathbf{e}_1$, of the $\rho\mathbf{v}$ term given by Eq. (A-12) yields

$$
\begin{aligned}
rA_r &\Rightarrow r(\rho + r\rho_1)rv_1, \\
\text{thus } \frac{1}{r}\frac{\partial}{\partial r}(rA_r) &\Rightarrow \frac{1}{r}\left[(\rho + r\rho_1)rv_1 + r\frac{\partial}{\partial r}(\rho + r\rho_1)rv_1 + r(\rho + r\rho_1)\frac{\partial}{\partial r}(rv_1)\right], \\
&= (\rho + r\rho_1)v_1 + \frac{\partial}{\partial r}(\rho + r\rho_1)rv_1 + (\rho + r\rho_1)\frac{\partial}{\partial r}(rv_1), \\
&= 2(\rho + r\rho_1)v_1 + \frac{\partial}{\partial r}(\rho + r\rho_1)rv_1. \qquad \text{(A-14)}
\end{aligned}
$$

Turning attention to the vertical component,$\mathbf{e}_3$, yields

$$
\begin{aligned}
A_z &\Rightarrow [v_z + rv_2][\rho + r\rho_1], \\
\text{thus } \frac{\partial A_z}{\partial z} &\Rightarrow \left[\frac{\partial v_z}{\partial z} + r\frac{\partial v_2}{\partial z}\right](\rho + r\rho_1) + (v_z + rv_2)\frac{\partial}{\partial z}(\rho + r\rho_1). \qquad \text{(A-15)}
\end{aligned}
$$

Substituting the radial and vertical components into the continuity gives

$$
\begin{aligned}
\frac{\partial \rho}{\partial t} + \nabla\cdot(\rho\mathbf{v}) \Rightarrow\ & \frac{\partial}{\partial t}(\rho + r\rho_1) + 2(\rho + r\rho_1)v_1 + \frac{\partial}{\partial r}(\rho + r\rho_1)rv_1 + \\
& + \left[\frac{\partial v_z}{\partial z} + r\frac{\partial v_2}{\partial z}\right](\rho + r\rho_1) + (v_z + rv_2)\frac{\partial}{\partial z}(\rho + r\rho_1). \qquad \text{(A-16)}
\end{aligned}
$$

Thus to the zeroth order (replacing r with εR and taking $\varepsilon \to 0$) one obtains

$$
\frac{\partial \rho}{\partial t} + 2\rho v_1 + \frac{\partial v_z}{\partial z}\rho + v_z\frac{\partial \rho}{\partial z} = 0. \qquad \text{(A-17)}
$$

Eq. (A-17) may be rewritten by considering the expansion of $(\nabla\cdot\mathbf{v})_{r=0}$. It is known that

$$
\begin{aligned}
\mathbf{v} &= (0,0,v_z) + r(v_1,0,v_2) + O(r^2), \\
&= rv_1\mathbf{e}_1 + (v_z + rv_2)\mathbf{e}_3 + O(r^2), \qquad \text{(A-18)}
\end{aligned}
$$

thus, after neglecting $O(r^2)$, the divergence of velocity is given by

$$
\nabla\cdot\mathbf{v} = \frac{1}{r}\frac{\partial}{\partial r}(r^2v_1) + \frac{\partial}{\partial z}(v_z + rv_2). \qquad \text{(A-19)}
$$

Taking the only zeroth order terms gives

$$
(\nabla\cdot\mathbf{v})_{r=0} = 2v_1 + \frac{\partial v_z}{\partial z}. \qquad \text{(A-20)}
$$

Thus Eq. (A-17) may be rewritten as

$$
\frac{\partial \rho}{\partial t} + \rho\Delta + v_z\frac{\partial \rho}{\partial z} = 0, \qquad \text{(A-21)}
$$

where $\Delta = (\nabla\cdot\mathbf{v})_{r=0}$.

A.1.2 Momentum

The momentum equation is given by Eq. (A-2). Examining the current density, $\mathbf{j}$, given that the magnetic field is $\mathbf{B} = (0,0,B_z(t,z)) + r(b_1,0,b_2)$, it can be seen that

$$\begin{aligned} \mathbf{j} = \frac{\nabla \times \mathbf{B}}{\mu} &= \frac{1}{\mu r}\begin{vmatrix} \mathbf{e}_1 & r\mathbf{e}_2 & \mathbf{e}_3 \\ \frac{\partial}{\partial r} & \frac{\partial}{\partial \phi} & \frac{\partial}{\partial z} \\ rb_1 & 0 & B_z + rb_2 \end{vmatrix}, \\ &= \frac{1}{\mu r}\left[0\mathbf{e}_1 + \left(\frac{\partial}{\partial z}(rb_1) - \frac{\partial}{\partial r}(B_z + rb_2)\right) r\mathbf{e}_2 + 0\mathbf{e}_3\right]. \end{aligned} \tag{A-22}$$

Thus $\mathbf{j}$ is clearly in the azimuthal direction and has a magnitude of (to the zeroth order) $-b_2/\mu$. Given that $\mathbf{j}$ is azimuthal and $\mathbf{B}$ is essentially axial, $\mathbf{j} \times \mathbf{B}$ must be radial (since $(0,\phi,o) \times (0,0,z) = (r,0,0)$). Examining, firstly, only the vertical component of the momentum equation, one may ignore the $\mathbf{j} \times \mathbf{B}$ term since it is radial, yielding

$$\rho\left(\frac{\partial \mathbf{v}}{\partial t} + (\mathbf{v}\cdot\nabla)\mathbf{v}\right) = -\nabla p + \rho\mathbf{g}. \tag{A-23}$$

Ignoring the $O(r^2)$ terms one sees that

$$\mathbf{v}_{e_3} = v_z + rv_2, \quad \frac{\partial \mathbf{v}_{e_3}}{\partial t} = \frac{\partial v_z}{\partial t} + r\frac{\partial v_2}{\partial t}, \tag{A-24}$$

and

$$\begin{aligned} (\mathbf{v}\cdot\nabla)\mathbf{v}|_{e_3} &= \left(v_z\frac{\partial}{\partial z} + rv_2\frac{\partial}{\partial z}\right)[v_z + rv_2], \\ &= v_z\frac{\partial V_z}{\partial z} + v_z r\frac{\partial v_2}{\partial z} + rv_2\frac{\partial v_z}{\partial z}. \end{aligned} \tag{A-25}$$

The pressure term is given by

$$-\nabla p|_{e_3} = -\frac{\partial p}{\partial z} - r\frac{\partial p_1}{\partial z}, \tag{A-26}$$

and the density term by

$$\rho\mathbf{g}|_{e_3} = -\rho g - r\rho_1 g. \tag{A-27}$$

Letting $r = \varepsilon R$ and considering the zeroth order terms ($\varepsilon \to 0$) one finds

$$\left(\frac{\partial v_z}{\partial t} + v_z\frac{\partial v_z}{\partial z}\right)\rho = -\frac{\partial p}{\partial z} - \rho g. \tag{A-28}$$

Now turning to the radial component of the momentum equation one sees that

$$[\rho + r\rho_1]\left(r\frac{\partial v_1}{\partial t} + (\mathbf{v}\cdot\nabla)\mathbf{v}|_{e_1}\right) = -\frac{\partial}{\partial r}(p + rp_1) + \mathbf{j} \times \mathbf{B}, \tag{A-29}$$

where

$$(\mathbf{v}\cdot\nabla)\mathbf{v}|_{e_1} = \left(rv_1\frac{\partial}{\partial r}\right)[rv_1] = rv_1^2. \tag{A-30}$$

The $\mathbf{j} \times \mathbf{B}$ has been shown to be radial and has magnitude $-b_1 B/\mu$, thus to the zeroth order the momentum equation yields

$$p_1 + B\frac{b_2}{\mu} = 0. \tag{A-31}$$

This equation shows that the total pressure on the axis is the same as the pressure on the boundary, i.e. it is constant across the tube. Thus a non-linear pressure balance condition is prescribed and given by

$$p + \frac{B^2}{2\mu} = p_e. \tag{A-32}$$

A.1.3 Induction

The induction equation is given by Eq. (A-3) and may be rewritten as

$$\frac{\partial \mathbf{B}}{\partial t} = \mathbf{v}(\nabla \cdot \mathbf{B}) - \mathbf{B}(\nabla \cdot \mathbf{v}) + (\mathbf{B} \cdot \nabla)\mathbf{v} - (\mathbf{v} \cdot \nabla)\mathbf{B}. \tag{A-33}$$

The time derivative of the magnetic field is given by

$$\frac{\partial \mathbf{B}}{\partial t} = \left[r\frac{\partial b_1}{\partial t}\right]\mathbf{e}_1 + \left[\frac{\partial B_z}{\partial t} + r\frac{\partial b_2}{\partial t}\right]\mathbf{e}_3. \tag{A-34}$$

The first and second terms in Eq. (A-33) may be dealt with by employing the solenoidal condition and letting $(\nabla \cdot \mathbf{v})_{r=0} = \Delta$ respectively. The third and fourth terms may be dealt with by considering the textbook cylindrical components of $(\mathbf{P} \cdot \nabla)\mathbf{Q}$, for two arbitrary vectors, $\mathbf{P}$ and $\mathbf{Q}$. Thus

$$(\mathbf{P} \cdot \nabla)\mathbf{Q}|_{e_1} = P_r\frac{\partial Q_r}{\partial r} + P_z\frac{\partial Q_r}{\partial z}, \tag{A-35}$$

$$(\mathbf{P} \cdot \nabla)\mathbf{Q}|_{e_3} = P_r\frac{\partial Q_z}{\partial r} + P_z\frac{\partial Q_z}{\partial z}. \tag{A-36}$$

Thus the third and fourth terms in Eq. (A-33) are given by

$$\begin{aligned}(\mathbf{B} \cdot \nabla)\mathbf{v} &= \left[rb_1\frac{\partial}{\partial r}(rv_1) + (B_z + rb_2)\frac{\partial}{\partial z}(rv_1)\right]\mathbf{e}_1 + \\ &+ \left[rb_1\frac{\partial}{\partial r}(v_z + rv_2) + (B_z + rb_2)\frac{\partial}{\partial z}(v_z + rv_2)\right]\mathbf{e}_3,\end{aligned} \tag{A-37}$$

$$\begin{aligned}(\mathbf{v} \cdot \nabla)\mathbf{B} &= \left[rv_1\frac{\partial}{\partial r}(rb_1) + (v_z + rv_2)\frac{\partial}{\partial z}(rb_1)\right]\mathbf{e}_1 + \\ &+ \left[rv_1\frac{\partial}{\partial r}(B_z + rb_2) + (v_z + rv_2)\frac{\partial}{\partial z}(B_z + rb_2)\right]\mathbf{e}_3.\end{aligned} \tag{A-38}$$

Thus to the zeroth order the radial component of the induction equation is given by

$$\frac{\partial b_1}{\partial t} = -b_1\Delta + B_z\frac{\partial v_1}{\partial z} - v_z\frac{\partial b_1}{\partial z}, \tag{A-39}$$

and to the zeroth order the vertical component is given by

$$\frac{\partial B_z}{\partial t} = -B_z\Delta + B_z\frac{\partial v_z}{\partial z} - v_z\frac{\partial B_z}{\partial z}. \tag{A-40}$$

A.1.4 Energy

The energy equation readily yields, to the zeroth order,

$$\frac{\partial p}{\partial t} + v\frac{\partial p}{\partial z} = \frac{\gamma p}{\rho}\left(\frac{\partial \rho}{\partial t} + v\frac{\partial \rho}{\partial z}\right). \tag{A-41}$$

A.1.5 Ideal Gas

The equation for ideal gas readily yields, to the zeroth order,

$$p(t,z) = \frac{k}{\hat{m}}T(t,z)\rho(t,z). \tag{A-42}$$

A.1.6 Solenoidal

Using the definition of divergence for cylindrical coordinates it is easily seen that to the zeroth order

$$2b_1 + \frac{\partial B}{\partial z} = 0. \tag{A-43}$$

A.2 Summary

Thus the non-linear thin flux tube equations for the study of longitudinal waves are given by (Roberts & Webb, 1978)

$$\rho\left(\frac{\partial v_z}{\partial t} + v_z v_z'\right) + p' + \rho g = 0, \tag{A-44}$$

$$\frac{\partial}{\partial t}\left(\frac{\rho}{B_z}\right) + \left(\frac{\rho v_z}{B_z}\right)' = 0, \tag{A-45}$$

$$\frac{\partial p}{\partial t} + v_z p' - c^2\left(\frac{\partial \rho}{\partial t} + v_z\rho'\right) = 0, \tag{A-46}$$

$$p + \frac{B_z^2}{2\mu} = p_e, \tag{A-47}$$

where Δ has been eliminated from the equations of continuity and induction to give a conservation of flux equation. The prime indicates a derivative in the z-direction. These equations will form the basis of the study into longitudinal wave propagation with the presence of a background flow.

B

Multiple Scales

The solution to Eq. (2.54) in the main text is sought in terms of a multiple scales approach rather than treating it as a regular problem, e.g Holmes (1995). Thus Eq. (2.54) holds, but one assumes two scales, $z_1 = z$ and $z_2 = \varepsilon z$, exist. The two scales are assumed independent, such that

$$\frac{d}{dz} = \frac{\partial}{\partial z_1} + \varepsilon \frac{\partial}{\partial z_2}, \tag{B-1}$$

$$\frac{d^2}{dz^2} = \frac{\partial^2}{\partial z_1^2} + 2\varepsilon \frac{\partial^2}{\partial z_1 \partial z_2} + \varepsilon^2 \frac{\partial^2}{\partial z_2^2}. \tag{B-2}$$

Thus one finds

$$\left[\frac{\partial^2}{\partial z_1^2} + 2\varepsilon \frac{\partial^2}{\partial z_1 \partial z_2} + \varepsilon^2 \frac{\partial^2}{\partial z_2^2}\right] q - a\varepsilon e^{z_1/2H} \left[\frac{\partial}{\partial z_1} + \varepsilon \frac{\partial}{\partial z_2^2}\right] q - (m^2 + b\varepsilon e^{z/2H}) q = 0. \tag{B-3}$$

Now let

$$q = q_0(z_1, z_2) + \varepsilon q_1(z_1, z_2) + \ldots, \tag{B-4}$$

such that upon substitution one obtains

$$\left[\frac{\partial^2}{\partial z_1^2} + 2\varepsilon \frac{\partial^2}{\partial z_1 \partial z_2} + \ldots\right](q_0 + \varepsilon q_1 + \ldots) - a\varepsilon e^{z_1/2H} \left[\frac{\partial}{\partial z_1} + \ldots\right](q_0 + \ldots)$$
$$-(m^2 + b\varepsilon e^{z/2H})(q_0 + \varepsilon q_1 + \ldots) = 0. \tag{B-5}$$

First consider terms of order ε^0, given by

$$\frac{\partial^2 q_0}{\partial z_1^2} - m^2 q_0 = 0, \tag{B-6}$$

which solves to give

$$q_0 = Ae^{-mz_1} + Be^{mz_1}, \tag{B-7}$$

where A, B are functions of s and z_2, but are left general for the moment. Next consider terms of order ε^1, given by

$$\frac{\partial^2 q_1}{\partial z_1^2} - m^2 q_1 = -2\frac{\partial^2 q_0}{\partial z_1 \partial z_2} + ae^{z_1/2H}\frac{\partial q_0}{\partial z_1} + be^{z_1/2H} q_0. \tag{B-8}$$

After substitution of Eq. (B-7) one obtains

$$\frac{\partial^2 q_1}{\partial z_1^2} - m^2 q_1 = e^{-mz_1}\left(2\frac{\partial A}{\partial z_2}m + (bA - amA)e^{z_1/2H}\right) + e^{mz_1}\left(-2\frac{\partial B}{\partial z_2}m + (bB + amB)e^{z_1/2H}\right). \tag{B-9}$$

This may be solved by first considering the CF, such that

$$\frac{\partial^2 q_1}{\partial z_1^2} - m^2 q_1 = 0, \tag{B-10}$$

and thus

$$q_1 = Ce^{-mz_1} + De^{mz_1}, \tag{B-11}$$

where C, D are again functions of s and z_2. For the PI take

$$q_1 = e^{-mz_1}[Ez_1 + Fe^{z_1/2H}] + e^{mz_1}[Jz_1 + Ke^{z_1/2H}], \tag{B-12}$$

which may be differentiated twice, substituted into the Eq. (B-9) and after equating terms one finds

$$E = -\frac{\partial A}{\partial z_2}, \tag{B-13}$$

$$F = \frac{4H^2(bA - amA)}{1 - 4Hm}, \tag{B-14}$$

$$J = -\frac{\partial B}{\partial z_2}, \tag{B-15}$$

$$K = \frac{4H^2(bB + amB)}{1 + 4Hm}. \tag{B-16}$$

Applying the boundary conditions

$$\lim_{z\to\infty} q_0(s,z) = 0, \quad \text{thus} \quad B = 0, \tag{B-17}$$

$$\lim_{z\to 0} q_0(s,z) = v(s), \quad \text{thus} \quad A = v(s), \tag{B-18}$$

$$\lim_{z\to\infty} q_1(s,z) = 0, \quad \text{thus} \quad D = 0, \tag{B-19}$$

$$\lim_{z\to 0} q_1(s,z) = 0, \quad \text{thus} \quad C = \frac{4H^2 v(s)(am - b)}{1 - 4mH}. \tag{B-20}$$

Thus one sees that $q_1 = CF + PI$ is given by

$$q_1 = e^{-mz_1}\left(-\frac{\partial v(s)}{\partial z_2}z_1 + \frac{4H^2 v(s)(am-b)}{1-4Hm}(1-e^{z_1/2H})\right). \tag{B-21}$$

Since the boundary condition $v(s)$ is a function of s only, secular terms are avoided. Letting $z_1 = z$ and recalling that $q = q_0 + \varepsilon q_1$ one obtains

$$q = v(s)e^{-mz}\left(1 + \frac{\varepsilon 4H^2(am-b)}{1-4Hm}(1-e^{z/2H})\right), \tag{B-22}$$

and thus we see that one obtains the same result as in the regular expansion case.

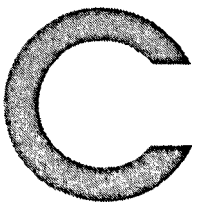

Alternative derivation for Section 4.2

C.1 Governing equations

This appendix outlines an alternative derivation for Section 4.2 based on a similar method employed in Chapter 2. The governing non-linear equations are now given by

$$\frac{\partial}{\partial t}\left(\frac{\rho}{B}\right)+\left(\frac{\rho v}{B}\right)'=0, \tag{C-1}$$

$$\rho\left(\frac{\partial v}{\partial t}+vv'\right)+p'+\rho g=\rho\nu v'', \tag{C-2}$$

$$\frac{\partial p}{\partial t}+vp'=c^2\left(\frac{\partial \rho}{\partial t}+v\rho'\right), \tag{C-3}$$

$$p+\frac{B^2}{2\mu}=p_e, \tag{C-4}$$

where the prime indicates the derivative in the z-direction. Performing linear analysis, such that $p\equiv p+p_0$, $\rho\equiv\rho+\rho_0$, $B\equiv B+B_0$ and $v\equiv u$, where the unsubscripted quantities denote perturbed quantities, yield the linearised equations

$$B_0\frac{\partial \rho}{\partial t}-\rho_0\frac{\partial B}{\partial t}+B_0^2\left(\frac{\rho_0 u}{B_0}\right)'=0, \tag{C-5}$$

$$\rho_0\frac{\partial u}{\partial t}+p'+\rho g=\rho_0\nu u'', \tag{C-6}$$

$$\frac{\partial p}{\partial t}+up_0'-c_0^2\left(\frac{\partial \rho}{\partial t}+u\rho_0'\right)=0, \tag{C-7}$$

$$p+\frac{B_0 B}{\mu}=p_e, \tag{C-8}$$

where p_e in the above equation represents the perturbation in external pressure. One may now follow Musielak *et al.* (1989) by introducing the following variable changes, such that

$$\rho_1 = \frac{\rho}{\rho_0}, \quad p_1 = \frac{p}{\rho_0}, \quad B_1 = \frac{B}{B_0}, \tag{C-9}$$

and the governing equations become

$$\frac{\partial \rho_1}{\partial t} - \frac{\partial B_1}{\partial t} + \frac{B_0}{\rho_0}\left(\frac{\rho_0 u}{B_0}\right)' = 0, \tag{C-10}$$

$$\frac{\partial u}{\partial t} + p_1' + \frac{\rho_0'}{\rho_0} p_1 + \rho_1 g - \nu u'' = 0, \tag{C-11}$$

$$\frac{\partial p_1}{\partial t} + u\frac{p_0'}{\rho_0} - c_0^2\left[\frac{\partial \rho_1}{\partial t} + u\frac{\rho_0'}{\rho_0}\right] = 0, \tag{C-12}$$

$$p_1 + v_A^2 B_1 - \frac{p_e}{\rho_0} = 0. \tag{C-13}$$

Denoting Eq. (C-10) to Eq. (C-13) by n_1, n_2, n_3 and n_4 respectively and performing the following procedure

$$\frac{c_0^2}{v_A^2}\frac{\partial n_4}{\partial t} + c_0^2 n_1 + n_2, \tag{C-14}$$

yields

$$\frac{\partial p_1}{\partial t} + c_T^2 \frac{B_0}{\rho_0}\left(\frac{\rho_0 u}{B_0}\right)' + \left(\frac{c_T^2 p_0'}{c_0^2 \rho_0} - c_T^2 \frac{\rho_0'}{\rho_0}\right) u - \frac{1}{\rho_0}\frac{c_T^2}{v_A^2}\frac{\partial p_e}{\partial t} = 0. \tag{C-15}$$

Additionally performing the following procedure

$$\frac{\partial n_3}{\partial t} - \frac{g}{v_A^2}\frac{\partial n_4}{\partial t} - g n_1, \tag{C-16}$$

yields

$$\frac{\partial^2 u}{\partial t^2} - \nu \frac{\partial}{\partial t}[u''] + \left[\frac{\partial}{\partial z} + \frac{\rho_0'}{\rho_0} - \frac{g}{v_A^2}\right]\frac{\partial p_1}{\partial t} - g\frac{B_0}{\rho_0}\left(\frac{\rho_0 u}{B_0}\right)' + \frac{g}{\rho_0 v_A^2}\frac{\partial p_e}{\partial t} = 0. \tag{C-17}$$

Eliminating $\partial p_1/\partial t$ between Eq. (C-15) and Eq. (C-17) and making the substitution $u(t,z) = \exp(z/4H)Q(t,z)$ yields Eq. (4.15) of the main text, namely

$$\frac{\partial^2 Q}{\partial t^2} - c_T^2 \frac{\partial^2 Q}{\partial z^2} + \Omega_T^2 Q - \nu \frac{\partial}{\partial t}\left(\frac{1}{16H^2} + \frac{1}{2H}\frac{\partial}{\partial z} + \frac{\partial^2}{\partial z^2}\right) Q = -\frac{e^{-z/4H}}{\rho_0(z)}\left(\frac{c_T}{v_A}\right)^2 \frac{\partial}{\partial t}\left(\frac{\partial p_e}{\partial z} + \frac{g}{c_0^2} p_e\right).$$

References

Alfvén, H., *Nature*, **150**, 405 (1942)

Aschwanden, M.J., Fletcher, L., Schrijver, C.J. & Alexander, D., *ApJ*, **520**, 880 (1999)

Aschwanden, M. *Physics of the Solar Corona*, Springer, (2006)

Ballai, I., *A&A*, **410**, L17 (2003)

Ballai, I., Erdélyi, R. & Hargreaves, J., *Physics of Plasmas*, **13**, 042108-1 (2006)

Banerjee, D., Erdélyi, R., Oliver, R. & O'Shea, E., *Sol. Phys.*, **246**, 3 (2007)

Berghmans, D. & Clette, F., *Sol. Phys.*, **186**, 207 (1999)

Bogdan, T.J., *Sol. Phys.*, **192**, 373 (2000)

Boyd, T.J.M. & Sanderson, J.J., *Plasma Dynamics*, Nelson, London (1969)

Braginskii, S.I., *Rev. Plasma phys.*, **1**, 205 (1965)

Buchlin, E. & Hassler, D.M. in *AAS/Solar Physics Division Meeting*, Vol. 32, 810 (2000)

Cheng, J. *A&A*, **264**, 243 (1992)

Choudhuri, A. R. *A&A*, **239**, 335 (1990)

Coulson, C.A., *Waves* (Interscience Publishers, New York, 1955), p. 15

Cowling, T.G., *Magnetohydrodynamics*, 2^{nd} Edition, Adam Higler, Bristol (1976)

Curdt, W. & Heinzel, P., *ApJ*, **503**, L95 (1998)

Defouw R.J *ApJ*, **209**, 266 (1976)

DeForest, C.E., & Gurman, J.B., *ApJ Lett.*, **501**, L217 (1998)

De Moortel, I., Ireland, J. & Walsh, R.W., *A&A*, **355**, L23 (2000)

De Moortel, I., Hood, A., Ireland, J. & Walsh, R.W., *Sol. Phys.*, **209**, 61 (2002a)

De Moortel, I., Hood, A., Ireland, J. & Walsh, R.W., *Sol. Phys.*, **209**, 89 (2002b)

De Moortel, I., Ireland, J., Hood, A. & Walsh, R.W., *A&A*, **387**, L13 (2002c)

De Pontieu, B. & Erdélyi, R., *Phil. Trans. Roy. Soc., A*, **364**, 383, (2006)

De Pontieu, B., Erdélyi, R. & de Wijn, A. G., *ApJ*, **595**, L63, (2003a)

De Pontieu, B., Tarbell, T. & Erdélyi, R., *ApJ*, **590**, 502 (2003b)

De Pontieu B., Erdélyi, R. & James, S.P., *Nature*, **430**, 536 (2004)

De Pontieu B., Erdélyi,R. & De Moortel, I., *ApJ*, **624**, 61L (2005)

De Pontieu, B., McIntosh, S.W., Carlsson, M., Hansteen, V.H., Tarbell, T.D., Schrijver, C.J., Title, A.M., Shine, R.A., Tsuneta, S., Katsukawa, Y., Ichimoto, K., Suematsu, Y., Shimizu, T. & Nagata, S., *Science*, **318**, 1574 (2007)

Edwin, P.M. & Roberts B., *Sol. Phys.*, **88**, 179 (1983)

Erdélyi, A., Magnus, W., Oberhettinger, F., & Tricomi,F.G., *Table of integral transforms, Volume 1*, (McGraw-Hill Book Co., Inc. New-York, 1954), p. 102

Erdélyi, R., *Phil. Trans. Roy. Soc., A*, **364**, 351 (2006)

Erdélyi, R., Magnetohydrodynamic Waves, in Hasan, S.S. and Banerjee, D. (eds.) *Kodai School on Solar Physics, AIP-CP*, **919**, pp.122-137 (2007)

Erdélyi, R. & Ballai, I., Heating of the Solar and Stellar Coronae: A Review, *Astron. Nachrichten*, **328**, 726 (2007)

Erdélyi, R., & Fedun, V., *Science*, **318**, 1572 (2007)

Erdélyi, R., & Goossens, M., *A&A*, **294**, 575 (1995)

Erdélyi, R. & Hargreaves, J.A., *A&A*, In Press (2008)

Erdélyi, R., Malins, C., Tóth, G. & De Pontieu, B., *A&A*, **467**, 1299 (2007)

Fan, Y., Fisher, G. H. & McClymont A. N., *ApJ*, **436**, 907 (1994)

Fawzy, D., Ulmschneider, P. & Cuntz M. *A&A*, **336**, 1029 (1998)

Ferriz-Mas, A. & Schüssler, M., *Geophys. Astrosphys. Flu. Dynam.*, **48**, 217 (1989a)

Ferriz-Mas, A., Schüssler, M. & Anton, V., *A&A*, **210**, 425 (1989b)

Fleck, B. & Schmitz, F., *A&A*, **250**, 235 (1991)

Giovanelli, R.G., Livingstone, W.C. & Harvey, J.V., *Sol. Phys.*, **59**, 49 (1978)

Gloeckler, G. & Geiss, J. *Space Sci. Rev.*, **86**, 127 (1998)

Hargreaves, J.A. & Erdélyi, R., *A& A, In Press* (2008)

Hasan, S.S. & Kalkofen, W., *ApJ*, **519**, 899 (1999)

Holmes, M., *Introduction to Perturbation Methods*, Springer-Verlag (1995)

Innes D.E., Inhester B., Axford W.I. & Wilhelm K. *Nature*, **386**, 811 (1997)

Joarder, P.S., Nakariakov, V.M. & Roberts, B., *Sol. Phys.*, **176**, 285 (1997)

Joarder, P.S. & Narayanan, A.S., *A&A*, **359**, 1211, (2000)

Kalkofen,W., Rossi, P., Bodo, G. & Massaglia, S., *ApJ*, **284**, 976 (1994)

King, D.B., Nakariakov, V.M., DeLuca, E.E., Golub, L. & McClements, K.G., *A&A*, **404**, L1 (2003)

Kliem, B., Dammasch I.E., Curdt, W & Wilhelm, K., *ApJ Lett.*, **568**, L61 (2002)

Lamb, H., *Proc. London Math. Soc.*, **7**, 122 (1908)

Lamb, H., *Hydrodynamics*, Cambridge University Press (1932)

Lighthill, M.J., *Royal Society of London Philosophical Transactions Series A*, **252**, 397 (1960)

Lites, B.W., Rutten, R.J. & Kalkofen, W., *ApJ*, **414**, 345 (1993)

Malins, C. & Erdélyi, R., *Sol. Phys.*, **246** 41 (2007)

Marsh, M.S. & Walsh, R.W., *ApJ*, **643** 540 (2006)

McAteer, R.T.J., Gallagher, P.T., Bloomfield, D.S.,Williams, D.R., Mathioudakis, M. & Keenan, F.P., *ApJ*, **602**, 436 (2004)

Moreno-Insertis, F., Schüssler, M., Ferriz-Mas, A., *A&A*, **312**, 317 (1996)

Musielak, Z.E., Rosner, R. & Ulmschneider, P., *ApJ*, **337**, 470 (1989)

Musielak, Z.E. & Ulmschneider, P., *A&A*, **370**, 541 (2001)

Musielak, Z.E. & Ulmschneider, P., *A&A*, **400**, 1057 (2003a)

Musielak, Z.E. & Ulmschneider, P., *A&A*, **406**, 725 (2003b)

MWO, Mt. Wilson Observatory, http://www.astro.ucla.edu/~obs/150_data.html

NASA, http://www.solarviews.com/cap/vss/VSS00031.html

Nakariakov, V.M., Coronal Oscillations in *Dynamic Sun*, (Ed.) Dwivedi, B.N., p.314 Cambridge University Press, New York (2003)

Nakariakov, V.M. & Ofman, L., *A&A*, **372**, L53 (2001)

Nakariakov, V.M., Ofman, L., DeLuca, E.E., Roberts, B. & Davila, J.M., *Science*, **285**, 862 (1999)

Nakariakov, V.M. & Roberts, B., *Sol. Phys.*, **159**, 213 (1995)

Nakariakov, V.M. & Verwichte, E., *Liv. Rev. Sol. Phys.* (2005)

Narayanan, A.S., *Plasma Phys. Control. Fusion*, **33**, 333, (1991)

Nightingale, R.W., Aschwanden, M.J. & Hurlburt, N.E., *Sol. Phys.*, **190**, 249 (1999)

Ofman, L., Romoli, M., Poletto, G., Noci, G. & Kohl, J.L., *ApJ Lett.*, **491**, L111 (1997)

Ofman, L. & Wang, T., *ApJ Lett.*, **580**, L85 (2002)

Okamoto, T.J., Tsuneta, S., Berger, T.E., Ichimoto, K., Katsukawa, Y., Lites, B.W., Nagata, S., Shibata, K., Shimizu, T., Shine, R.A., Suematsu, Y., Tarbell, T.D. & Title, A.M., *Science*, **318**, 1577 (2007)

Osin, A., Volin, S. & Ulmschneider, P., *A&A*, **351**, 359 (1999)

Perez, M.E., Doyle, J.G., Erdélyi, R. & Sarro, L.M., *A&A*, **342**, 279 (1999)

Priest, E.R., *Solar Magnetohydrodynamics*, D. Reidel Publishing Company (1982)

Rae, I. & Roberts, B., *ApJ*, **265**, 761 (1982)

Roberts, B., *Sol. Phys.*, **69**, 27 (1981)

Roberts, B., *Sol. Phys.*, **87**, 77 (1983)

Roberts, B., Magnetohydrodynamic waves in the Sun, in Priest, E. R. & Hood, A. (ed) *Advances in solar system magnetohydrodynamics*, CUP (1991)

Roberts, B., *Sol. Phys.*, **193**, 139 (2000)

Roberts, B., MHD waves in the solar atmosphere, in (sci. eds.) R. Erdélyi, J.L. Ballester and B. Fleck, SOHO 13 *Waves, Oscillations and Small Scale Transient Events in the Solar Atmosphere, ESA-SP*, **547**, 1 (2004)

Roberts, B., *Phil. Trans. Roy. Soc. Lon.*, Series A, **364**, 447 (2006)

Roberts, B., Edwin, P.M., Benz, A.O., *ApJ*, **279** 857 (1984)

Roberts, B. & Webb, A.R., *Sol. Phys.*, **56**, 5 (1978)

Royal Swedish Academy of Sciences, http://www.solarphysics.kva.se/NatureNov2002/

Schiff, J.L., *The Laplace transform:theory and applications*, Springer, New York (1999)

Spriut, H.C., *A&A*, **98**, 155 (1981)

Spriut, H. C. & Roberts, B., *Nature*, **304**, 401 (1983)

Solanki, S.K., *Space Sci. Rev.*, **63**, 1 (1993)

Somasundaram, K., Venkatraman, S., & Sengottuvel, M.P., *Plasma Phys. Control. Fusion*, **41**, 1421 (1999)

Spitzer, L., *Physics of fully ionized gases*, Interscience, New York (1962)

Sutmann, G., Musielak, Z.E. & Ulmschneider, P., *A&A.*, **340**, 556 (1998)

Taroyan, Y. & Erdélyi, R. *Sol. Phys.*, In Press (2008)

Taroyan, Y., Erdélyi, R., Wang, T.J. & Bradshaw, S.J., *ApJ*, **659**, L173 (2007)

Teriaca, L., Doyle, J.G., Erdélyi, R. & Sarro, L.M. *A&A*, **352**, L99 (1999)

Terra-Homem, M., Erdélyi, R. & Ballai, I. *Sol. Phys.*, **217**, 199 (2003)

Tirry, W.J., Cadez, W.M., Erdélyi, R. & Goossens, M., *A&A*, **332**, 768 (1998)

Thomas, J.H., *ApJ*, **333**, 407 (1988)

Vernazza, J.E., Avertt, E.H. & Loeser, R., *ApJS*, **45**, 635 (1981)

Wang, T.J., Solanki, S.K., Curdt, W., Innes, D.E. & Dammasch, I.E., *ApJ*, **574**, L101 (2002)

Wang, T.J., Solanki, S.K., Curdt, W., Innes, D.E., Dammasch, I.E. & Kliem, B., *A&A*, **406**, 1105 (2003a)

Wang, T.J., Solanki, S.K., Innes, D.E., Curdt, W., Marsch, E., *A&A*, **402**, L17 (2003b)

Watanabe, T. *Publ. Astron. Soc. Japan*, **27**, 385 (1975)

Williams, D.R., Phillips, K.J.H., Rudawy, P., Mathioudakis, M., Gallagher, P.T., O'Shea, E., Keenan, F.P., Read, P. & Rompolt, B., *Mon. Not. R. Astron. Soc.*, **326**, 428 (2001)

Williams, D.R., Mathioudakis, M., Gallagher, P.T., Phillips, K.J.H., McAteer, R.T.J, Keenan, F.P., Rudawy, P & Katsiyannis, A.C., *Mon. Not. R. Astron. Soc.*, **336**, 747 (2002)

Wunsch, D., *Complex variables and applications*, Pearson Addison-Wesley, Boston (2005)

Zirker, J.B., *Journey from the Center of the Sun*, Princeton Science Library (2004)